

Electronic Supporting Information for  
**Harnessing Borane-Potassium Cooperativity for sulfurated ring-  
opening copolymerisation**

## Table of Contents

<b>Section S1:</b> General methods	3
<b>Section S2:</b> ROCOP with PTA/OX	4
➔ GPC	16
➔ End group analysis	18
<b>Section S3:</b> ROCOP with different monomers	21
➔ GPC	46
<b>Section S4:</b> Thermal Analysis	48
<b>Section S5:</b> Self nucleation experiments	60
<b>Section S6:</b> Insitu IR experiments	65
<b>Section S7:</b> References	66

## Section S1: General methods

Solvents and reagents were obtained from commercial sources and used as received unless stated otherwise. If “dried solvents” were used these were obtained by different procedures. THF was dried over K/benzophenone and distilled under argon, collected, and stored over pre-dried 4 Å sieves before use. The catalyst  $\text{BEt}_3$  (1 M solution in THF) was transferred to a Schlenk tube under inert conditions, degassed and stored in the glove box. 18-crown-6 was used as received. Oxetane (OX), OX-Me<sub>2</sub>, OX-OEt, OX-OBn, OX-OAll were dried over calcium hydride for 24 h, vacuum distilled and then dried over Na for 24 h, vacuum distilled and degassed before storing in the glove box. Propylene oxide (PO), carbon disulfide (CS<sub>2</sub>), ethyl isothiocyanate - EtNCS, PhNCS (phenyl), and CyNCS (cyclohexyl) were dried over CaH<sub>2</sub>, distilled, degassed and stored in the glovebox. Phthalic thioanhydride (PTA) and succinic thioanhydride (STA) were synthesised according to the literature.<sup>[1]</sup> KOAc@18c6 and KCl@18c6 were synthesised according to literature, washed with pentane, dried under vacuum and stored in the glove box.<sup>[2]</sup>

Nuclear Magnetic Resonance (NMR) spectra were recorded by using a Jeol JNM-ECA 400II, Bruker Advance 300 and 500 MHz spectrometer. <sup>1</sup>H and <sup>13</sup>C{<sup>1</sup>H} chemical shifts are referenced to the residual proton resonance of the deuterated solvents. Infrared spectra were measured using a Perkin Elmer Spectrum 100 FTIR spectrometer with DuraSampIR accessory in total reflection at room temperature. In situ – IR measurements were performed using Mettler Toledo “ReactIR 15” using liq. N<sub>2</sub> for cooling. Thermogravimetric Analysis (TGA) data was measured using a Mettler Toledo STAR<sup>e</sup> System “TGA/DSC 3+”. Differential scanning calorimetry (DSC) was measured on a Mettler Toledo “STAR<sup>e</sup> System DSC 3+” at a heating rate of 10.0 K/min. The molecular weight and polydispersity of the polymers were determined by a Waters 515 Gel permeation chromatography (GPC) instrument equipped with two linear PLgel columns (Mixed-C) following guard column and a differential refractive index detector using tetrahydrofuran as the eluent at a flow rate of 1.0 mL/min at 30 °C and a series of narrow polystyrene standards for the calibration of the columns. Each polymer sample was dissolved in HPLC-grade THF (5 mg/mL) and filtered through a 0.20 µm porous filter frit prior to analysis.

### Theoretical methods

The geometries and energies of all systems included in this study were fully optimized at the RI-BP86-D4/def2-TZVP level of theory. The calculations have been performed by using the program TURBOMOLE version 7.7.<sup>[3]</sup> For the calculations we have used the BP86<sup>[4]</sup> functional with the D4 correction for dispersion.<sup>[5]</sup> In order to reproduce solvent effects, we have used the conductor-like screening model COSMO,<sup>[6]</sup> which is a variant of the dielectric continuum solvation models. The minimum nature of the complexes and compounds have been confirmed by doing frequency calculations. The transition states were initially located using the NEB tool of ORCA 4.2 and re-optimized using Turbomole 7.7. They only present one negative frequency that corresponds to the movement of atoms connecting the intermediates. In some cases, very small frequencies (< -8 cm<sup>-1</sup>) are observed that could not be eliminated and correspond to small vibrations of the crown ether.

### General polymerisation protocol:

The appropriate amount of catalyst (1 eq., 7.86 µmol), cocatalyst (1 eq., 7.86 µmol) and the monomers (300 eq., 2.36 mmol and 600 eq., 4.17 mmol) [for PTA/OX ROCOP: 0.387g PTA and 0.307mL OX was used] were added to an oven dried vial equipped with a magnetic stirrer and sealed with a melamine cap containing a Teflon inlay inside an argon filled glovebox. The vial was then brought outside the glovebox and placed in a pre-heated aluminium block at the specified temperature for the specified time. At the specified end point, the polymerisation mixture was cooled down to room temperature, an aliquot was removed and analysed by <sup>1</sup>H NMR for the determination of the conversion. The mixture was then dissolved in 5 mL DCM and added dropwise to 40 mL of MeOH causing precipitation of the polymer, which was then isolated by centrifugation. This precipitation was repeated once more from DCM/pentane, and the obtained polymer was dried in a vacuum oven before further analysis.

## Section S2: ROCOP with PTA/OX

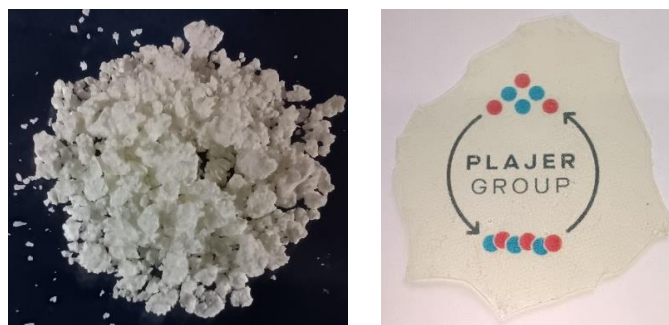


Figure S 1: Digital photographs of powder and film of PTA/OX copolymer.

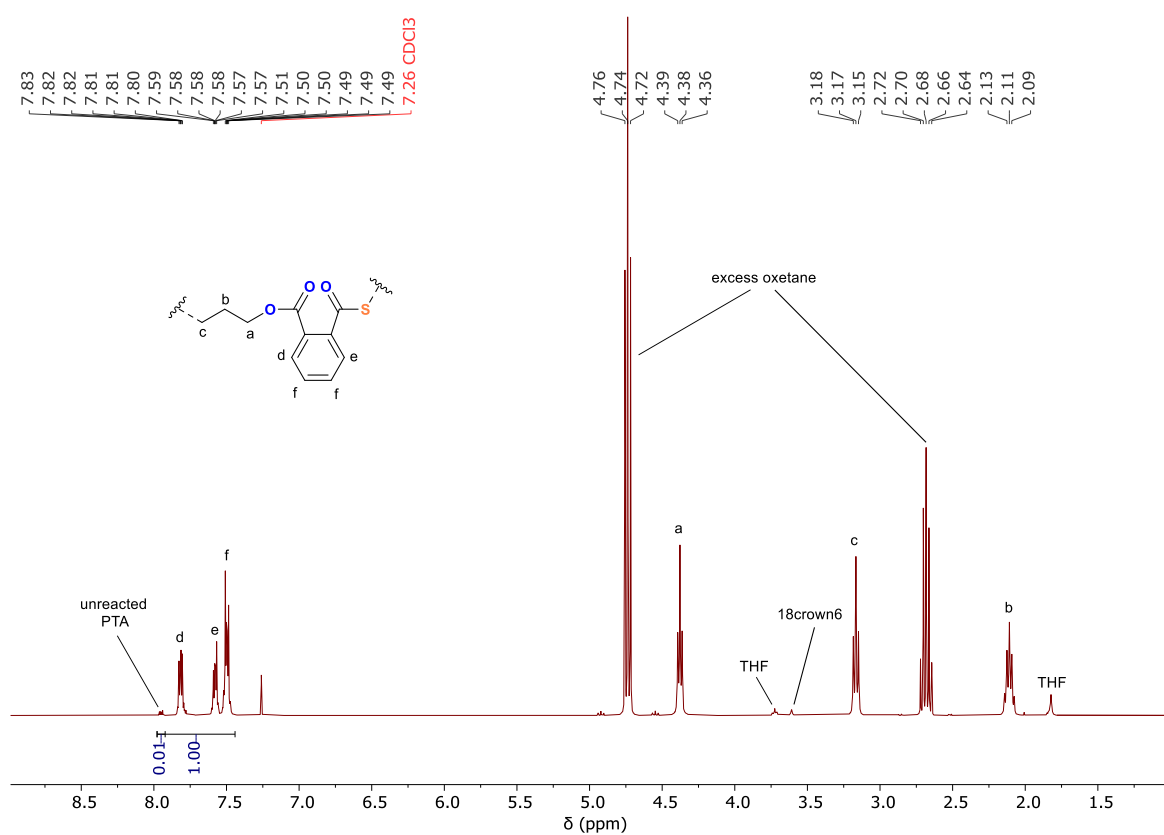
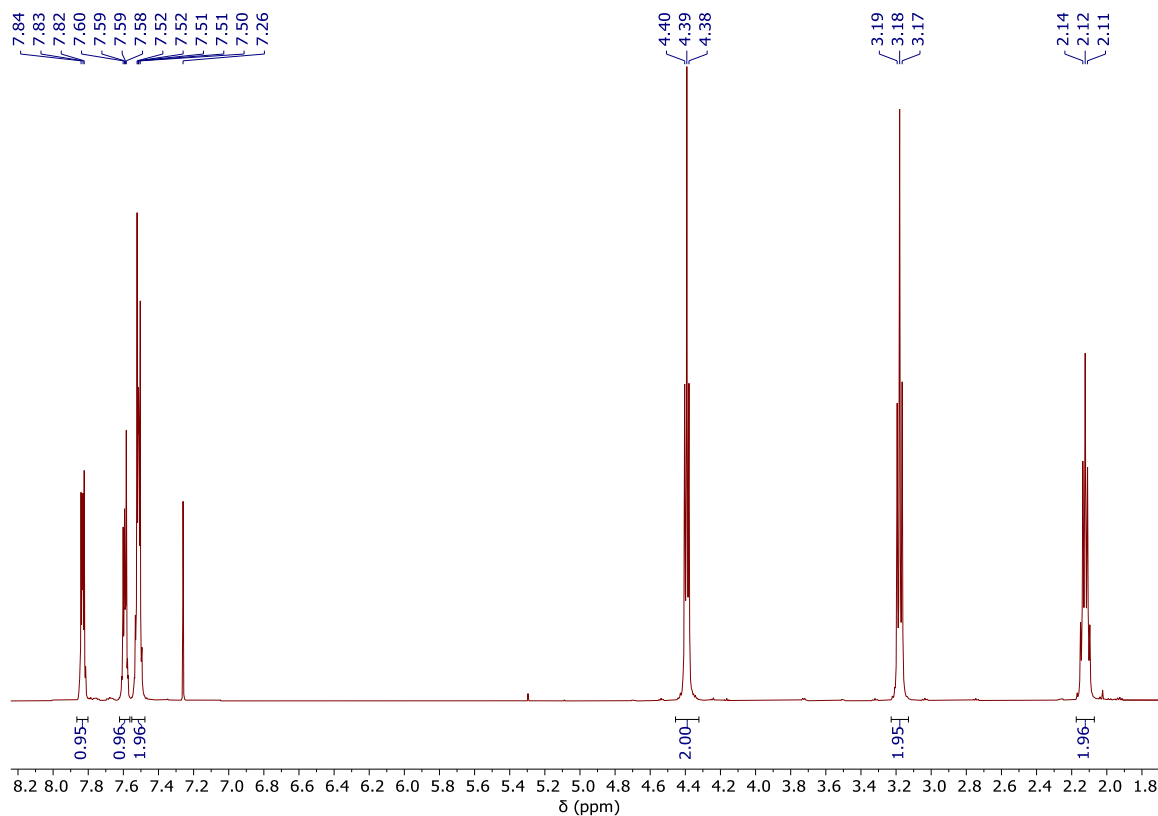
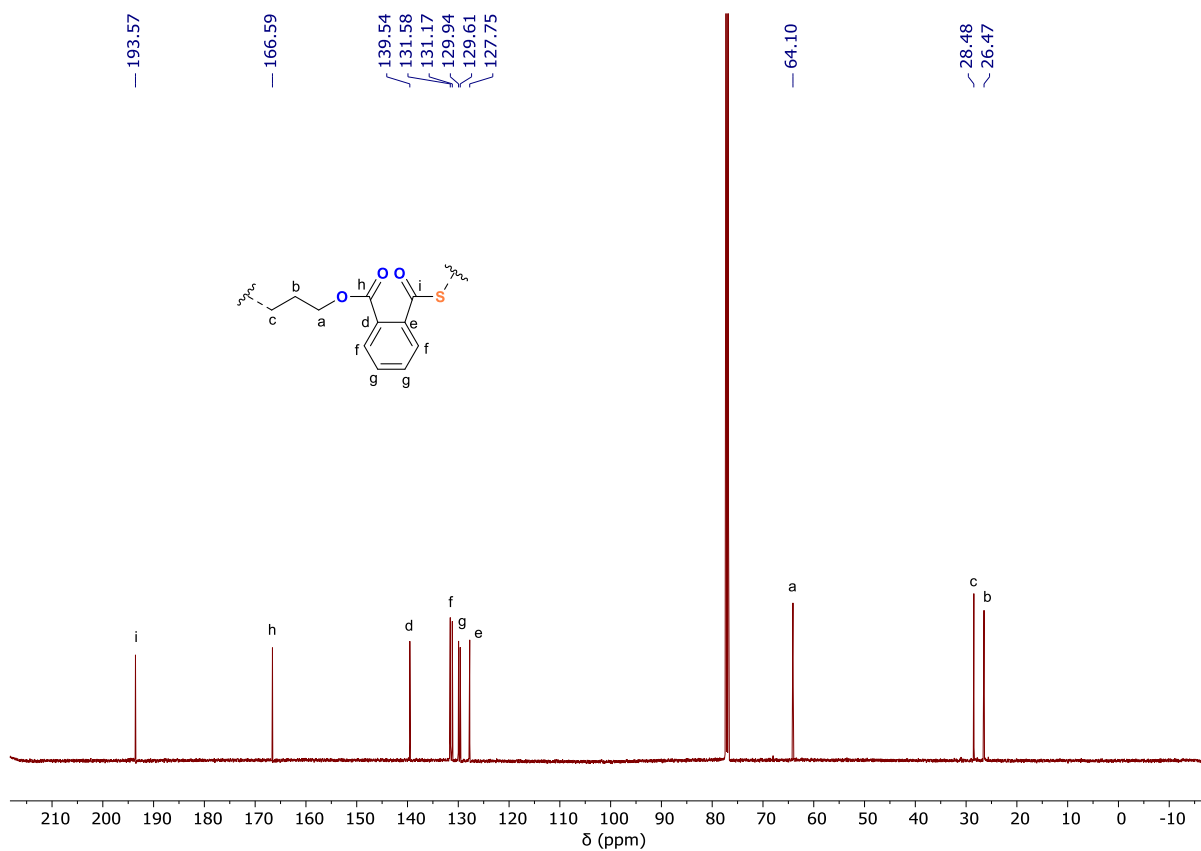


Figure S 2: <sup>1</sup>H NMR spectrum (400MHz, CDCl<sub>3</sub>) of the final aliquot from PTA/OX ROCOP (table 1, run 9).



**Figure S 3:**  $^1\text{H}$  NMR spectrum (500MHz,  $\text{CDCl}_3$ ) of the isolated PTA/OX copolymer (table 1, run 9). Peak assignments as per Fig. S 2 for all PTA/OX copolymers.



**Figure S 4:**  $^{13}\text{C}$  NMR spectrum (500MHz,  $\text{CDCl}_3$ ) of the isolated PTA/OX copolymer (table 1, run 9).

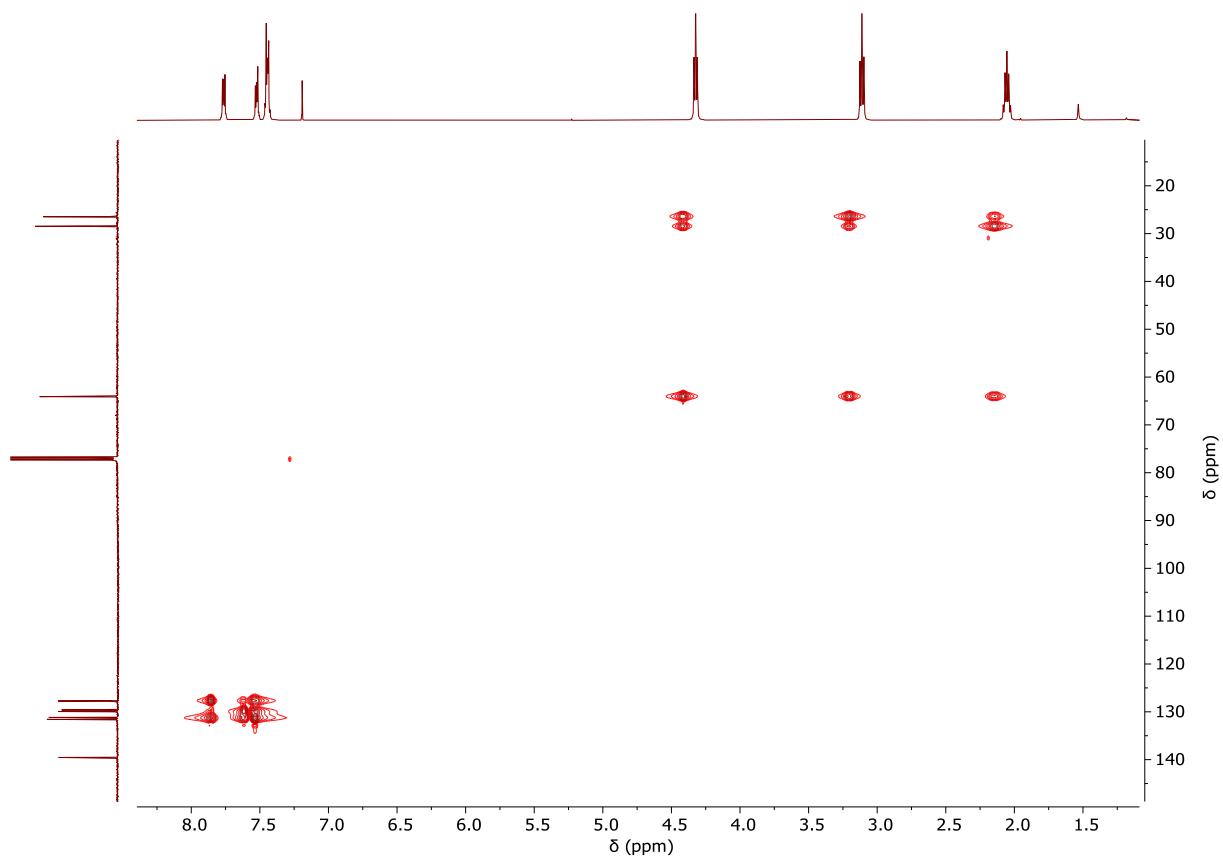


**Figure S 5:**  $^1\text{H}$  -  $^{13}\text{C}$  HSQC NMR spectrum (500 MHz,  $\text{CDCl}_3$ ) of isolated PTA/OX copolymer (table 1, run 9).

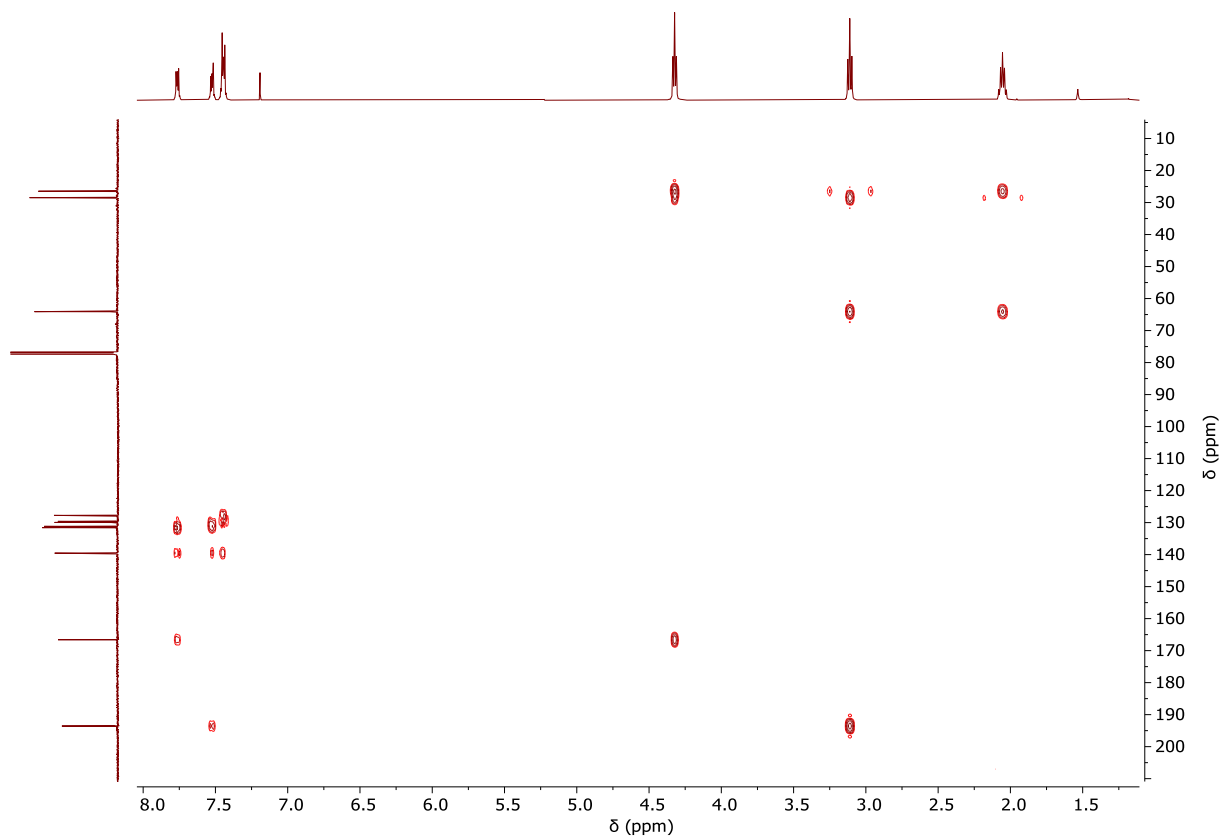


**Figure S 6:**  $^1\text{H}$  -  $^{13}\text{C}$  HMBC NMR spectrum (500 MHz,  $\text{CDCl}_3$ ) of isolated PTA/OX copolymer (table 1, run 9).

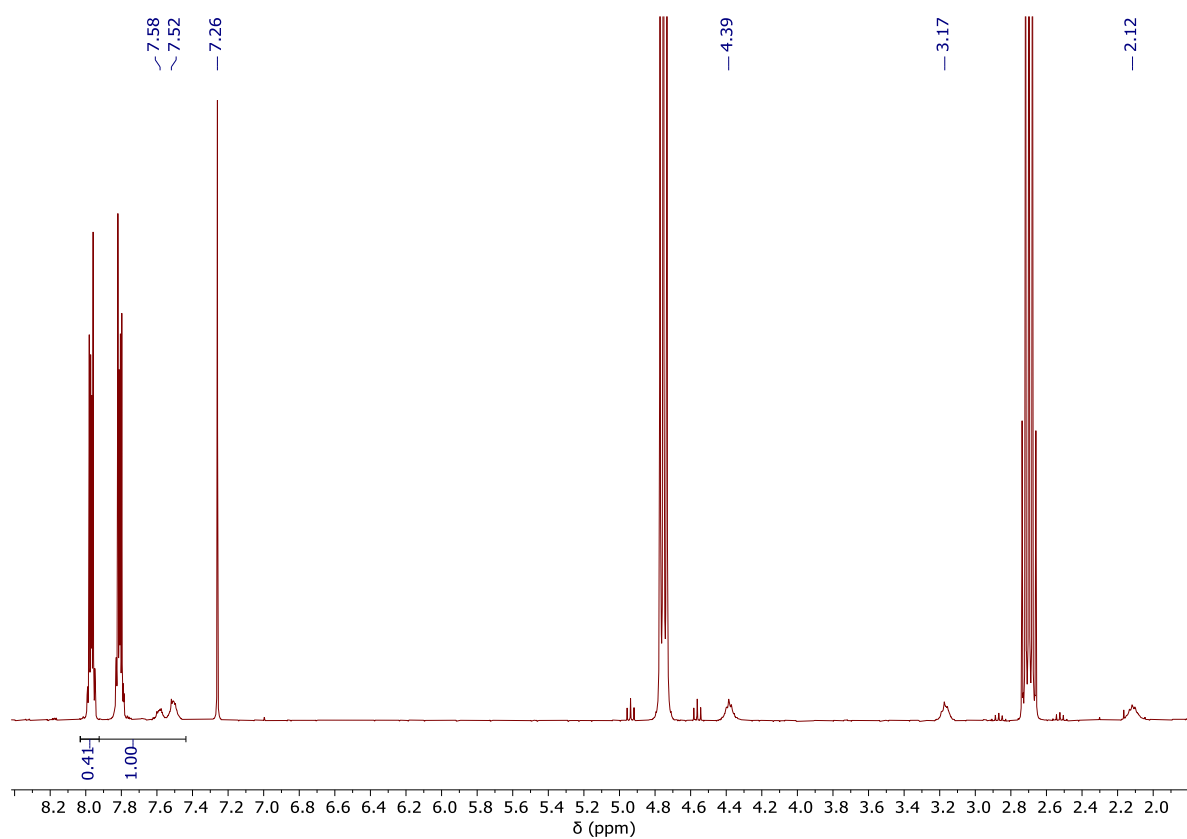


**Figure S 7:** <sup>1</sup>H NMR spectrum (400MHz, CDCl<sub>3</sub>) of the final aliquot from PTA/OX ROCOP (table 1, run 1).

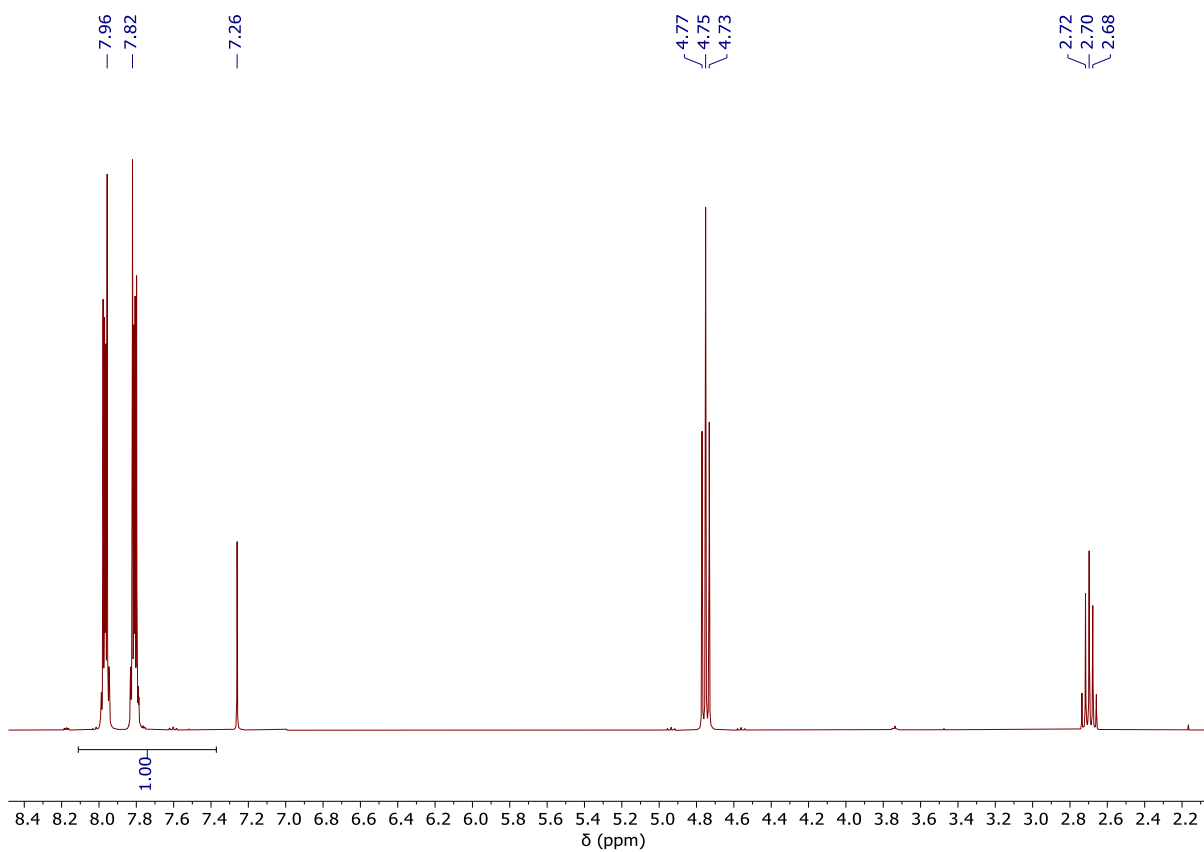


**Figure S 8:** <sup>1</sup>H NMR spectrum (400MHz, CDCl<sub>3</sub>) of the final aliquot from PTA/OX ROCOP (table 1, run 2).

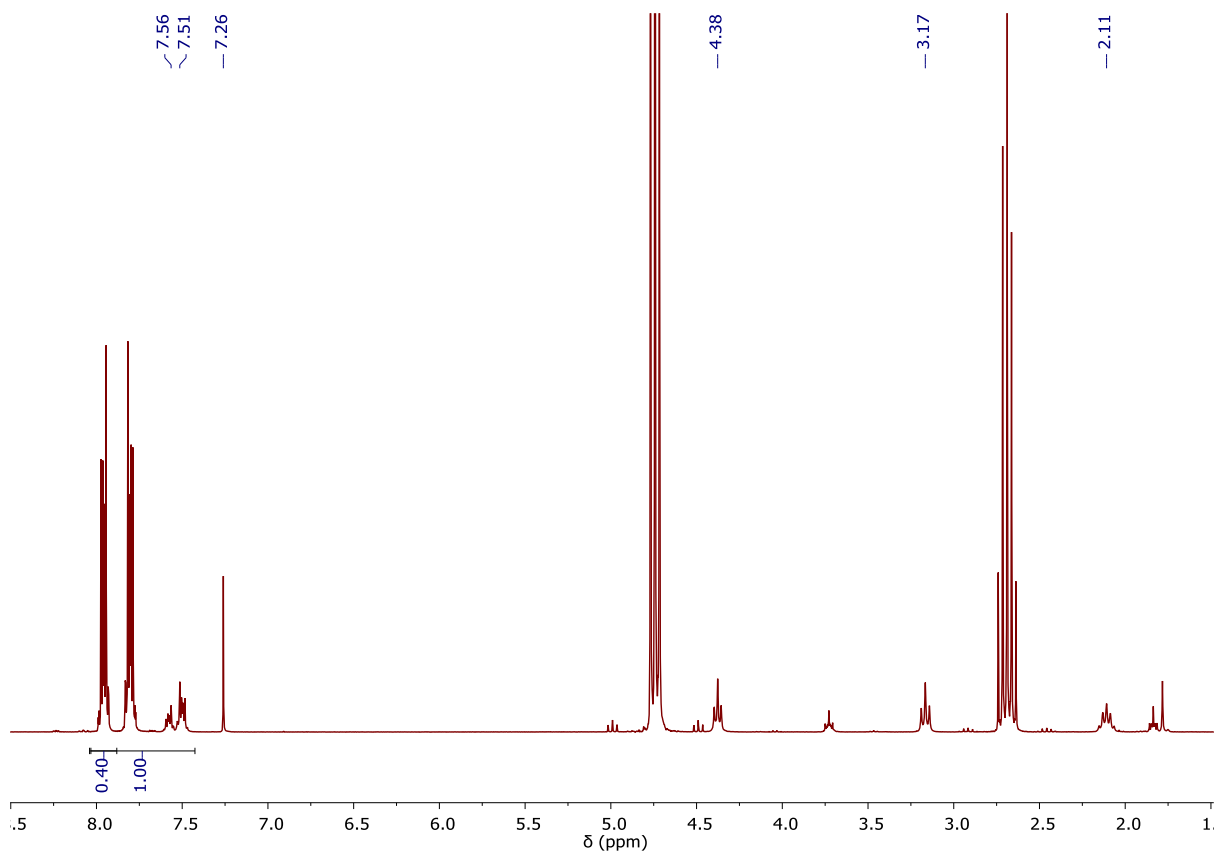


**Figure S 9:**  $^1\text{H}$  NMR spectrum (300MHz,  $\text{CDCl}_3$ ) of the final aliquot from PTA/OX ROCOP (table 1, run 3).

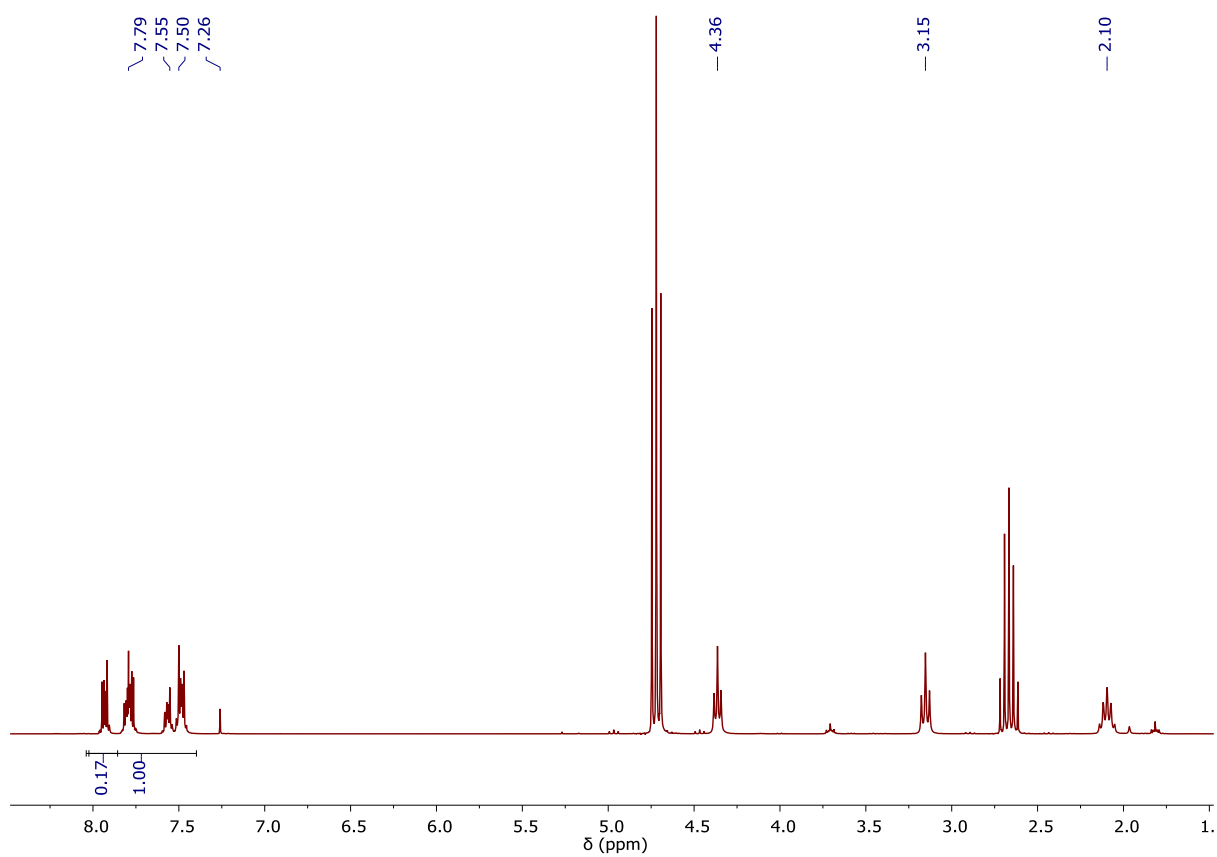


**Figure S 10:**  $^1\text{H}$  NMR spectrum (300MHz,  $\text{CDCl}_3$ ) of the final aliquot from PTA/OX ROCOP (table 1, run 4).



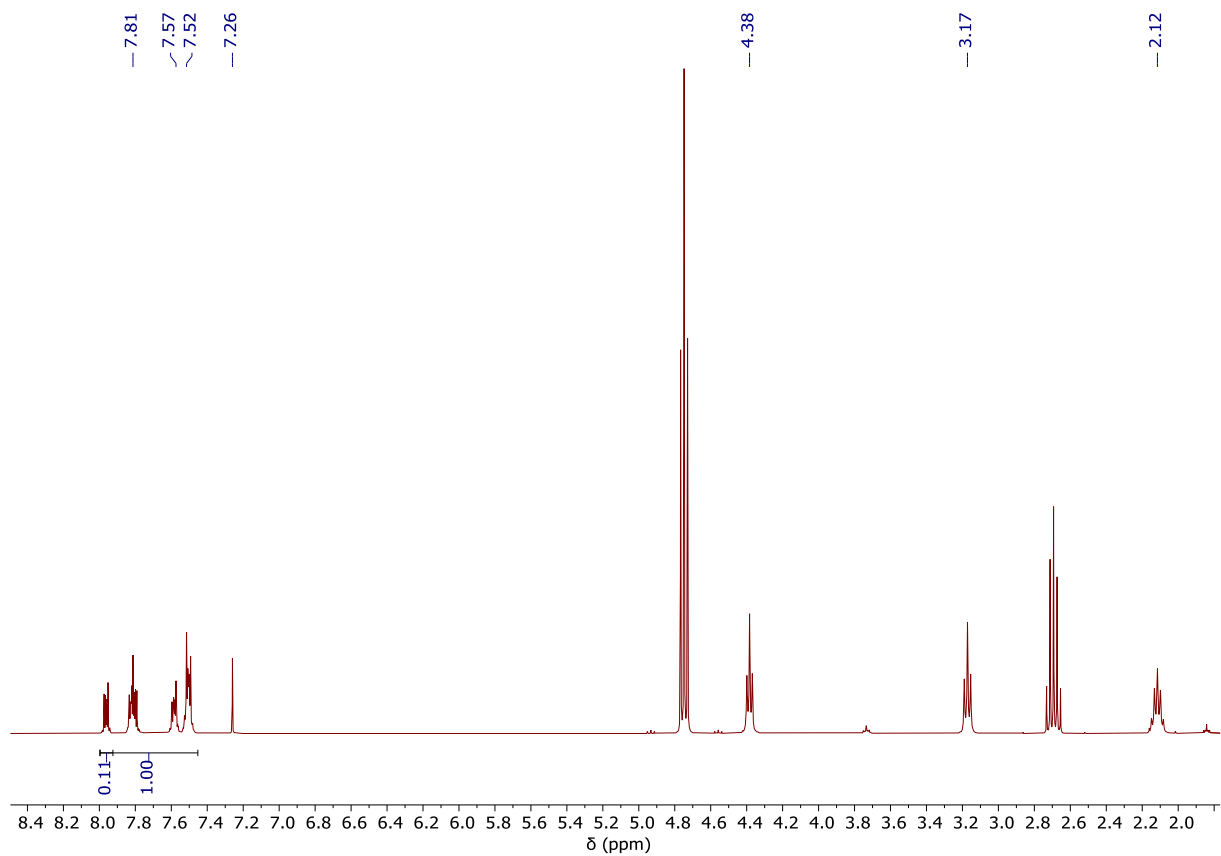


**Figure S 11:**  $^1\text{H}$  NMR spectrum (400MHz,  $\text{CDCl}_3$ ) of the final aliquot from PTA/OX ROCOP (table 1, run 5).

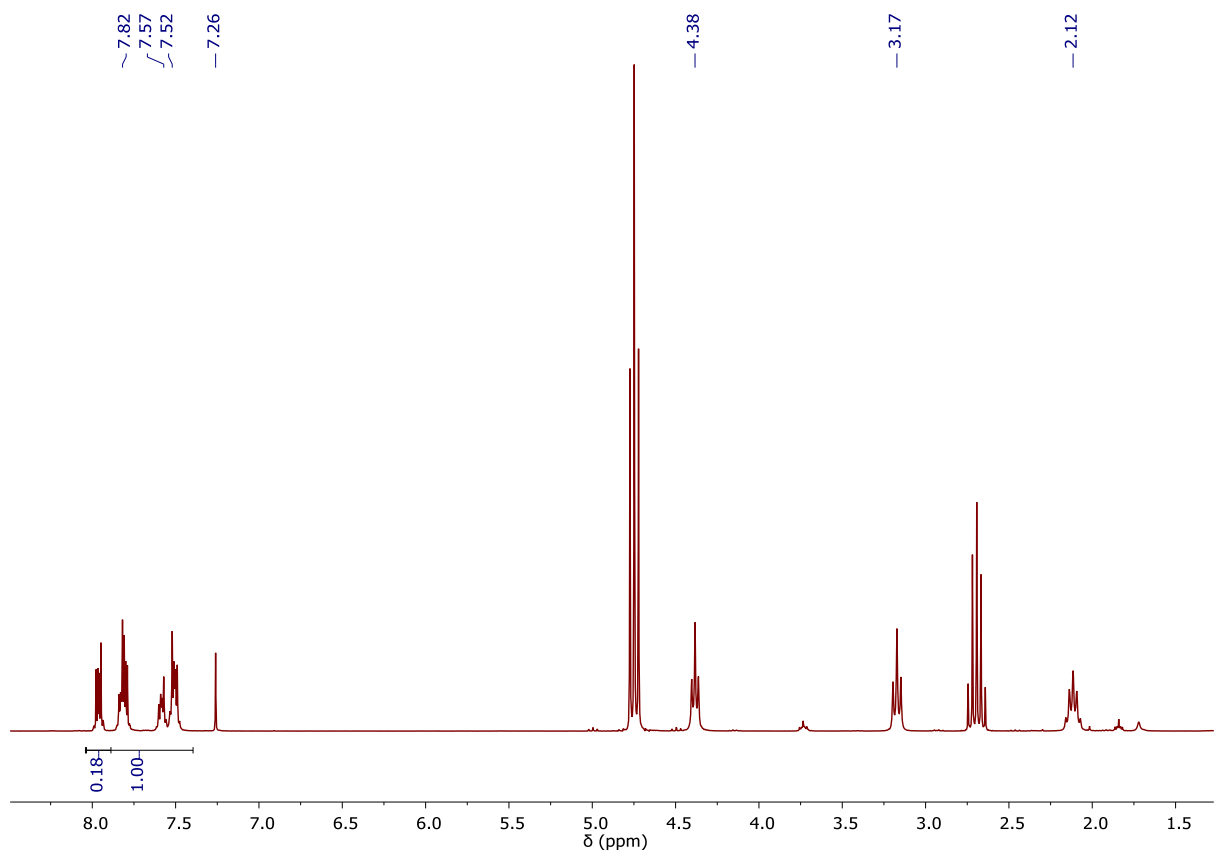


**Figure S 12:**  $^1\text{H}$  NMR spectrum (300MHz,  $\text{CDCl}_3$ ) of the final aliquot from PTA/OX ROCOP (table 1, run 6).

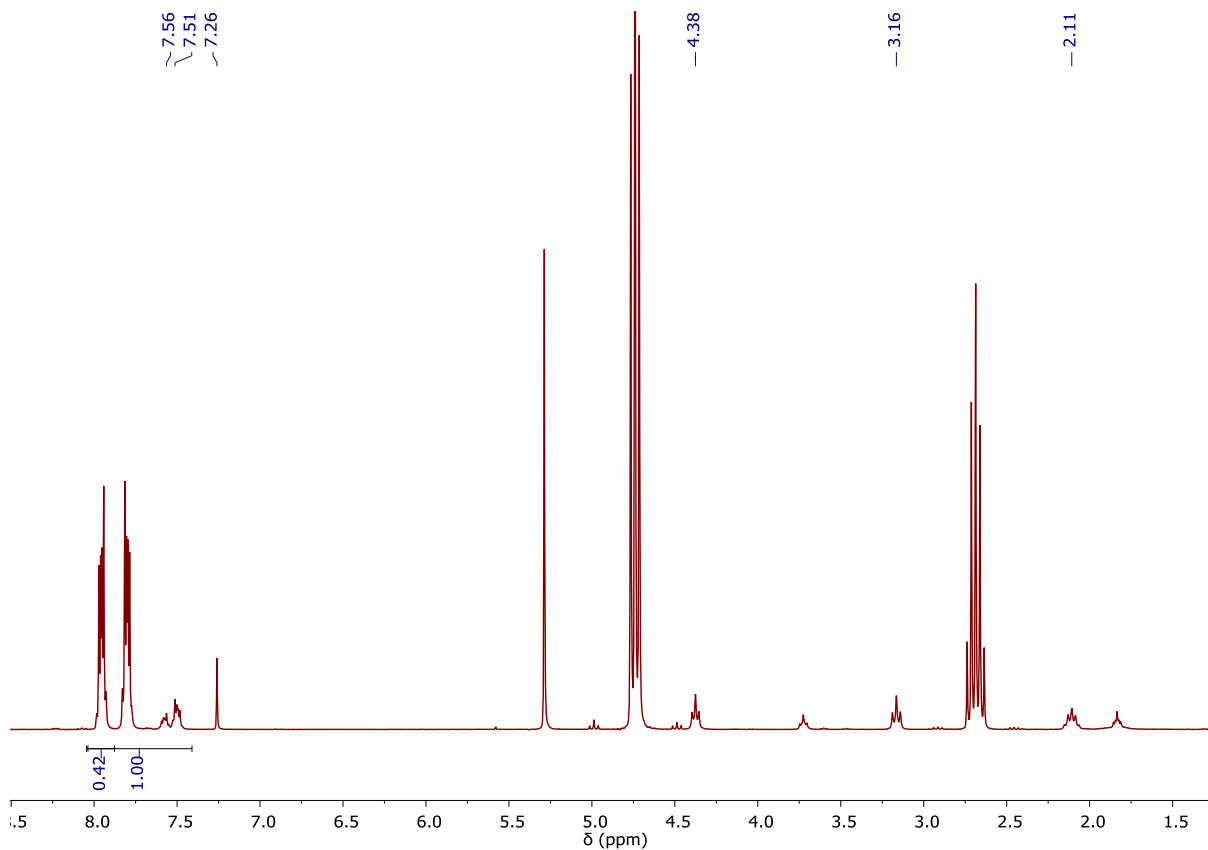


**Figure S 13:**  $^1\text{H}$  NMR spectrum (300MHz,  $\text{CDCl}_3$ ) of the final aliquot from PTA/OX ROCOP (table 1, run 7).

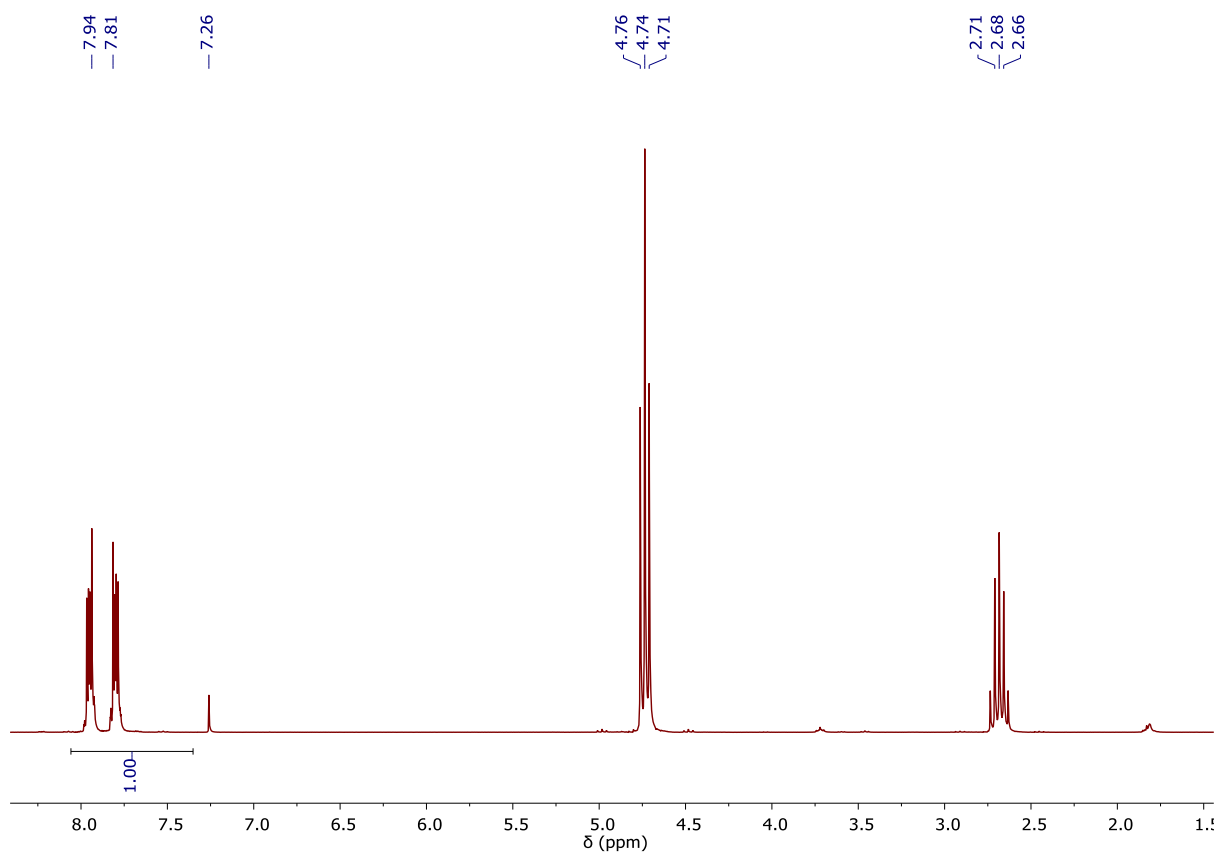


**Figure S 14:**  $^1\text{H}$  NMR spectrum (300MHz,  $\text{CDCl}_3$ ) of the final aliquot from PTA/OX ROCOP (table 1, run 8).

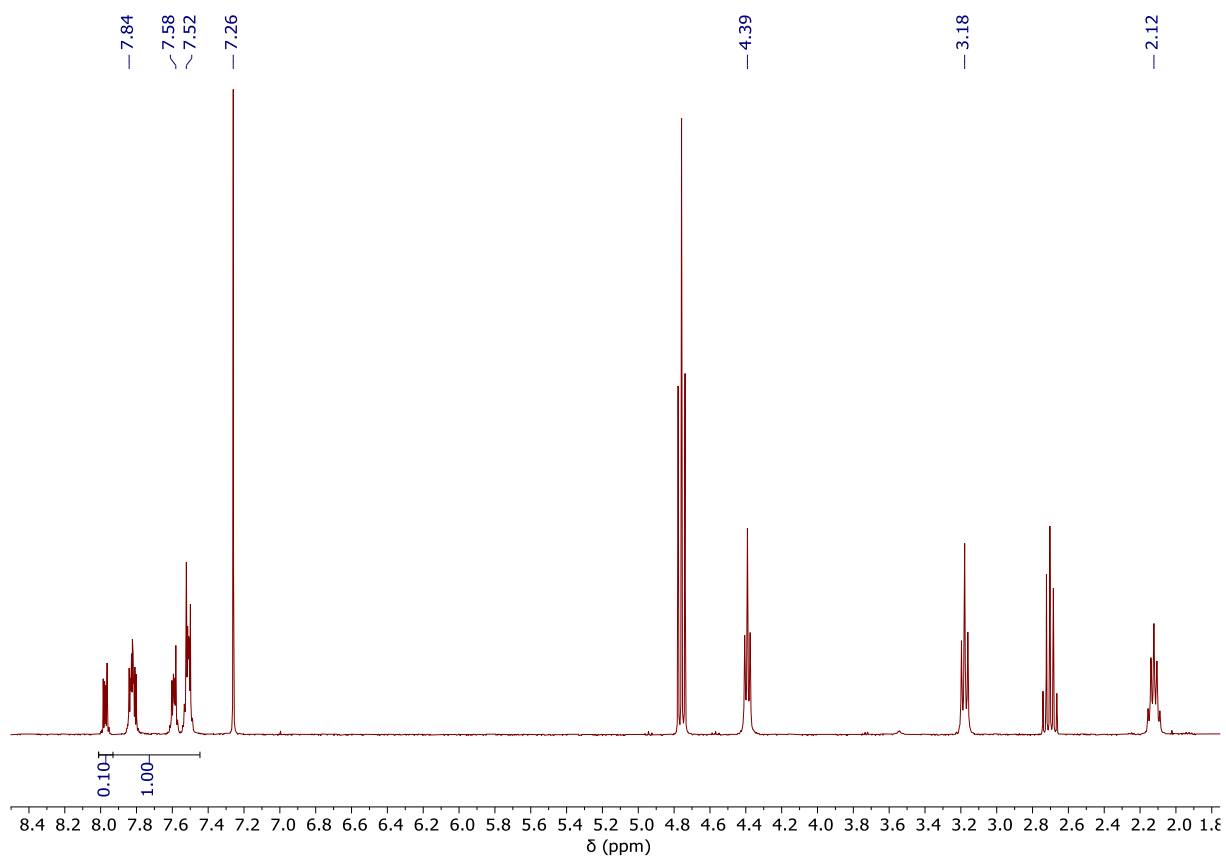


**Figure S 15:**  $^1\text{H}$  NMR spectrum (400MHz,  $\text{CDCl}_3$ ) of the final aliquot from PTA/OX ROCOP (table 1, run 10).

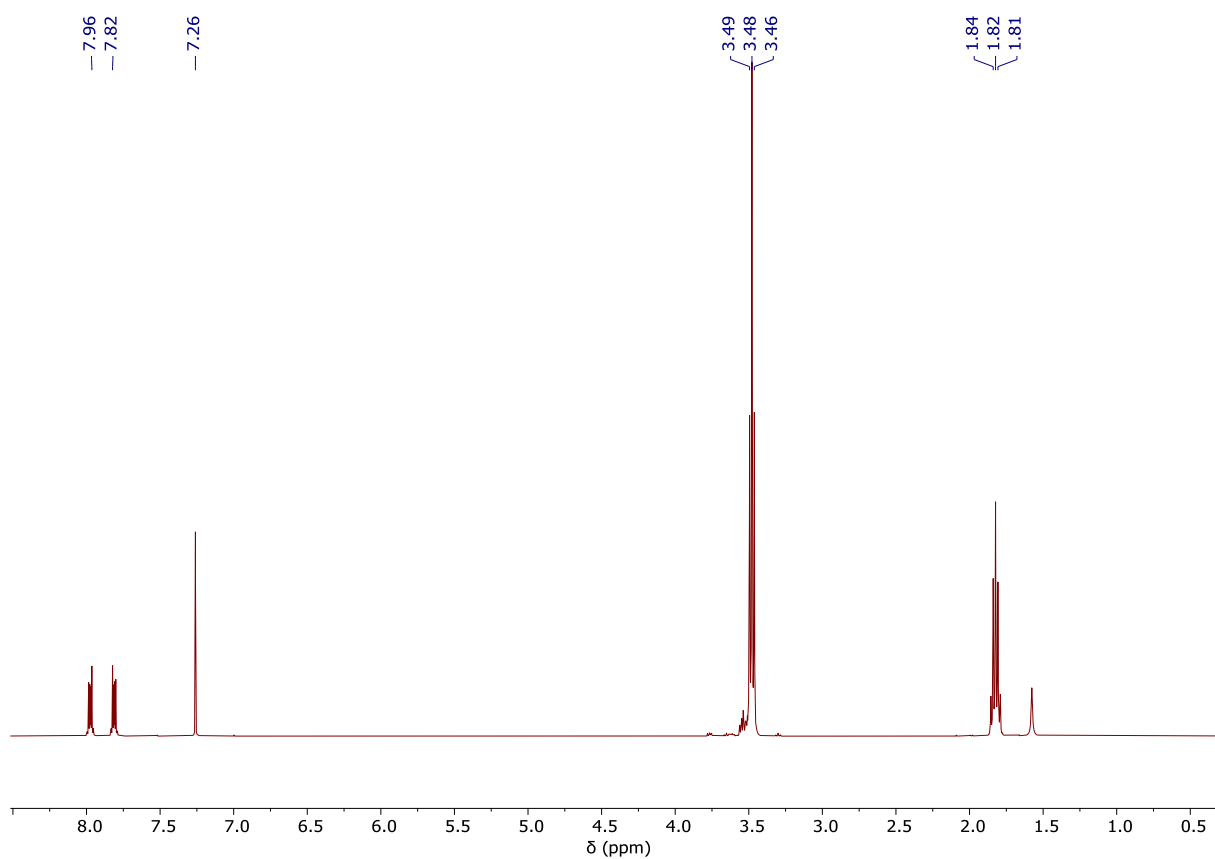


**Figure S 16:**  $^1\text{H}$  NMR spectrum (400MHz,  $\text{CDCl}_3$ ) of the final aliquot from PTA/OX ROCOP (table 1, run 11).

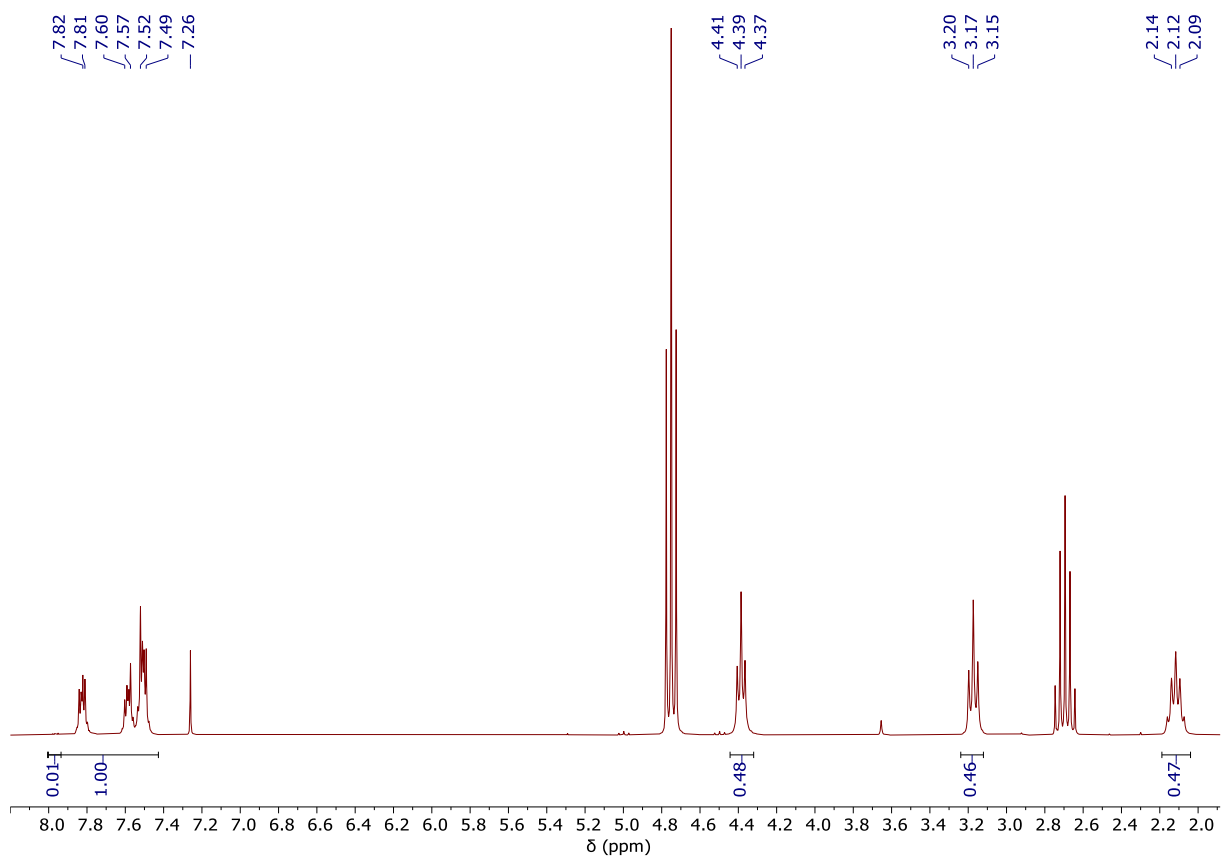


**Figure S 17:**  $^1\text{H}$  NMR spectrum (400MHz,  $\text{CDCl}_3$ ) of the final aliquot from PTA/OX ROCOP (table 1, run 12).

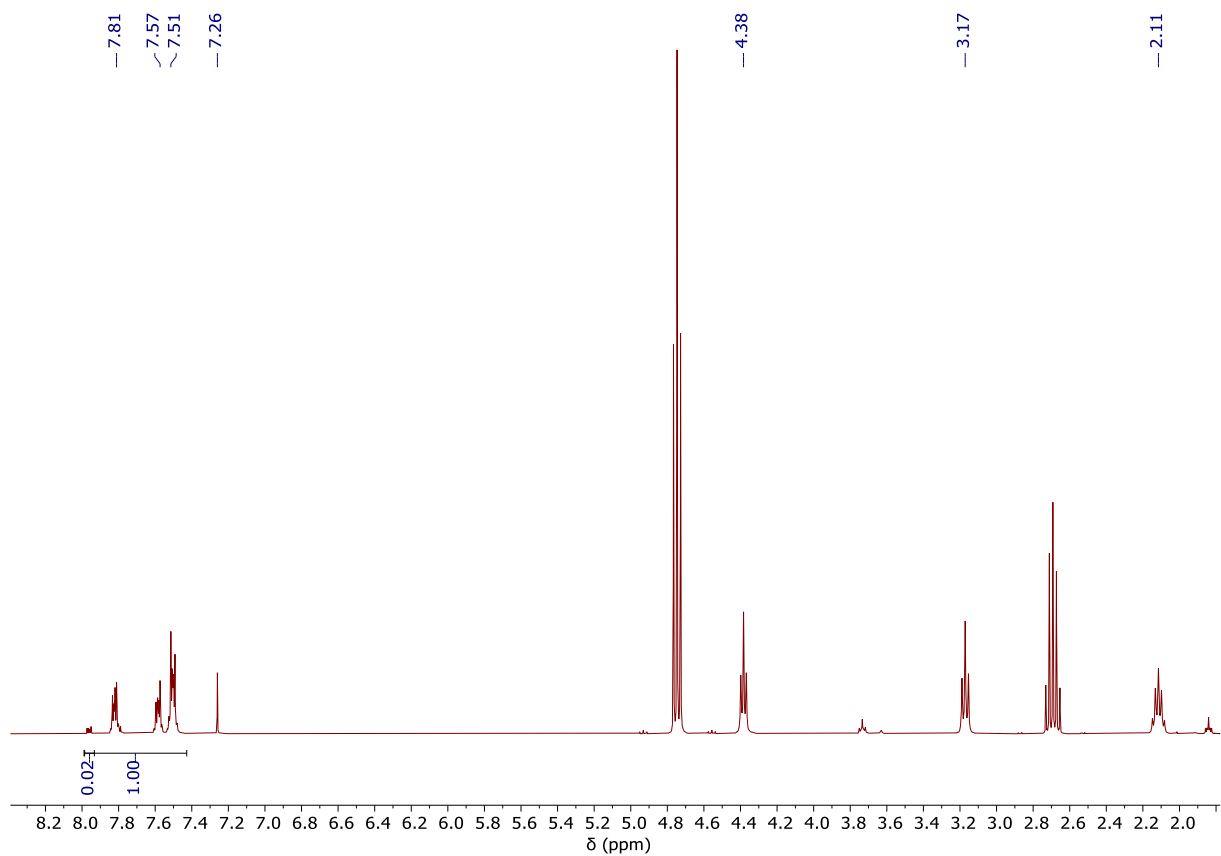


**Figure S 18:**  $^1\text{H}$  NMR spectrum (400MHz,  $\text{CDCl}_3$ ) of the final aliquot PTA/OX ROCOP (table 1, run 13).

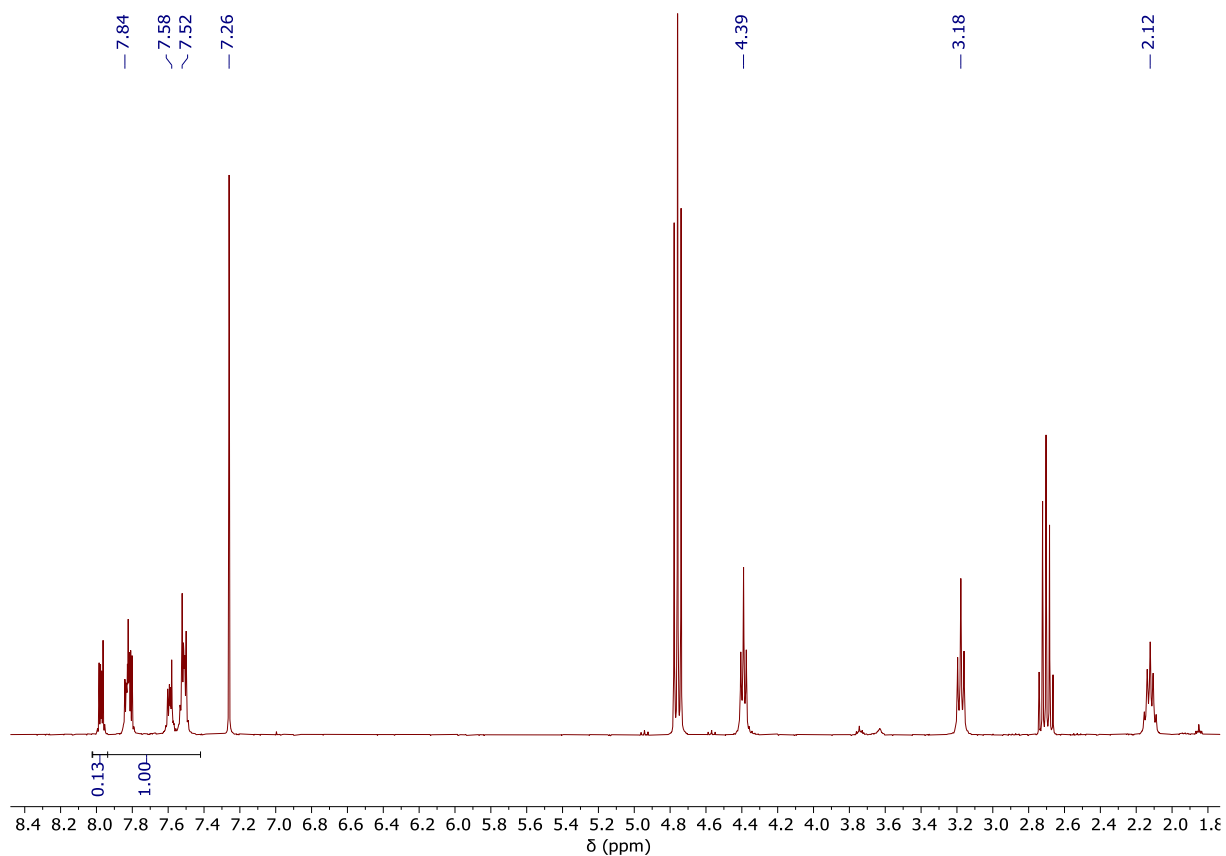


**Figure S 19:** <sup>1</sup>H NMR spectrum (400MHz, CDCl<sub>3</sub>) of the final aliquot from PTA/OX ROCOP (table 1, run 14).

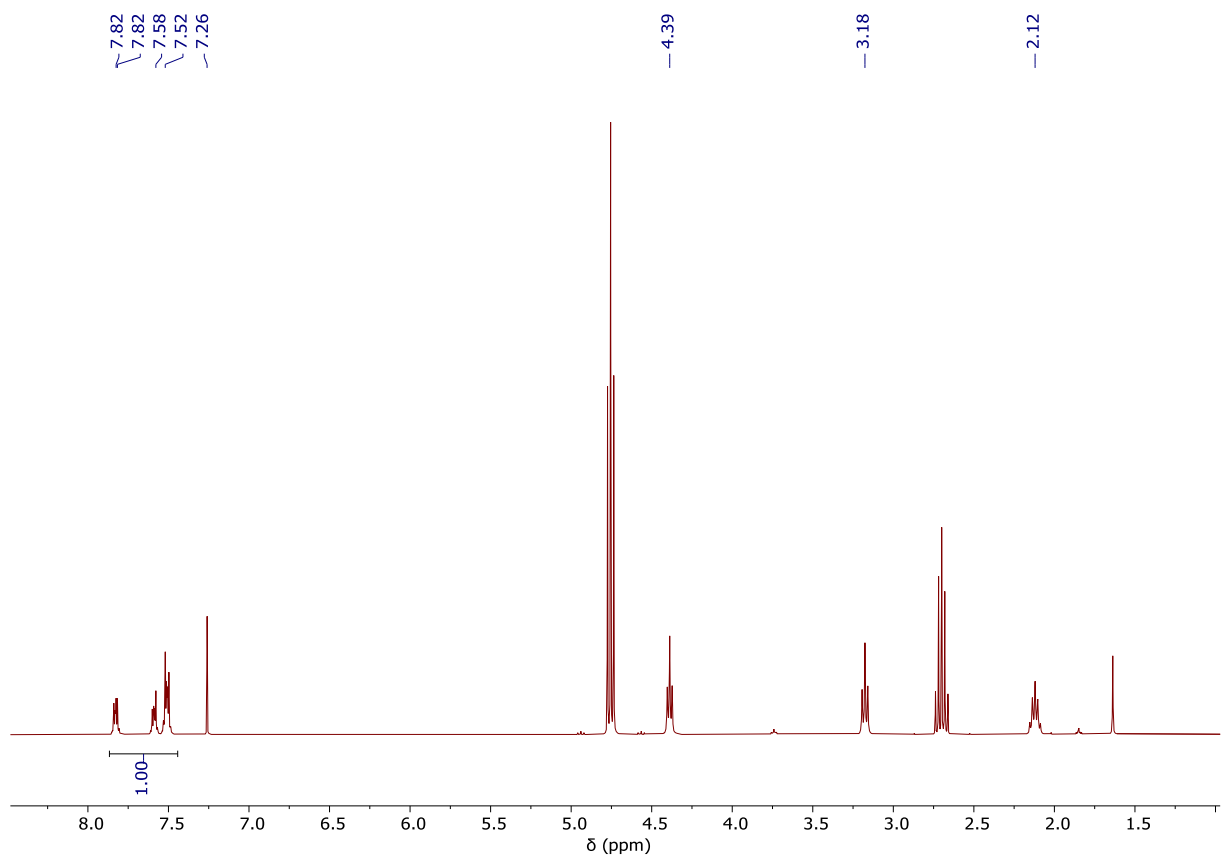


**Figure S 20:** <sup>1</sup>H NMR spectrum (400MHz, CDCl<sub>3</sub>) of the final aliquot from PTA/OX ROCOP (table 1, run 15).

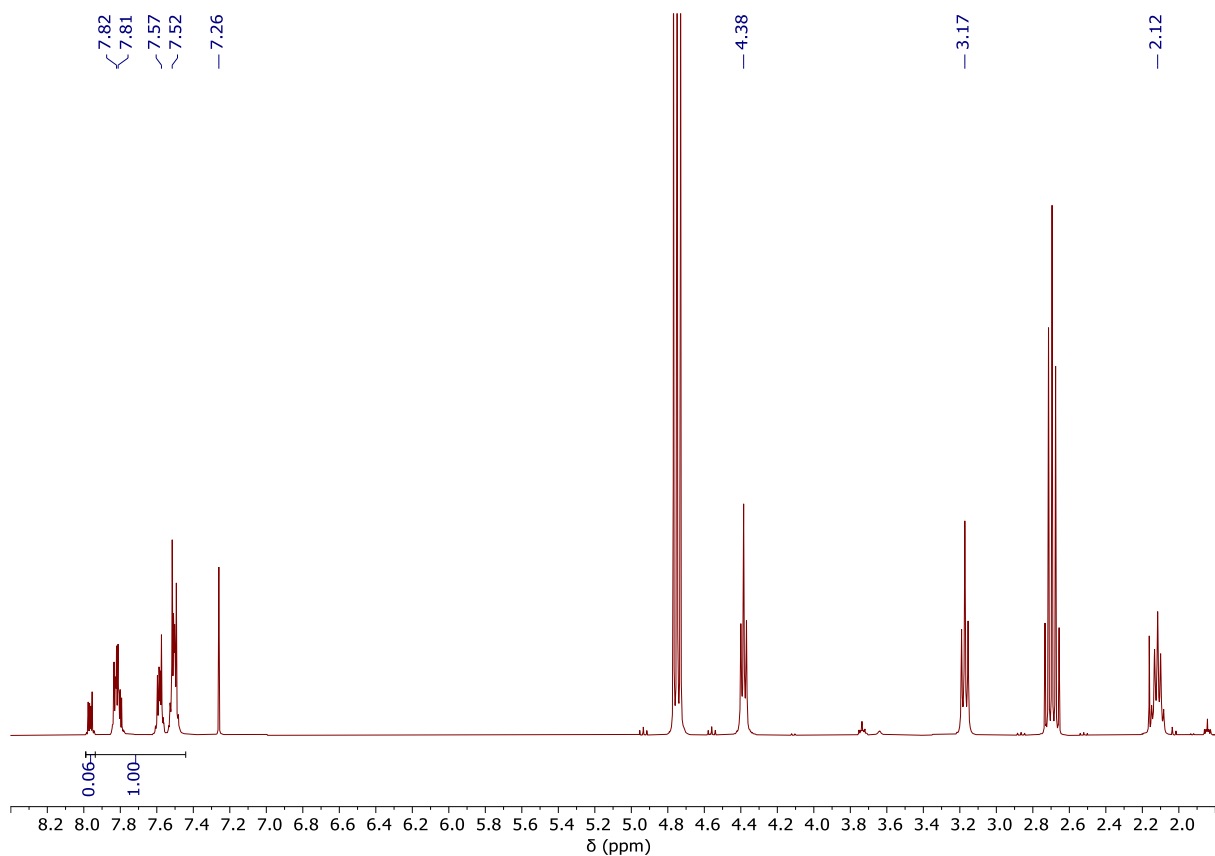


**Figure S 21:**  $^1\text{H}$  NMR spectrum (400MHz,  $\text{CDCl}_3$ ) of the final aliquot from PTA/OX ROCOP (table 1, run 16).

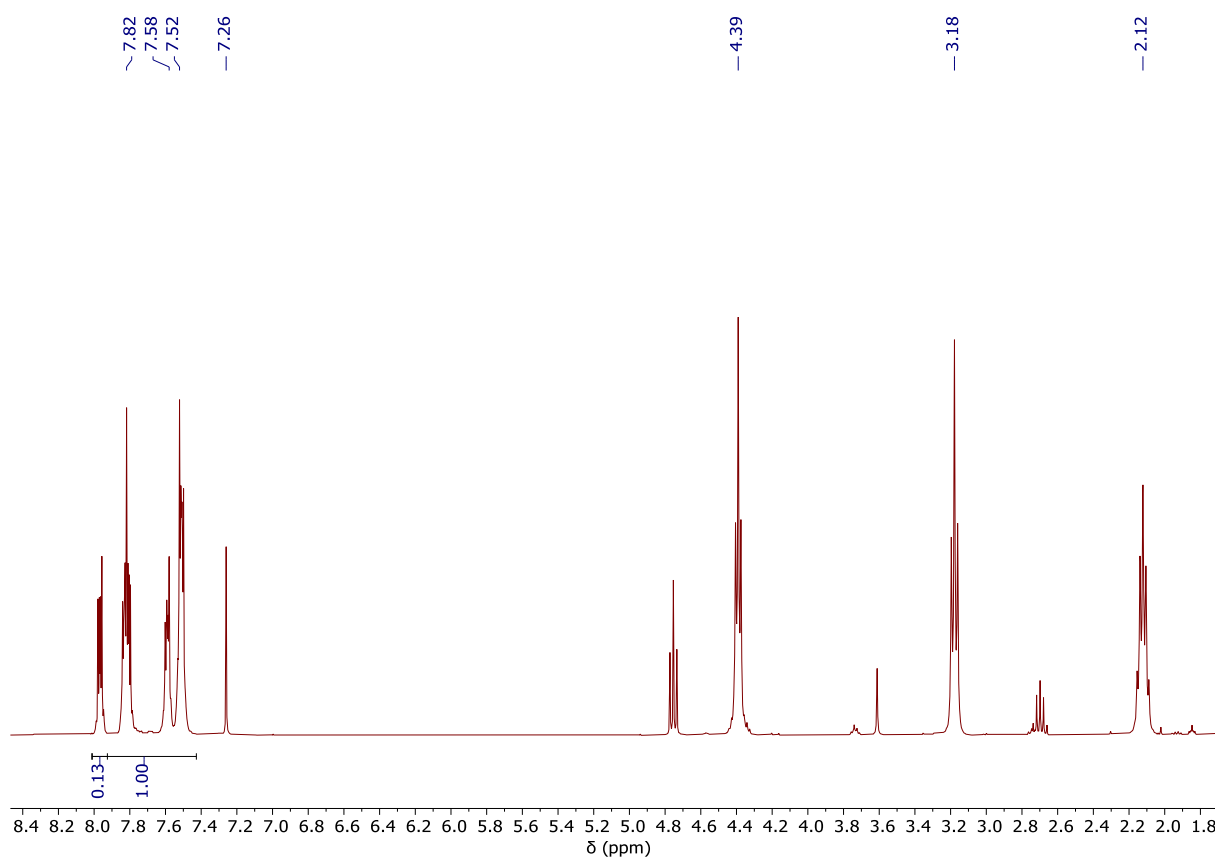


**Figure S 22:**  $^1\text{H}$  NMR spectrum (400MHz,  $\text{CDCl}_3$ ) of the final aliquot from PTA/OX ROCOP (table 1, run 17).

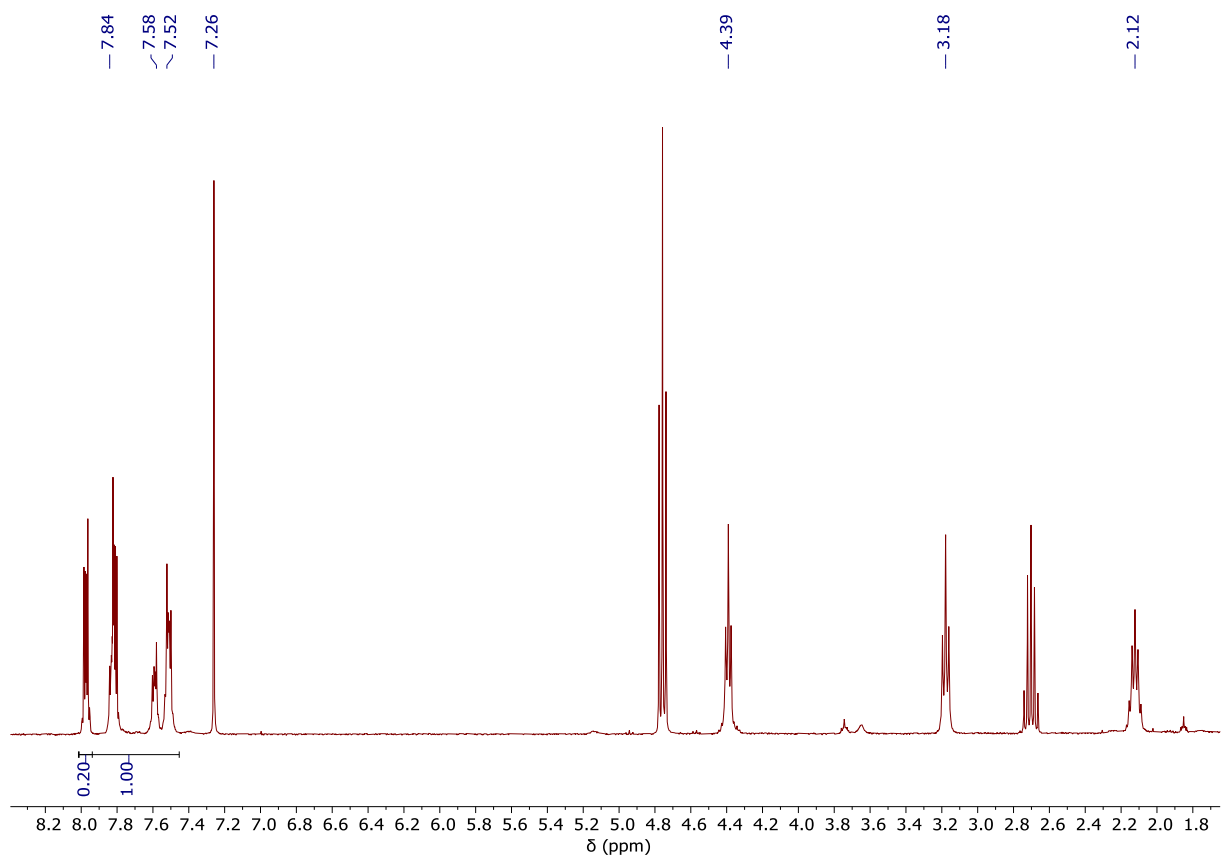


**Figure S 23:**  $^1\text{H}$  NMR spectrum (400MHz,  $\text{CDCl}_3$ ) of the final aliquot from PTA/OX ROCOP (table 1, run 18).

## Gel Permeation Chromatography (GPC):

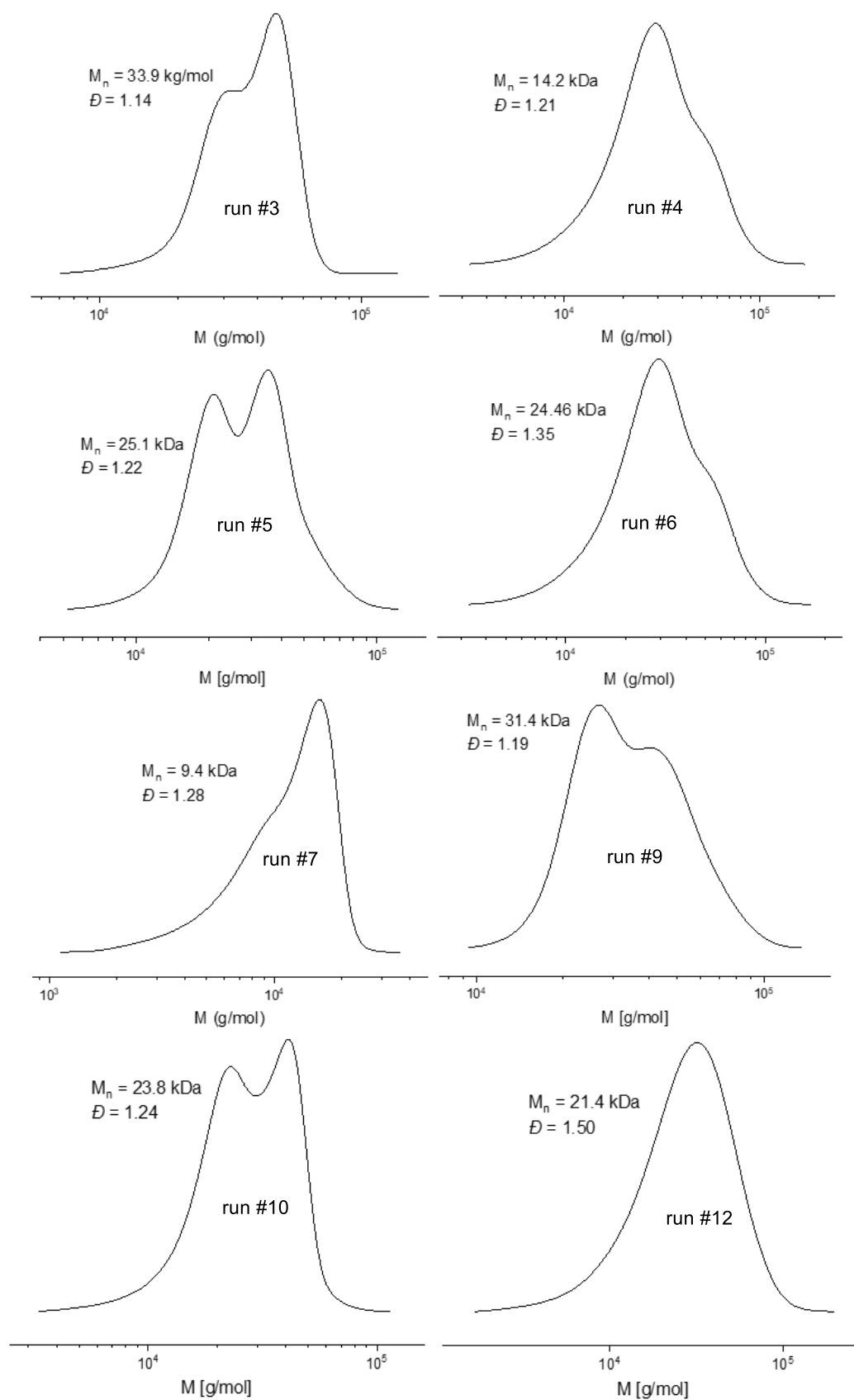


Figure S 24: GPC traces corresponding to table 1, run #3 to #12.



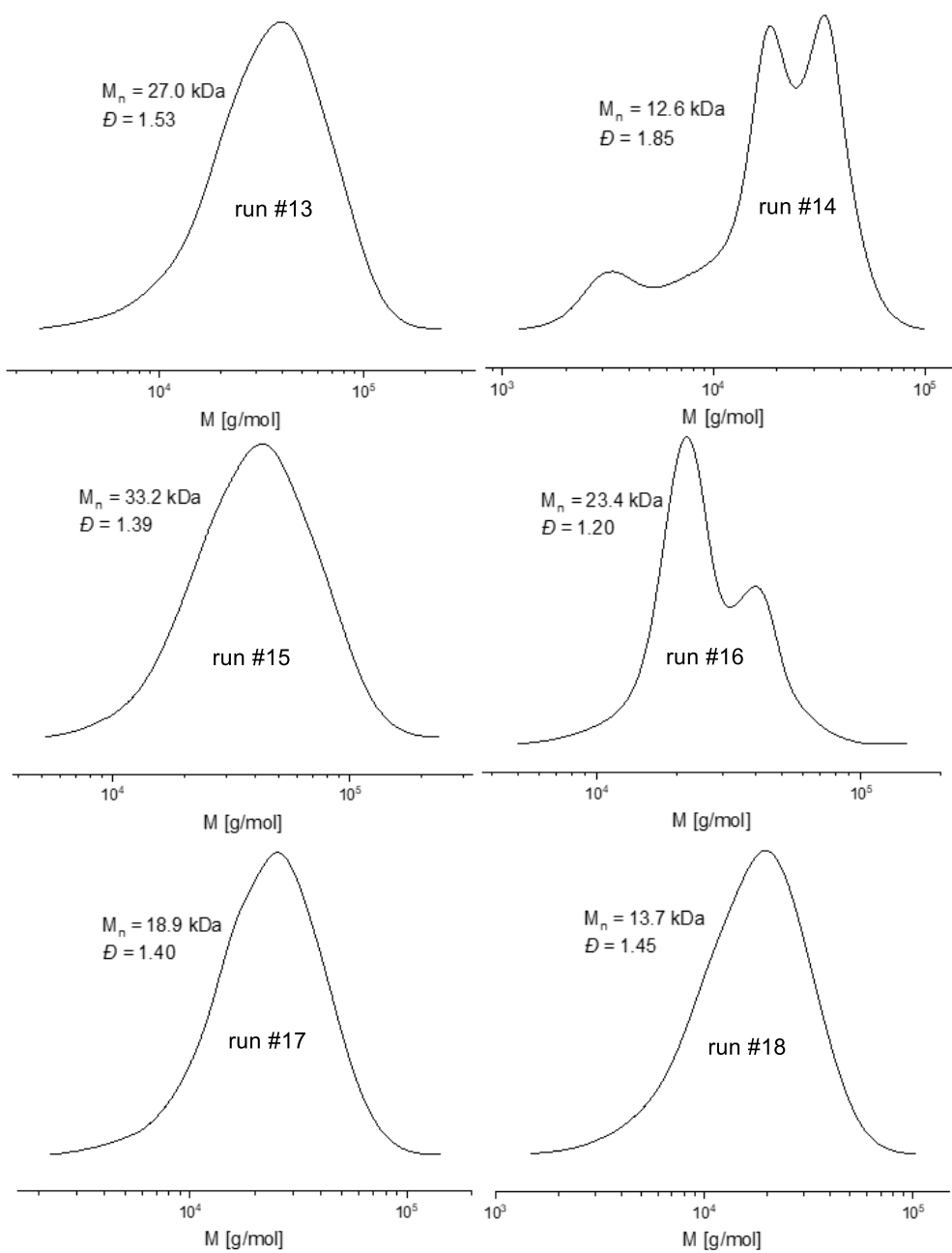


Figure S 25: GPC traces corresponding to table 1, run #13 to #18.

End group analysis:

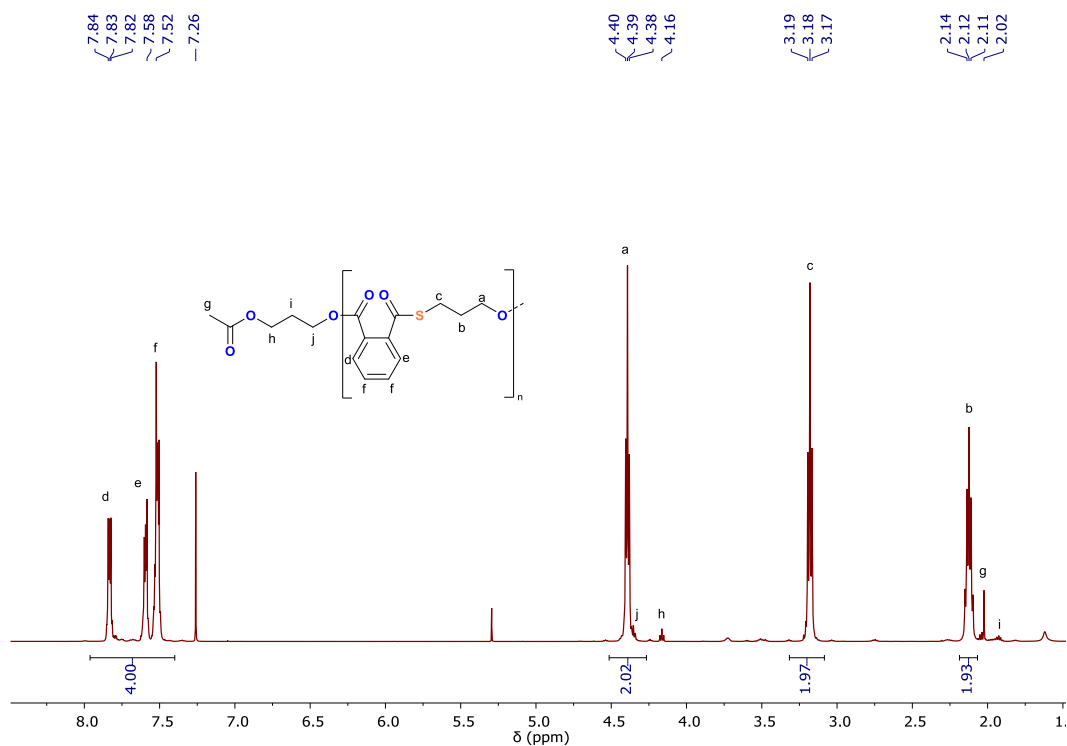


Figure S 26:  $^1\text{H}$  NMR spectrum (500MHz,  $\text{CDCl}_3$ ) of PTA/OX copolymer. Signals corresponding to  $-\text{CH}_3$  group from acetate initiator is seen at 2.02 ppm. Run at Cat.:coCat.:PTA:OX ratio of 1:1:20:40.

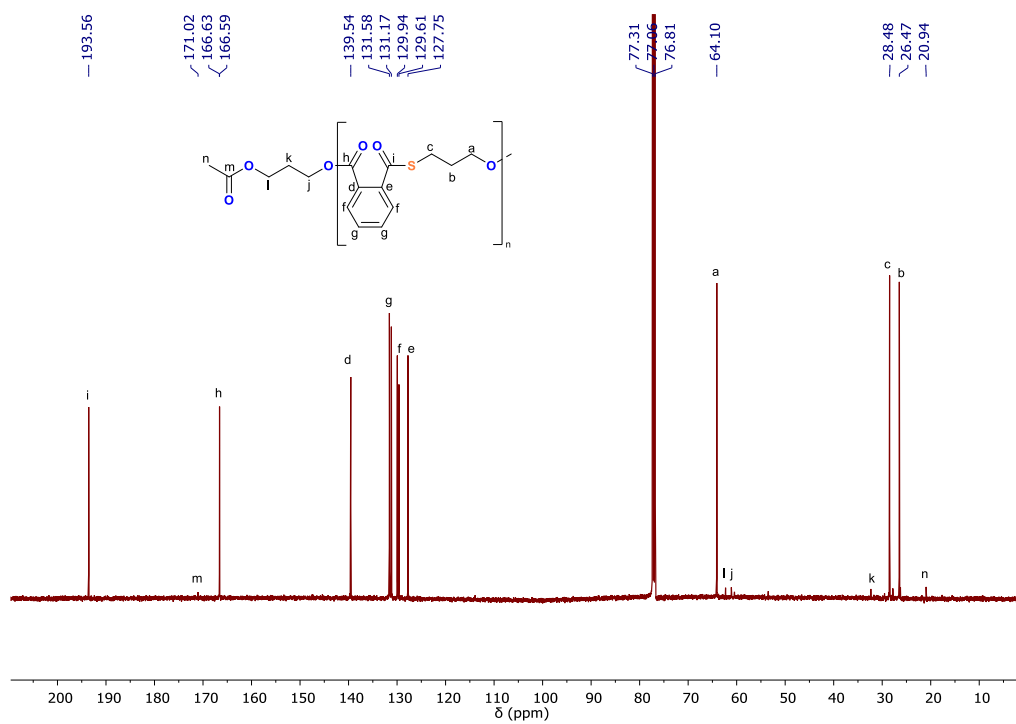
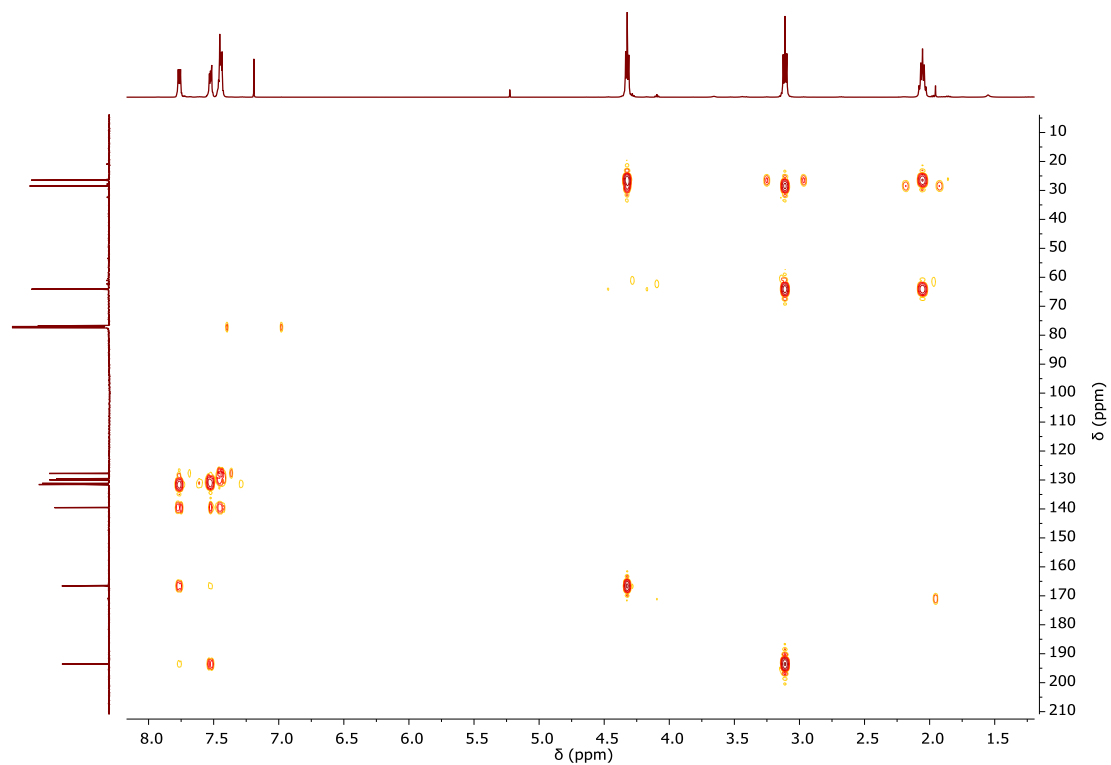
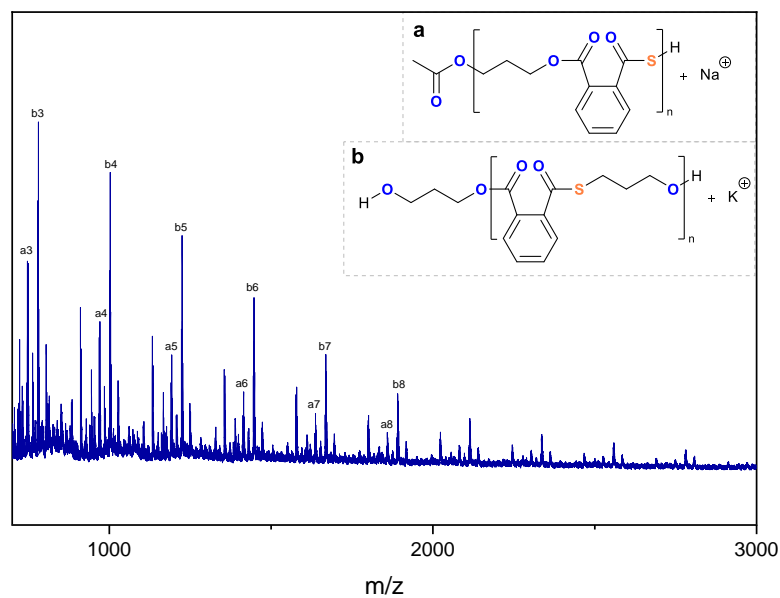


Figure S 27:  $^{13}\text{C}$  NMR spectrum (500MHz,  $\text{CDCl}_3$ ) of above PTA/OX copolymer.



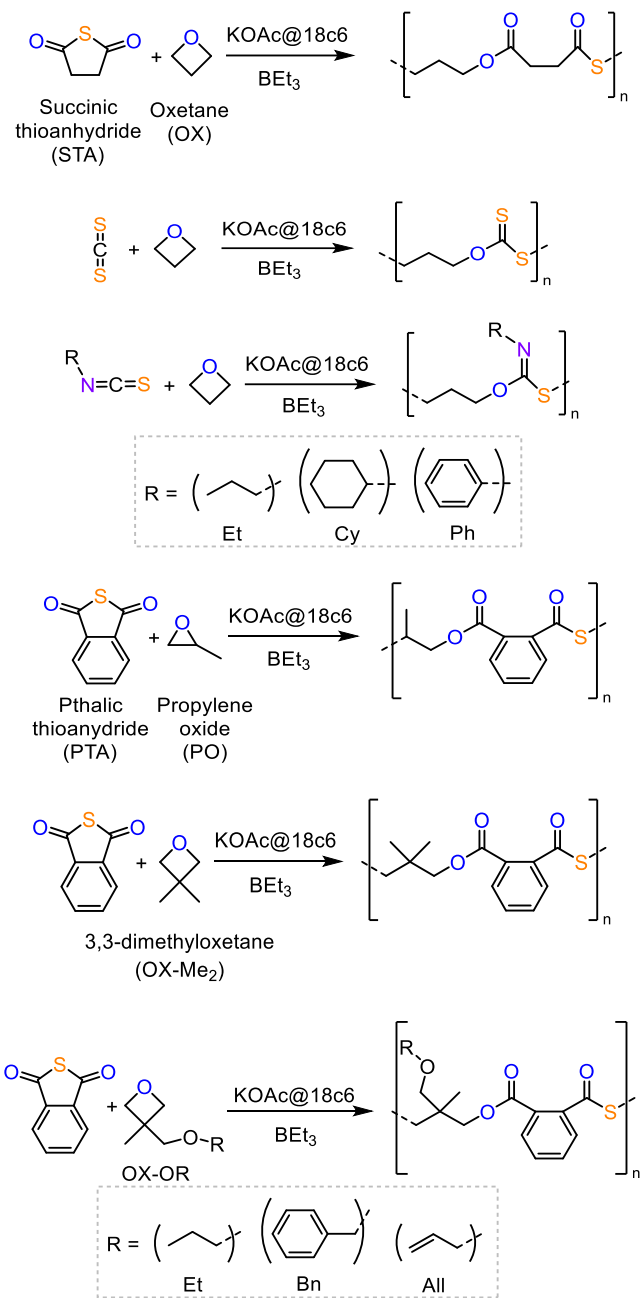
**Figure S 28:**  $^1\text{H} - ^{13}\text{C}$  HMBC NMR spectrum (500MHz,  $\text{CDCl}_3$ ) of above PTA/OX copolymer



n	Measured m/z for a	Measured m/z for b
3	748.97	780.97
4	971.01	1002.99
5	1193.02	1225.02
6	1415.04	1447.05
7	1637.10	1669.08
8	1859.13	1891.14

**Figure S 29:** MALDI-TOF spectrum of above PTA/OX copolymer. Matrix 2,5-dihydroxybenzoic acid with sodium trifluoroacetate.

### Section S3: ROCOP with different monomers



**Scheme S 1:** Schemes corresponding to table 2.

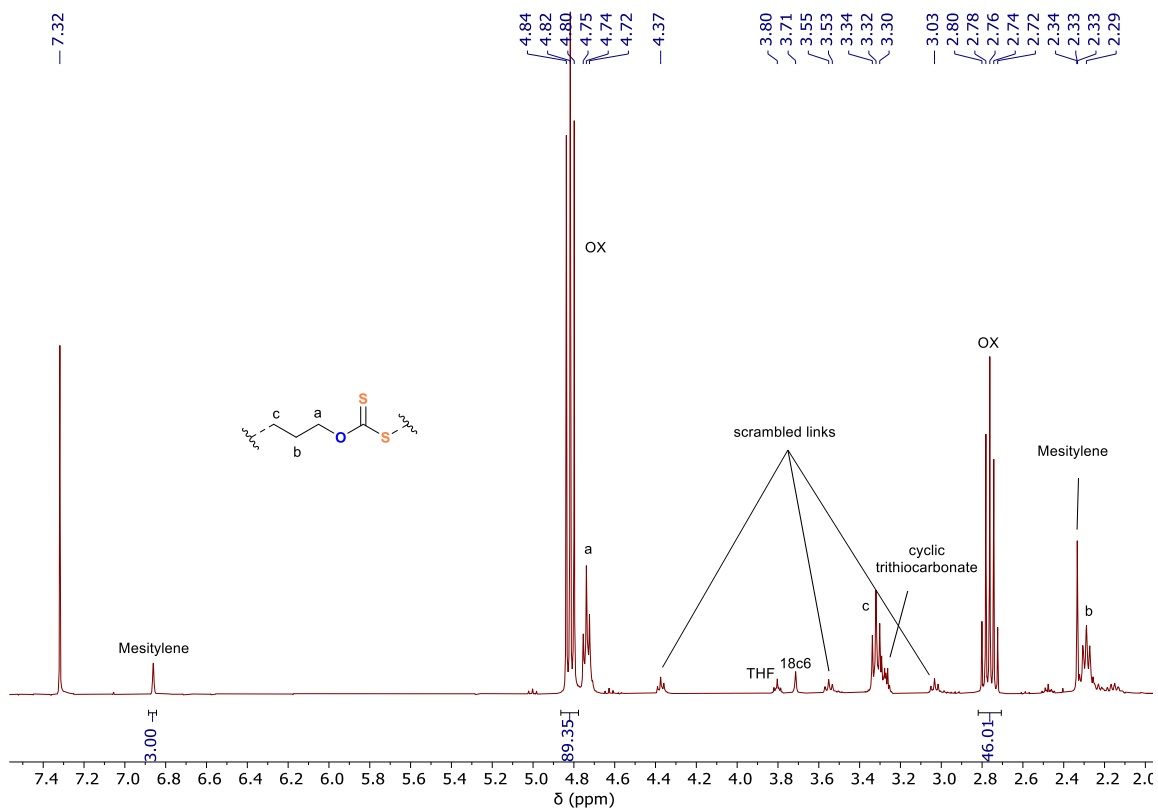


Figure S 30:  $^1\text{H}$  NMR spectrum (400MHz,  $\text{CDCl}_3$ ) of the final aliquot from  $\text{CS}_2/\text{OX}$  ROCOP (table 2, run 11).

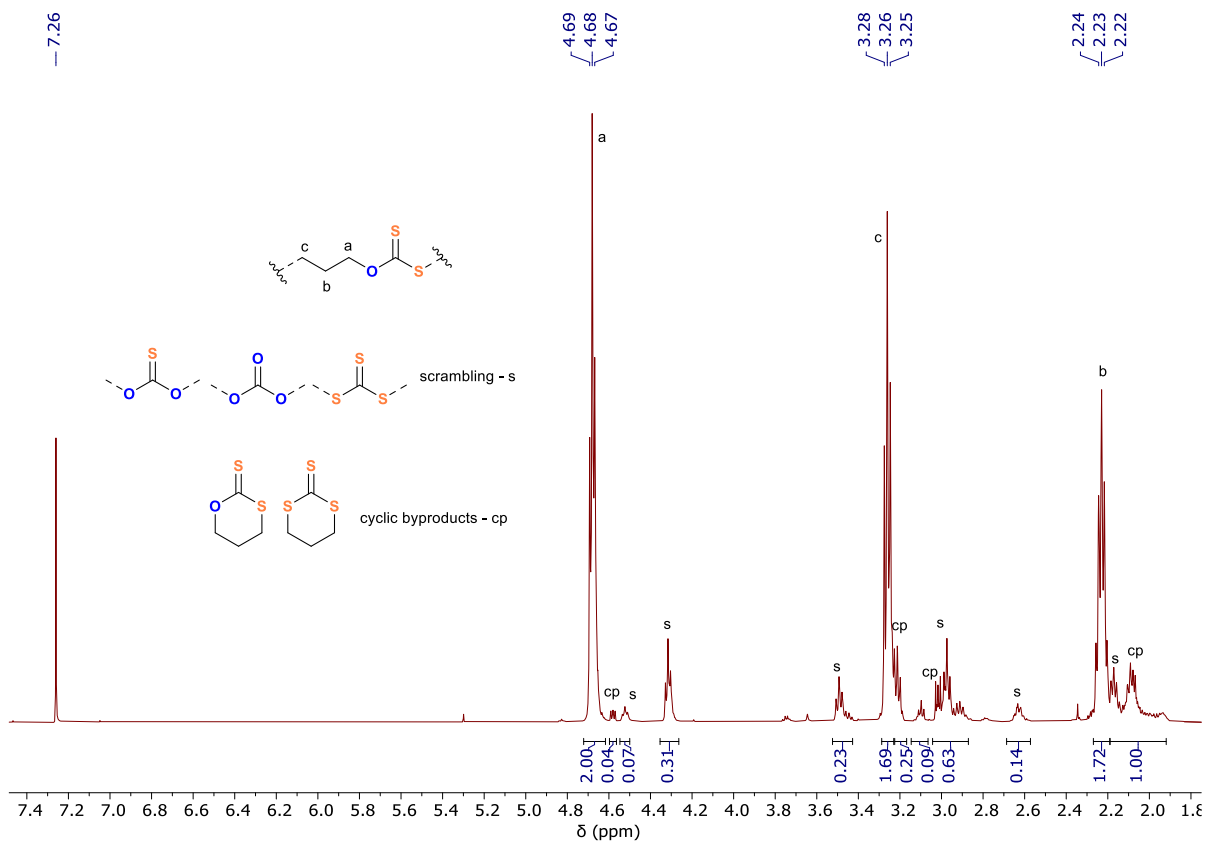
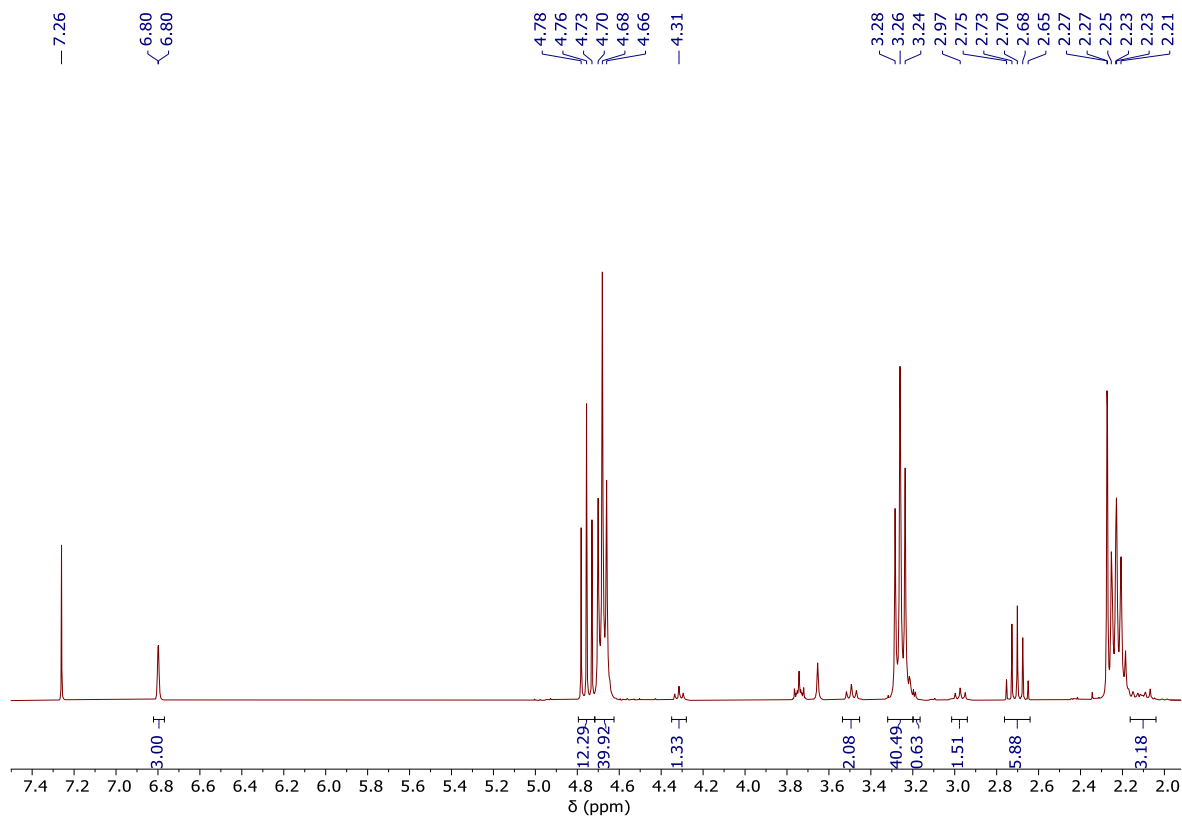
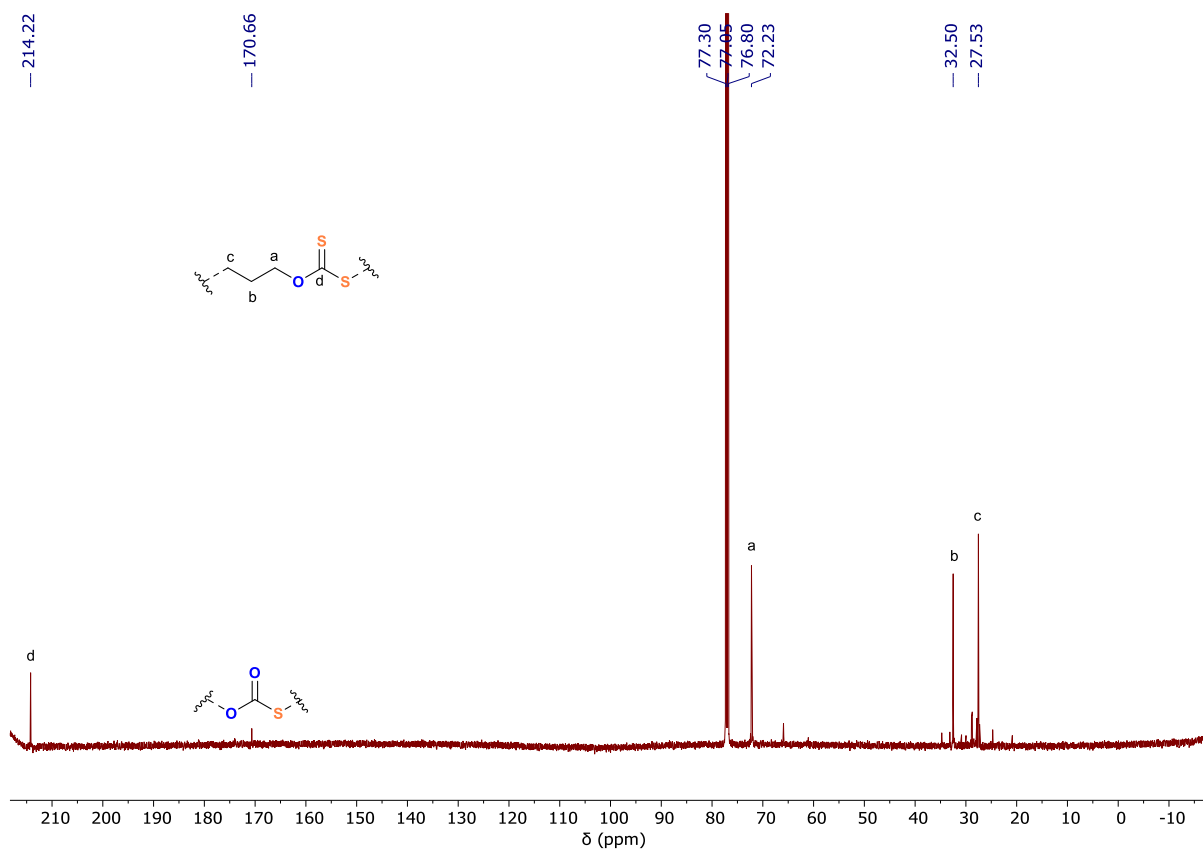


Figure S 31:  $^1\text{H}$  NMR spectrum (500MHz,  $\text{CDCl}_3$ ) of isolated  $\text{CS}_2/\text{OX}$  copolymer (table 2, run 11).



**Figure S 32:**  $^1\text{H}$  NMR spectrum (400MHz,  $\text{CDCl}_3$ ) of the final aliquot from  $\text{CS}_2/\text{OX}$  ROCOP (table 2, run 12). Peak assignments as per Fig. S 31.



**Figure S 33:**  $^{13}\text{C}$  NMR spectrum (500MHz,  $\text{CDCl}_3$ ) of isolated  $\text{CS}_2/\text{OX}$  copolymer (table 2, run 11).

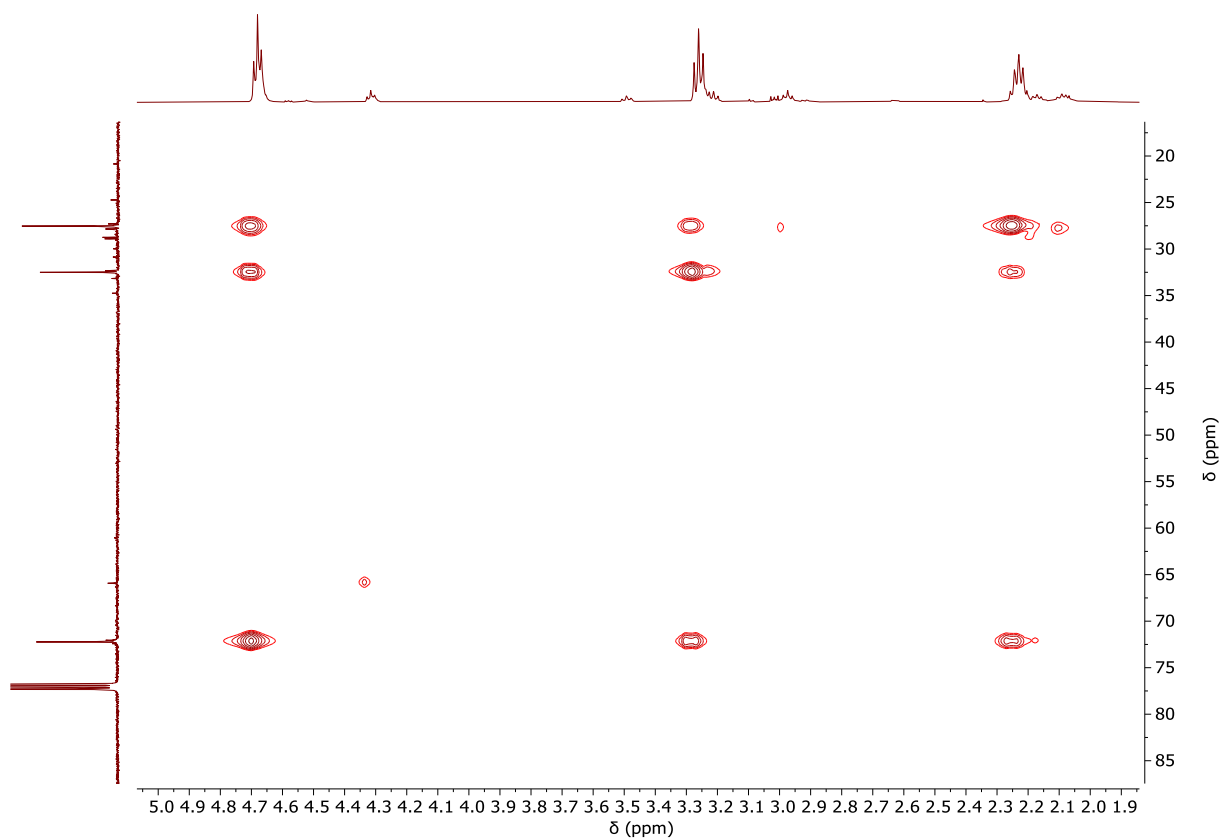


Figure S 34:  $^1\text{H}$  -  $^{13}\text{C}$  HSQC NMR spectrum (500MHz,  $\text{CDCl}_3$ ) of isolated  $\text{CS}_2/\text{OX}$  copolymer (table 2, run 11).

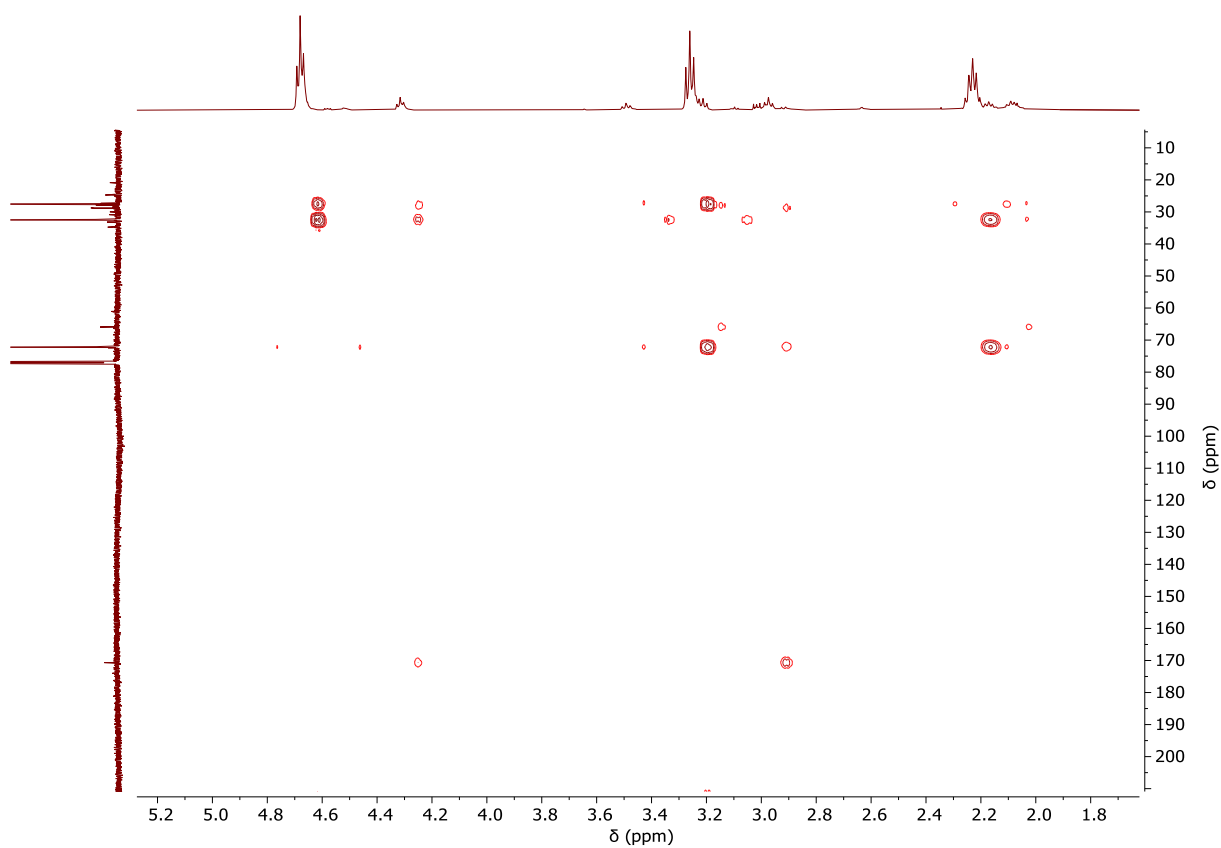


Figure S 35:  $^1\text{H}$  -  $^{13}\text{C}$  HMBC NMR spectrum (500MHz,  $\text{CDCl}_3$ ) of isolated  $\text{CS}_2/\text{OX}$  copolymer (table 2, run 11).

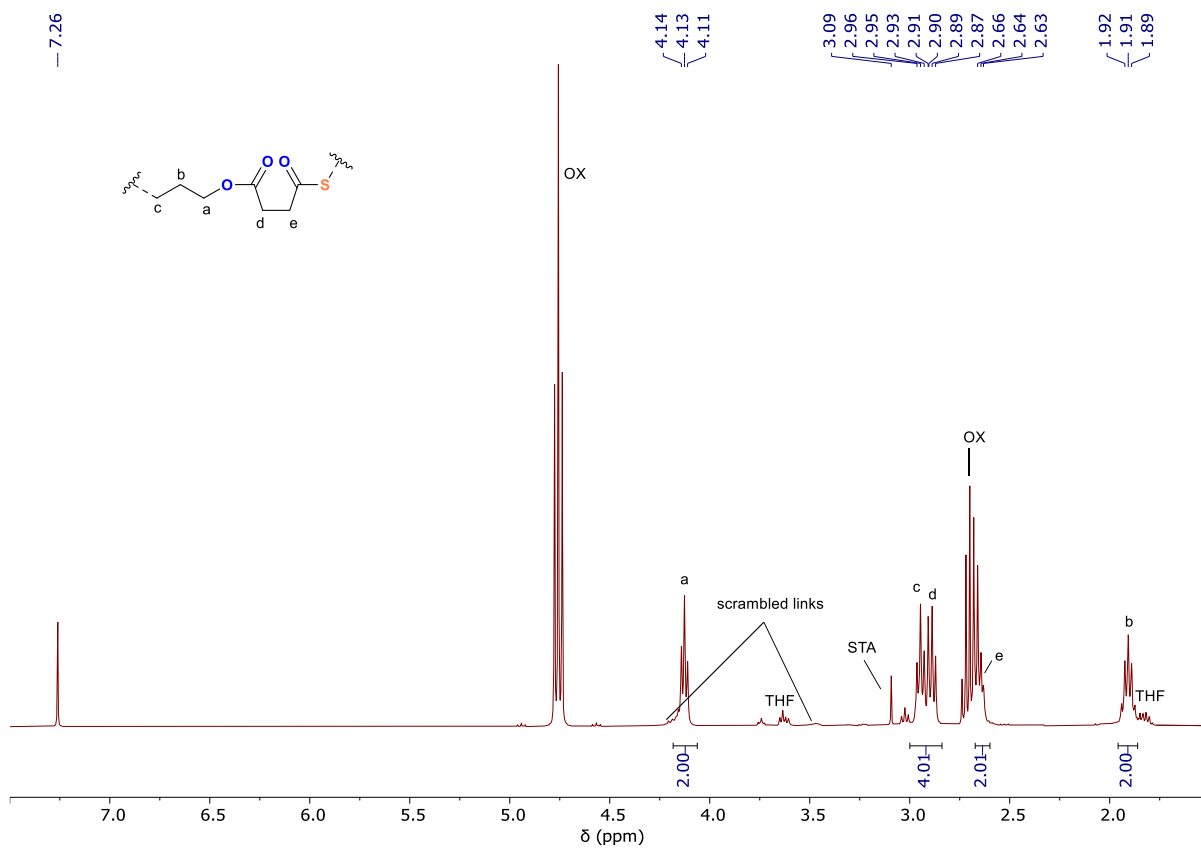


Figure S 36: <sup>1</sup>H NMR spectrum (400MHz, CDCl<sub>3</sub>) of the final aliquot from STA/OX ROCOP (table 2, run 2).

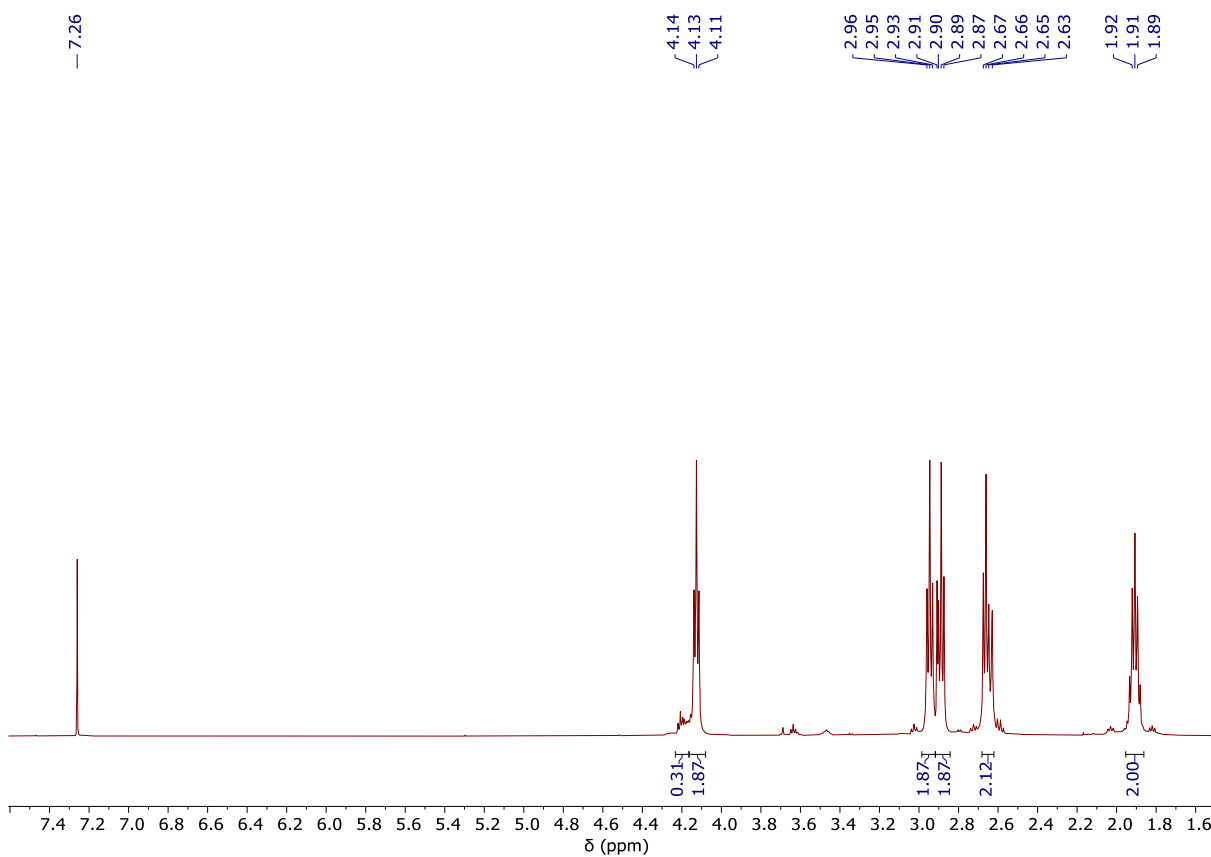


Figure S 37: <sup>1</sup>H NMR spectrum (500MHz, CDCl<sub>3</sub>) of isolated STA/OX copolymer (table 2, run 2). Peak assignments as per Fig. S 36.



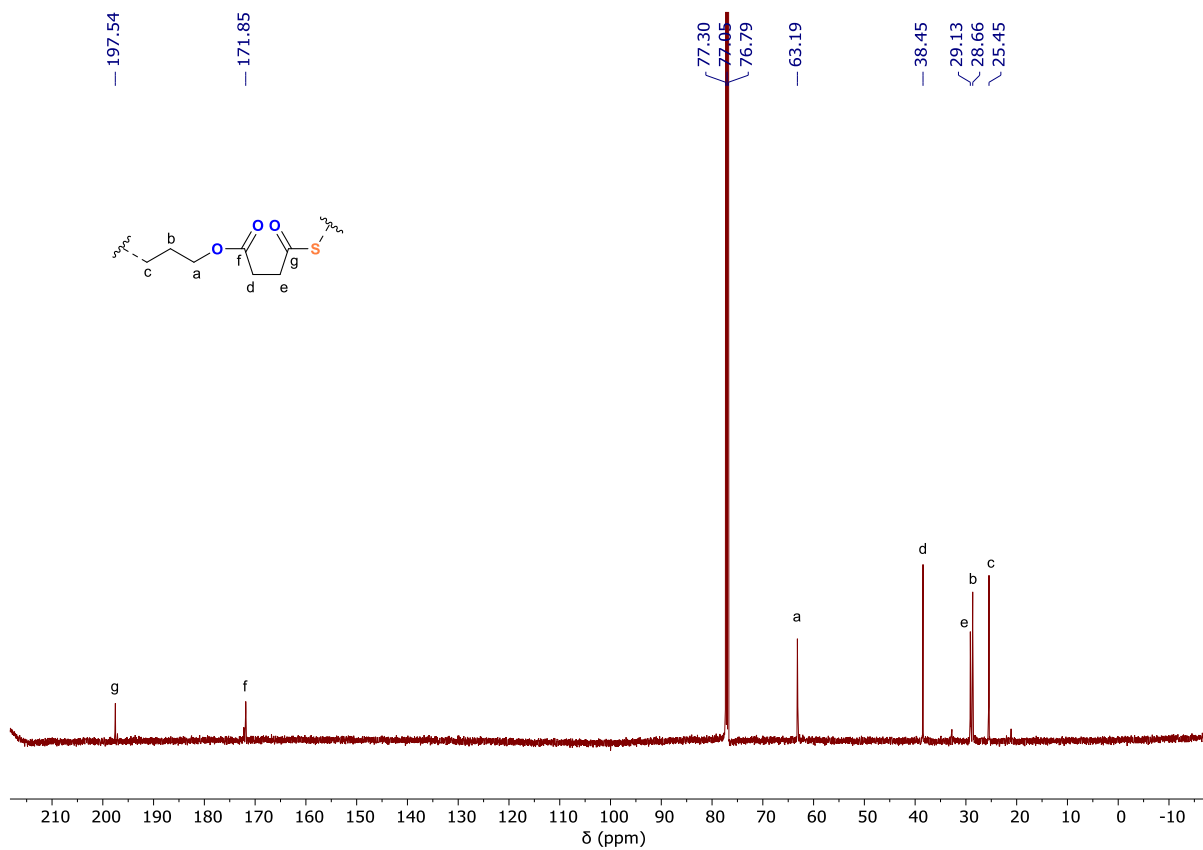


Figure S 38: <sup>13</sup>C NMR spectrum (500MHz, CDCl<sub>3</sub>) of isolated STA/OX copolymer (table 2, run 2).

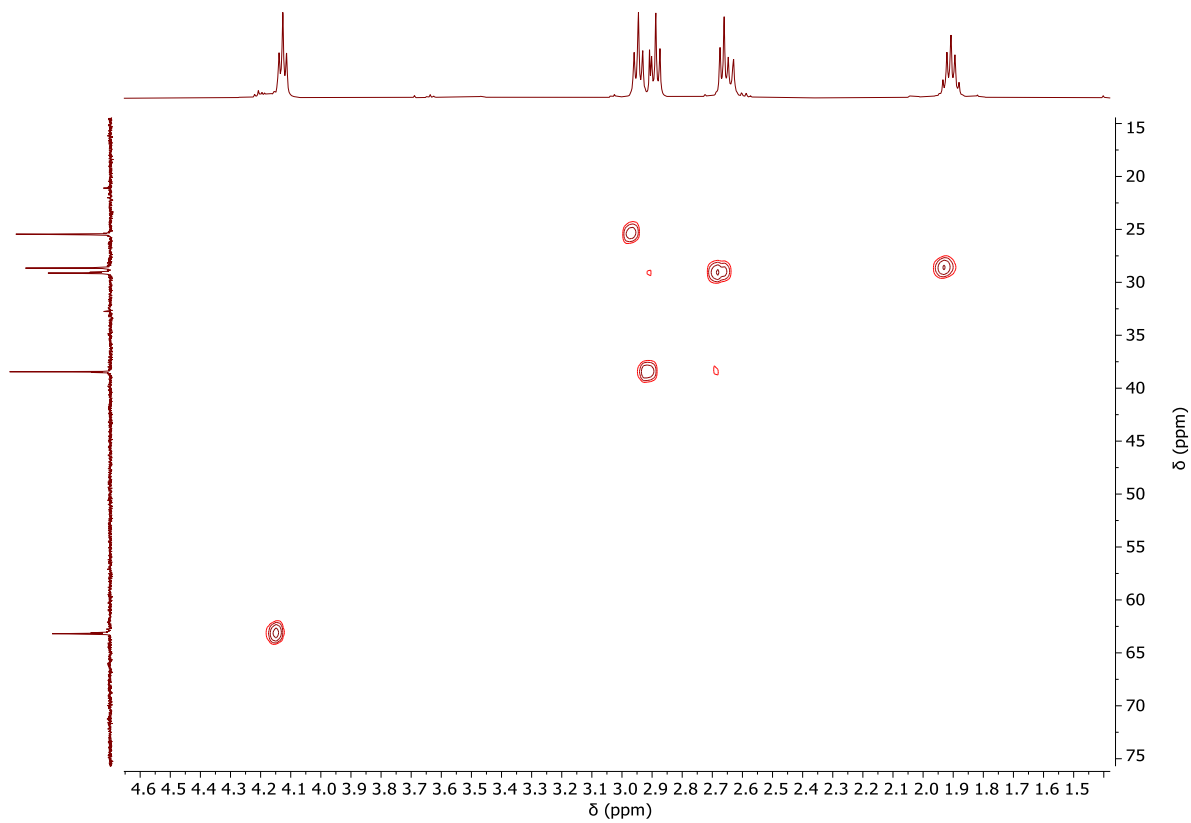


Figure S 39: <sup>1</sup>H - <sup>13</sup>C HSQC NMR spectrum (500MHz, CDCl<sub>3</sub>) of isolated STA/OX copolymer (table 2, run 2).

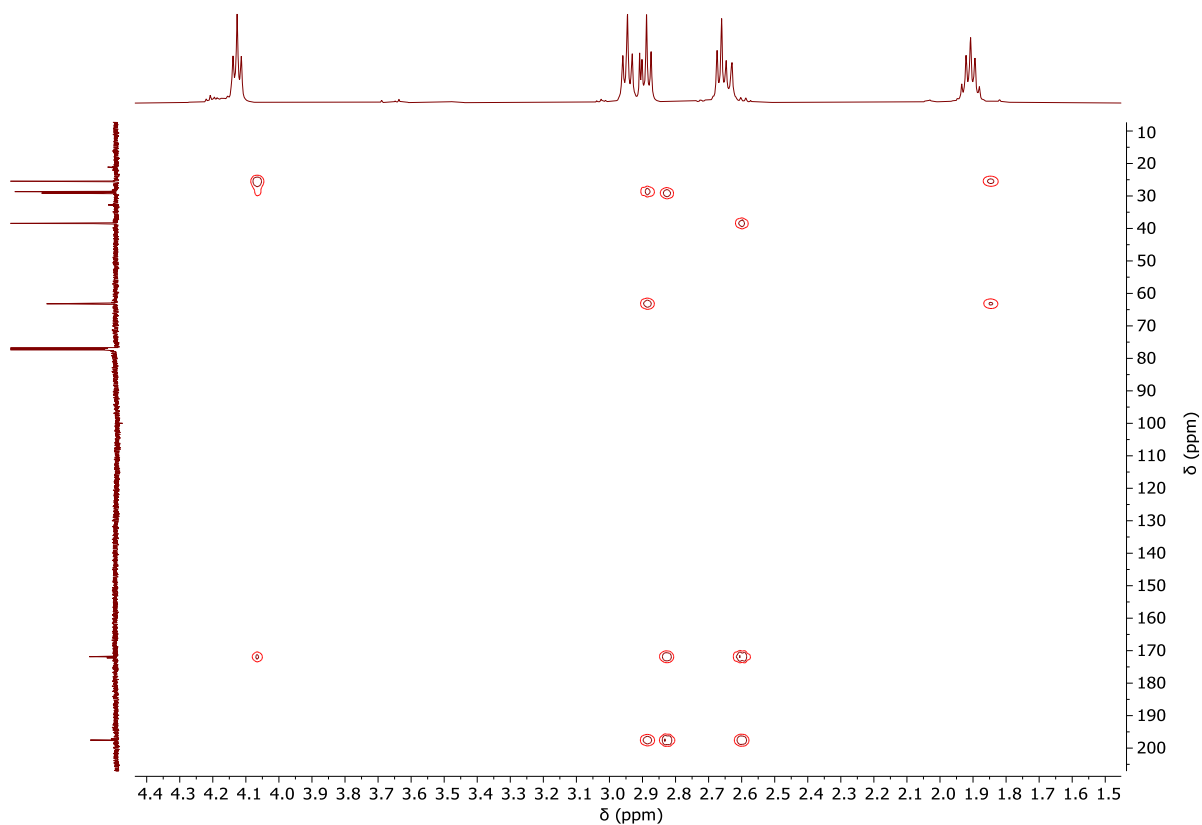


Figure S 40:  $^1\text{H}$  -  $^{13}\text{C}$  HMBC NMR spectrum (500MHz,  $\text{CDCl}_3$ ) of isolated STA/OX copolymer (table 2, run 2).

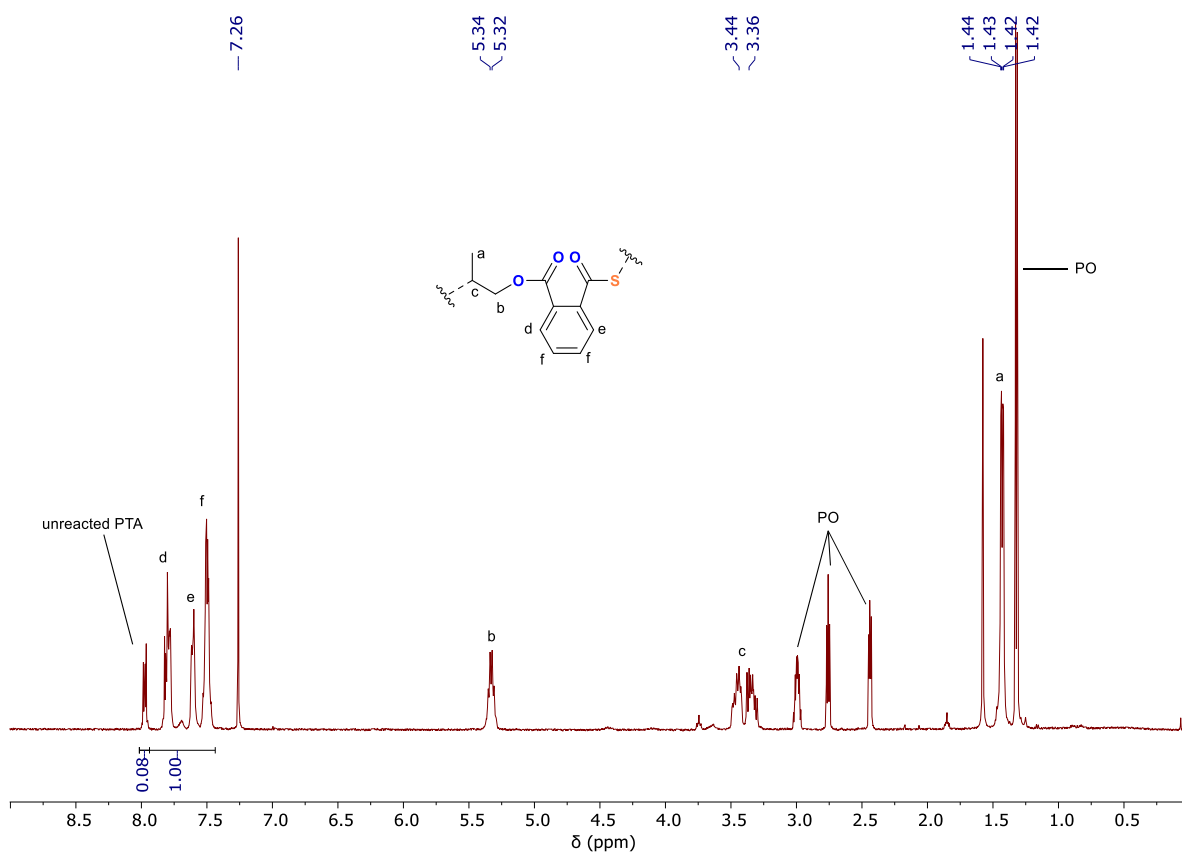
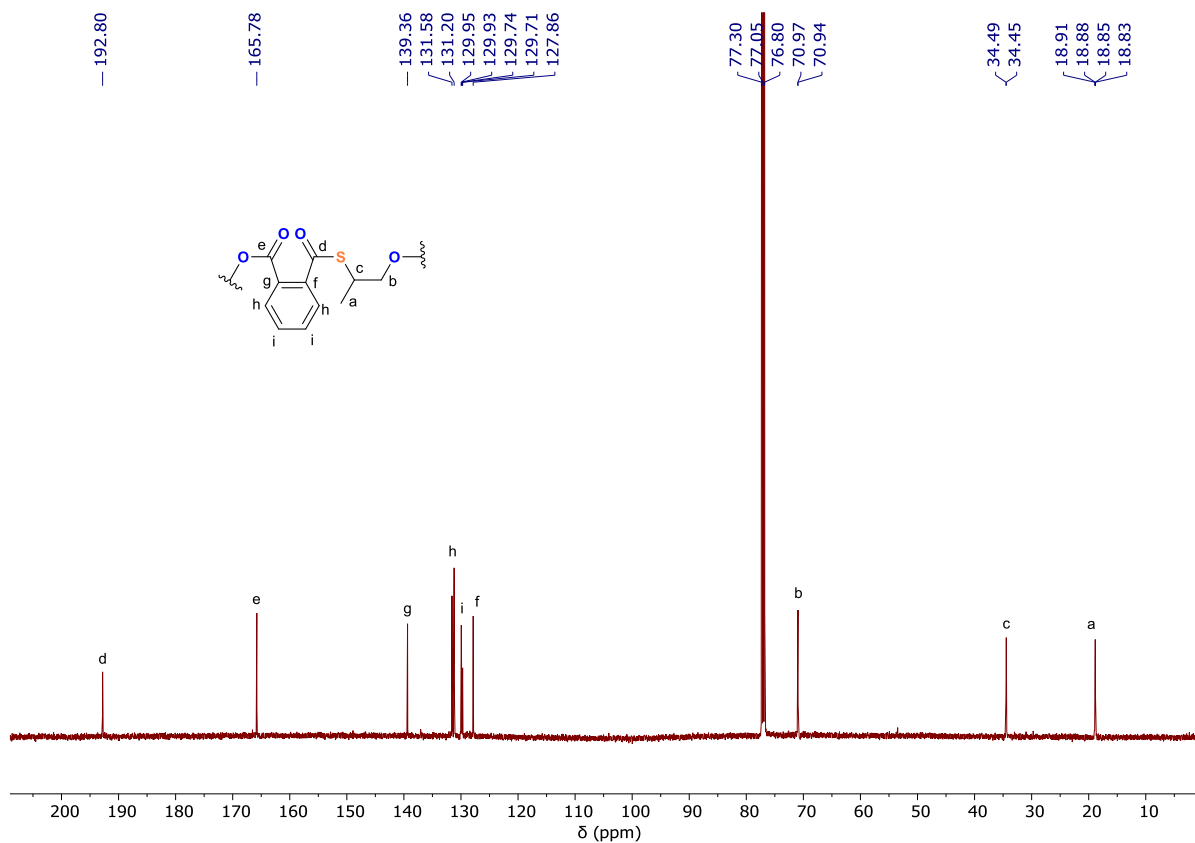
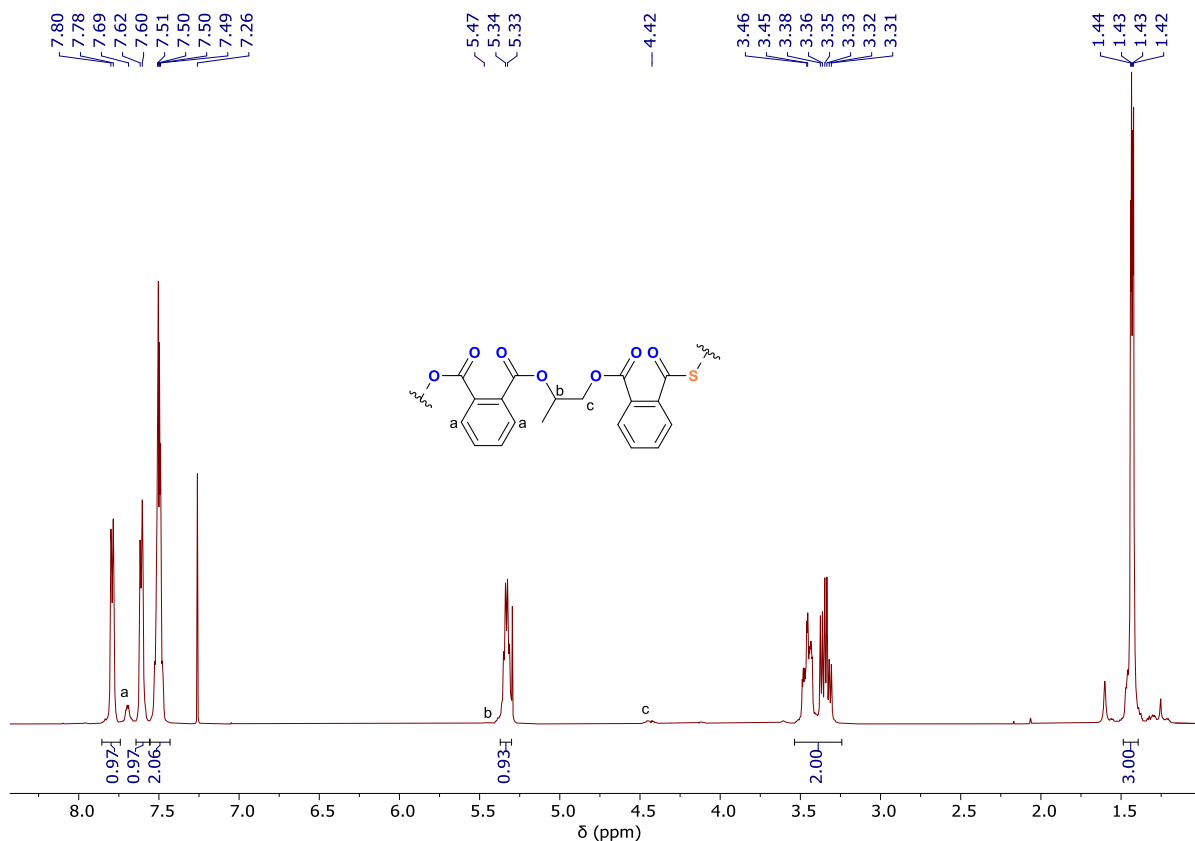


Figure S 41:  $^1\text{H}$  NMR spectrum (400MHz,  $\text{CDCl}_3$ ) of the final aliquot from PTA/PO ROCOP (table 2, run 7).



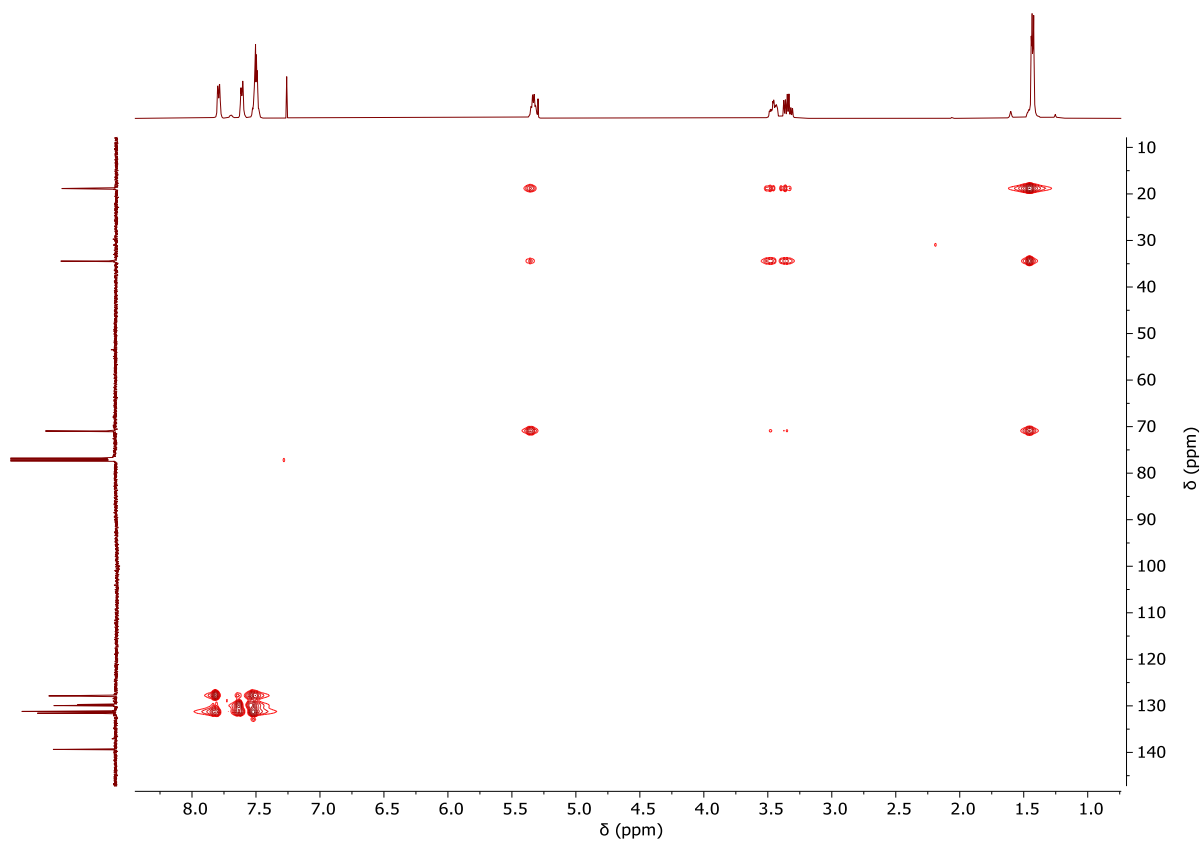


Figure S 44:  $^1\text{H}$  -  $^{13}\text{C}$  HSQC NMR spectrum (500MHz,  $\text{CDCl}_3$ ) of isolated PTA/PO copolymer (table 2, run 7).

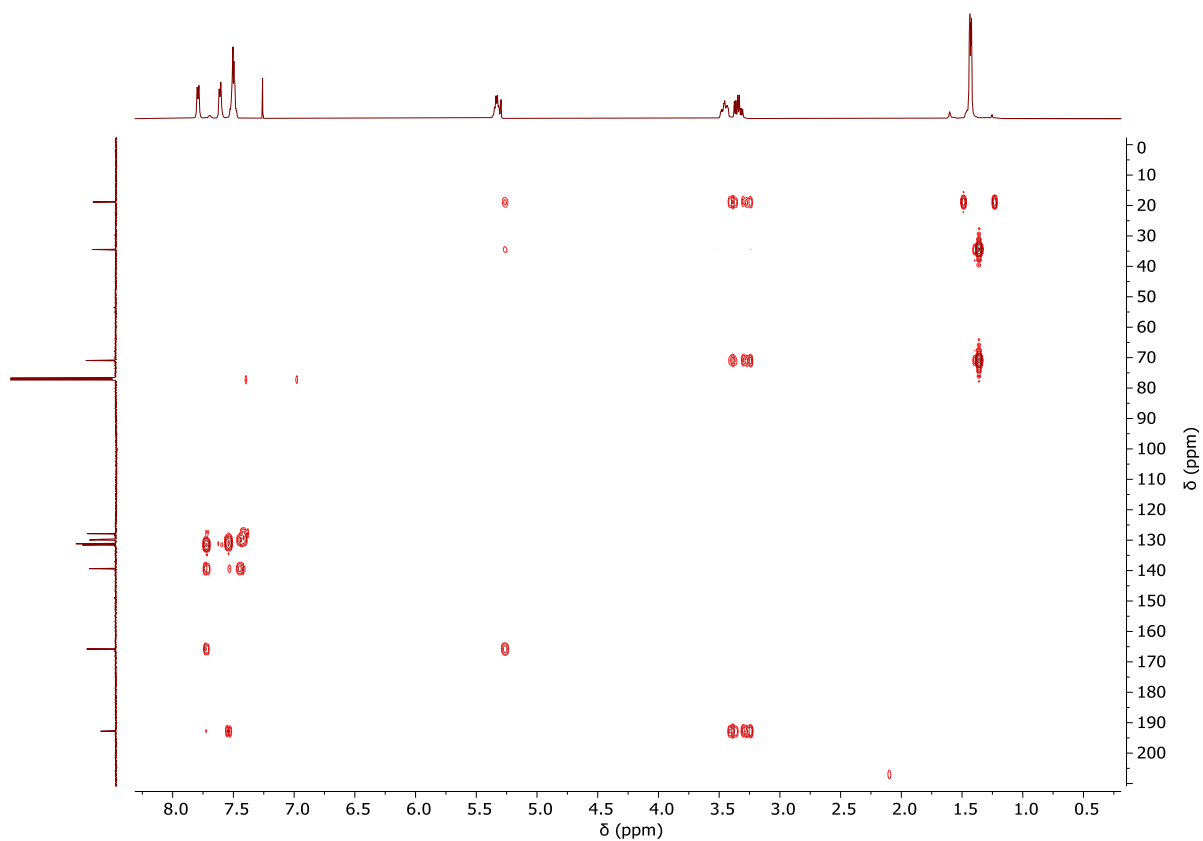


Figure S 45:  $^1\text{H}$  -  $^{13}\text{C}$  HMBC NMR spectrum (500MHz,  $\text{CDCl}_3$ ) of isolated PTA/PO copolymer (table 2, run 7).

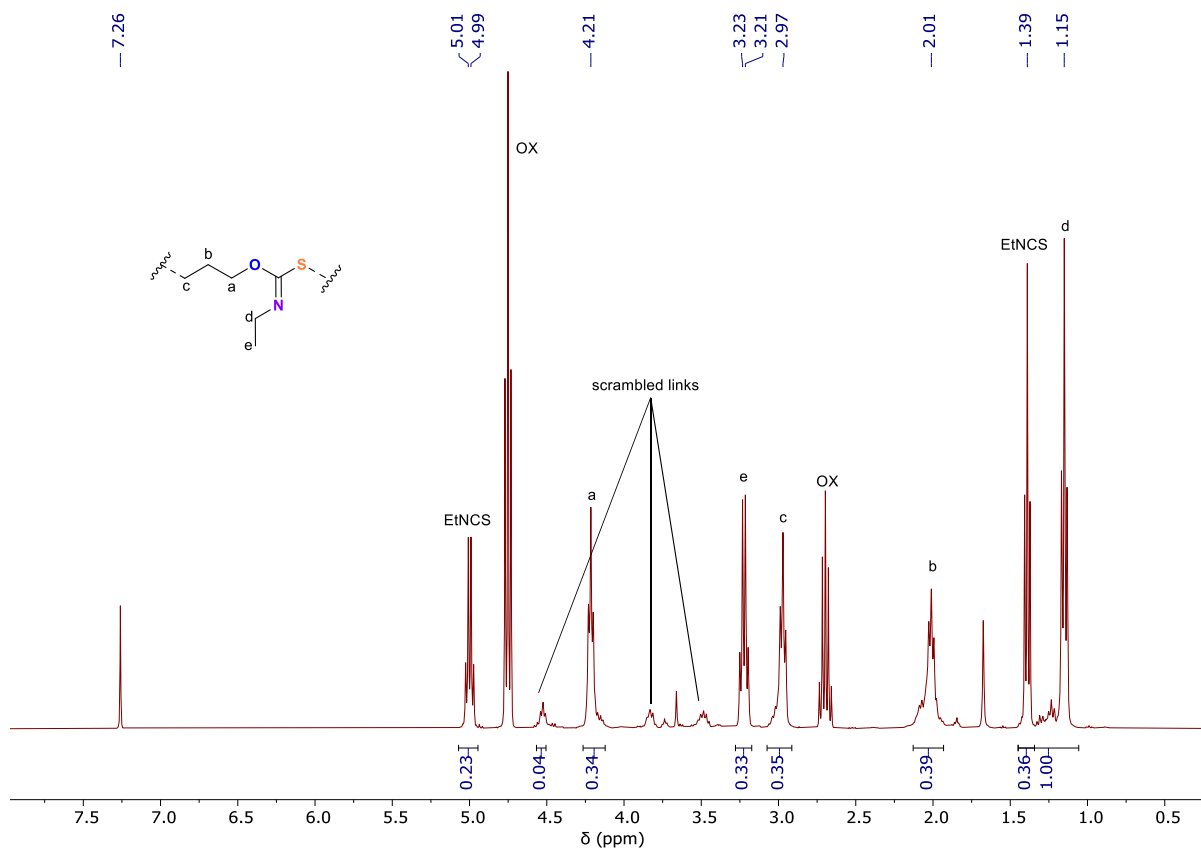


Figure S 46: <sup>1</sup>H NMR spectrum (400MHz, CDCl<sub>3</sub>) of the final aliquot from EtNCS/OX ROCOP (table 2, run 10).

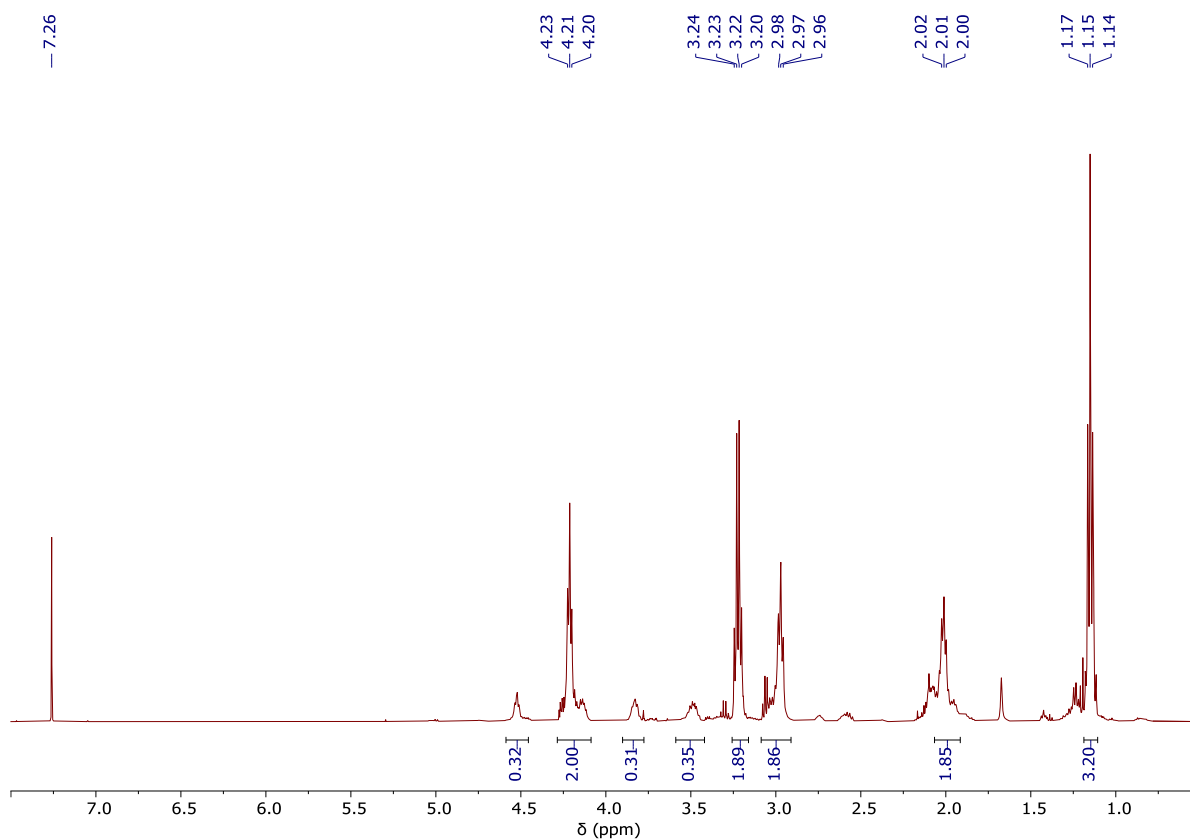


Figure S 47: <sup>1</sup>H NMR spectrum (500MHz, CDCl<sub>3</sub>) of isolated EtNCS/OX copolymer (table 2, run 10). Peak assignments as per Fig. S 46.

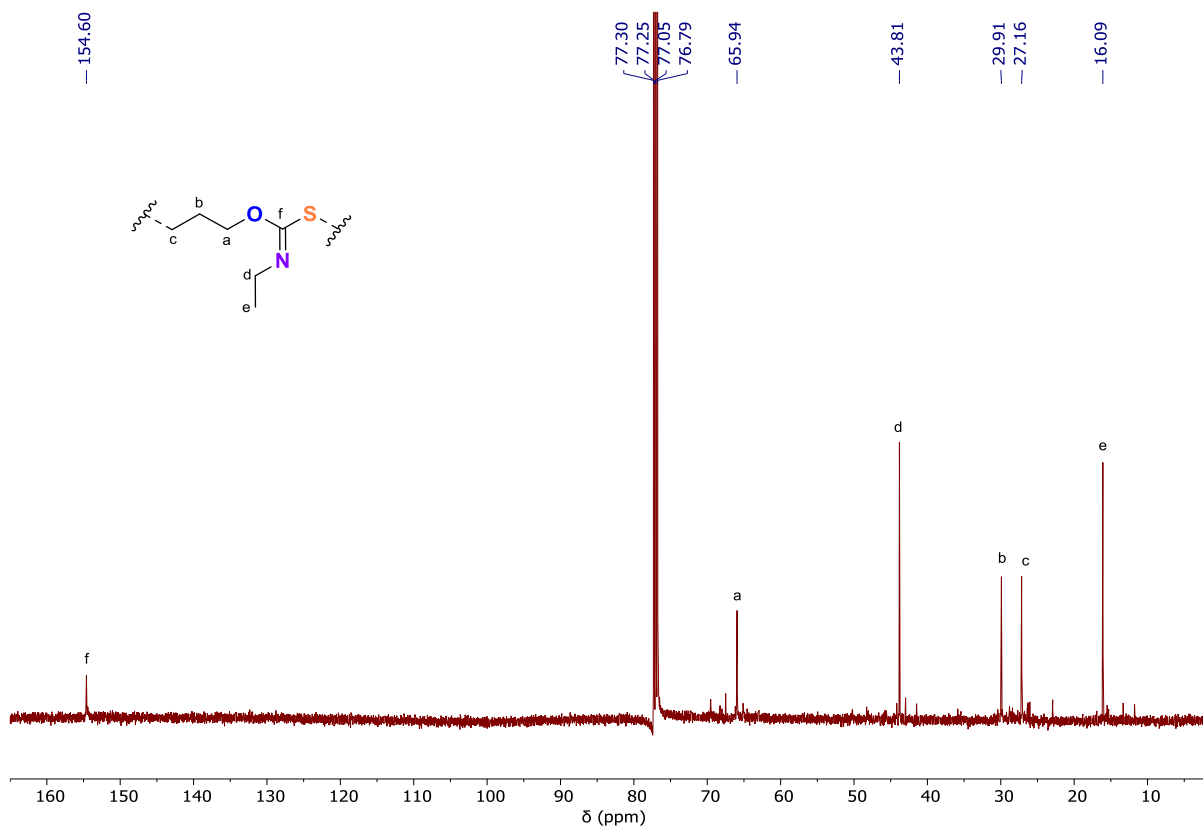


Figure S 48: <sup>13</sup>C NMR spectrum (500MHz, CDCl<sub>3</sub>) of isolated EtNCS/OX copolymer (table 2, run 10).

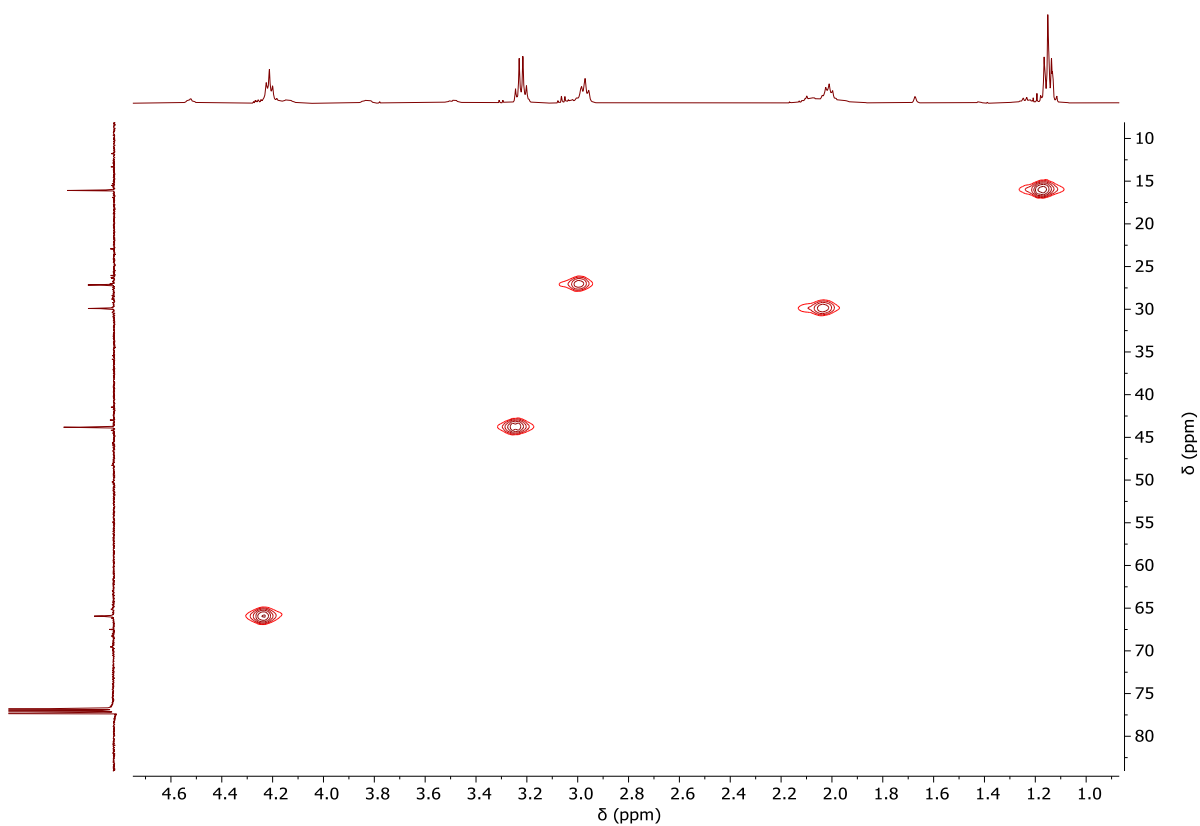


Figure S 49: <sup>1</sup>H - <sup>13</sup>C HSQC NMR spectrum (500MHz, CDCl<sub>3</sub>) of isolated EtNCS/OX copolymer (table 2, run 10).

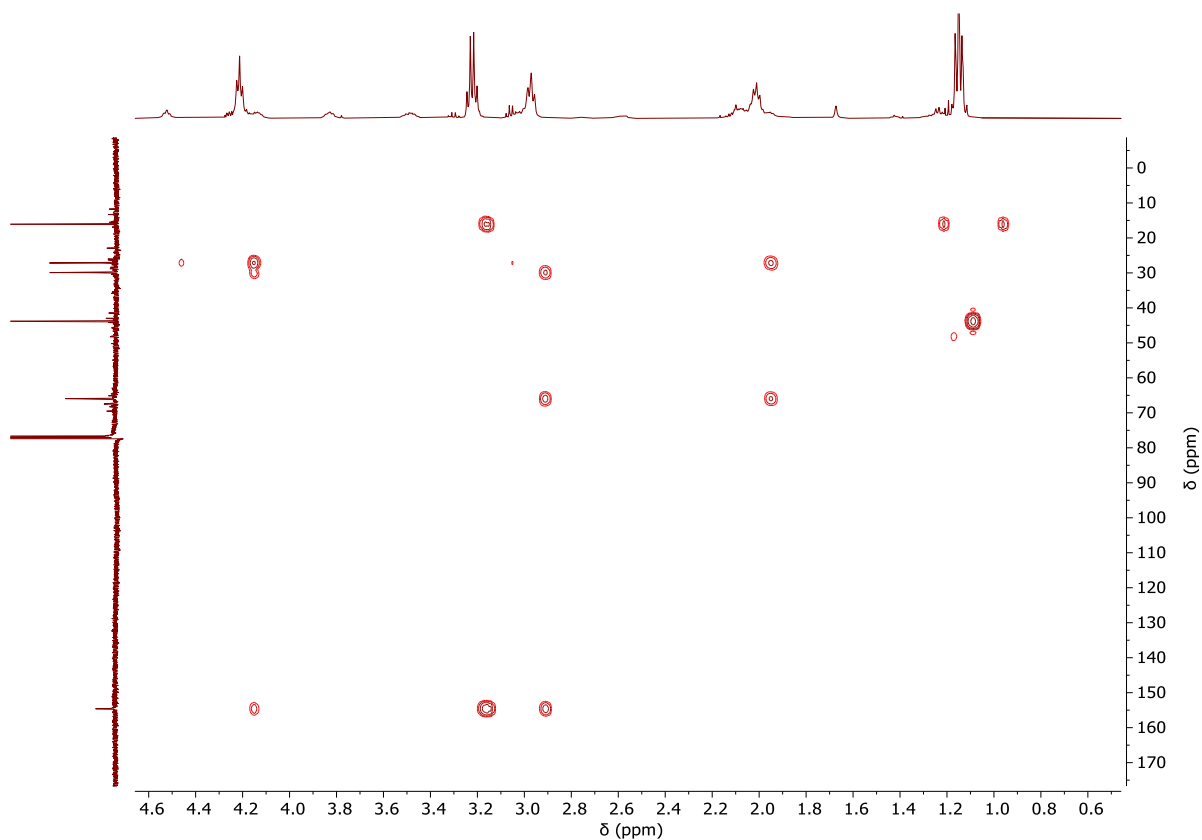


Figure S 50:  $^1\text{H} - ^{13}\text{C}$  HMBC NMR spectrum (500MHz,  $\text{CDCl}_3$ ) of isolated EtNCS/OX copolymer (table 2, run 10).

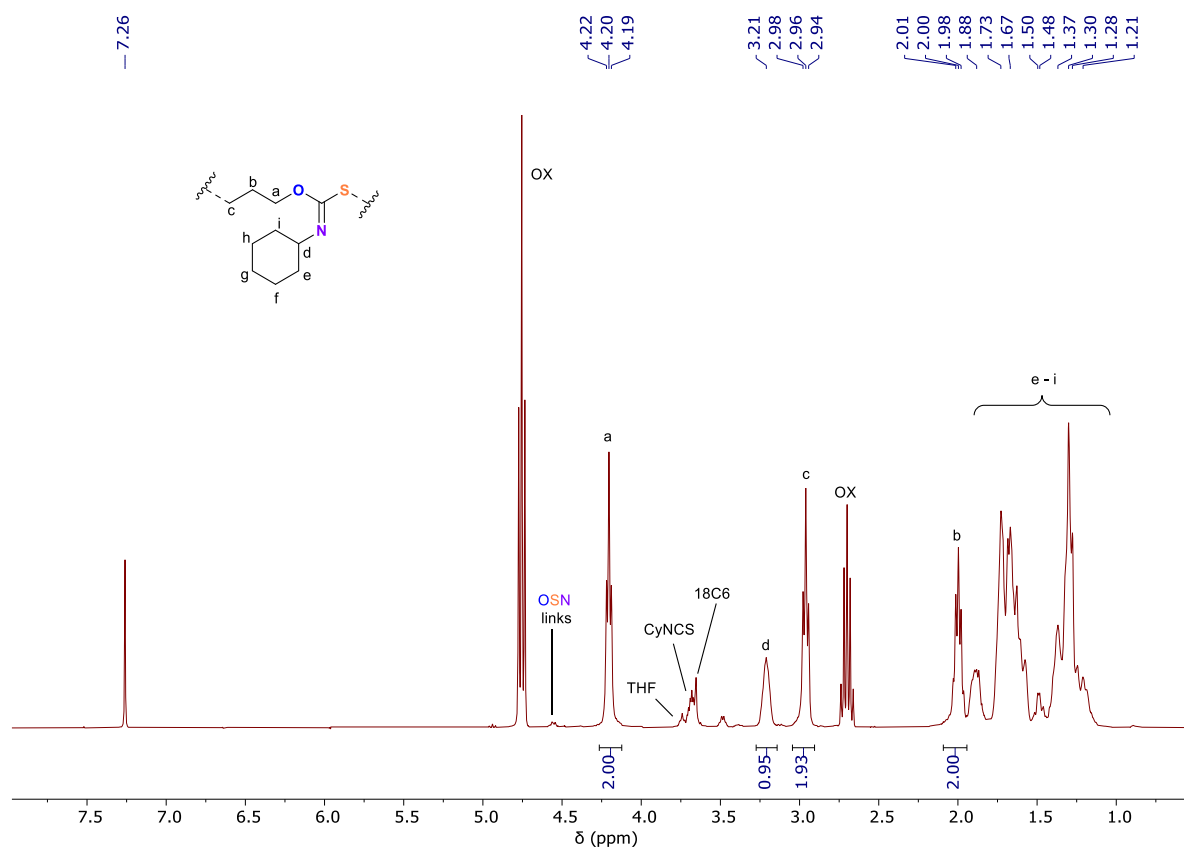
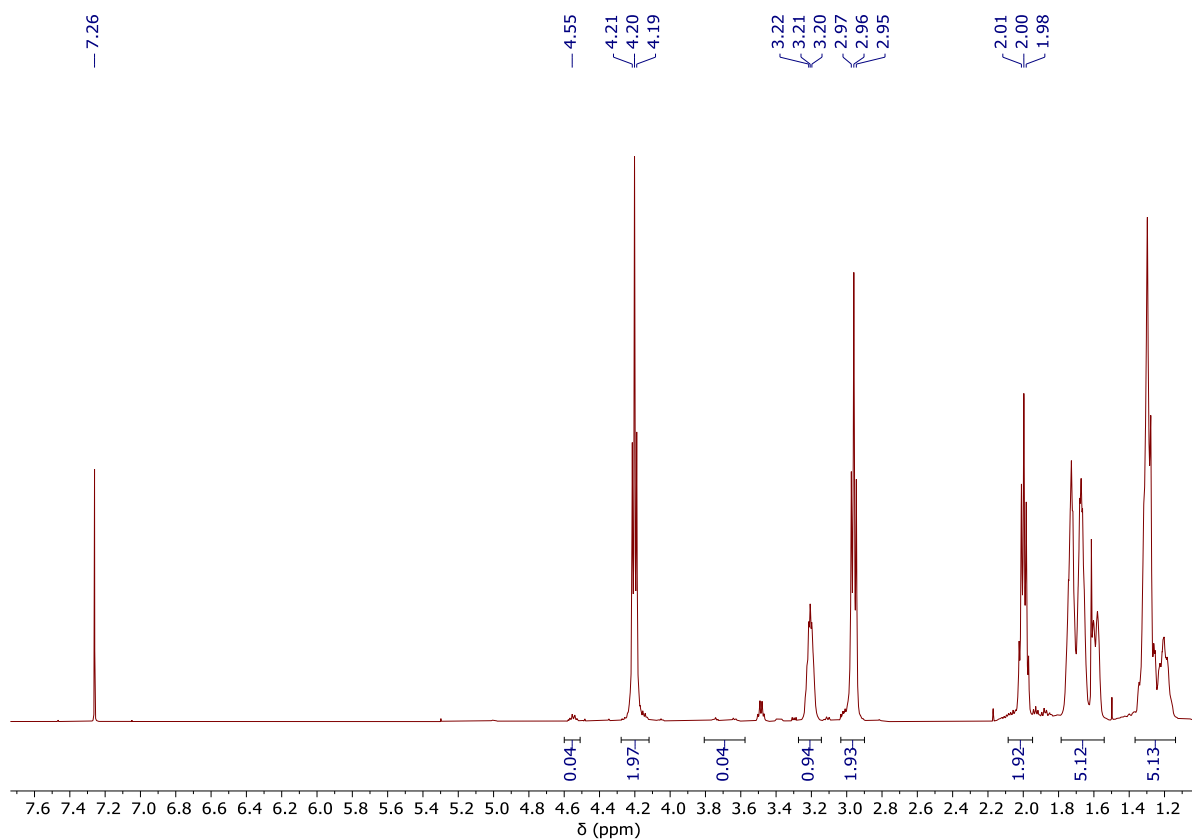
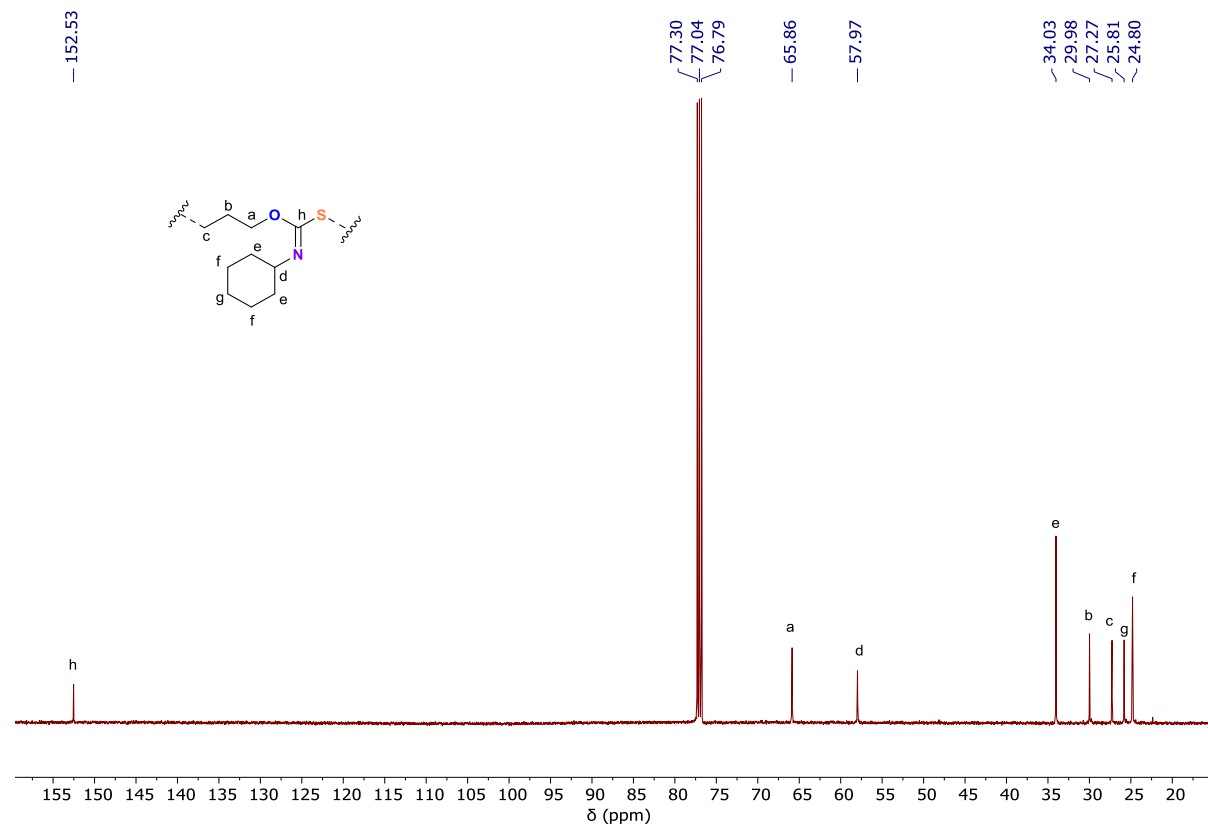


Figure S 51:  $^1\text{H}$  NMR spectrum (400MHz,  $\text{CDCl}_3$ ) of the final aliquot from CyNCS/OX ROCOP (table 2, run 9).



**Figure S 52:**  $^1\text{H}$  NMR spectrum (500MHz,  $\text{CDCl}_3$ ) of isolated CyNCS/OX copolymer (table 2, run 9). Peak assignments as per Fig. S 51.



**Figure S 53:**  $^{13}\text{C}$  NMR spectrum (500MHz,  $\text{CDCl}_3$ ) of isolated CyNCS/OX copolymer (table 2, run 9).



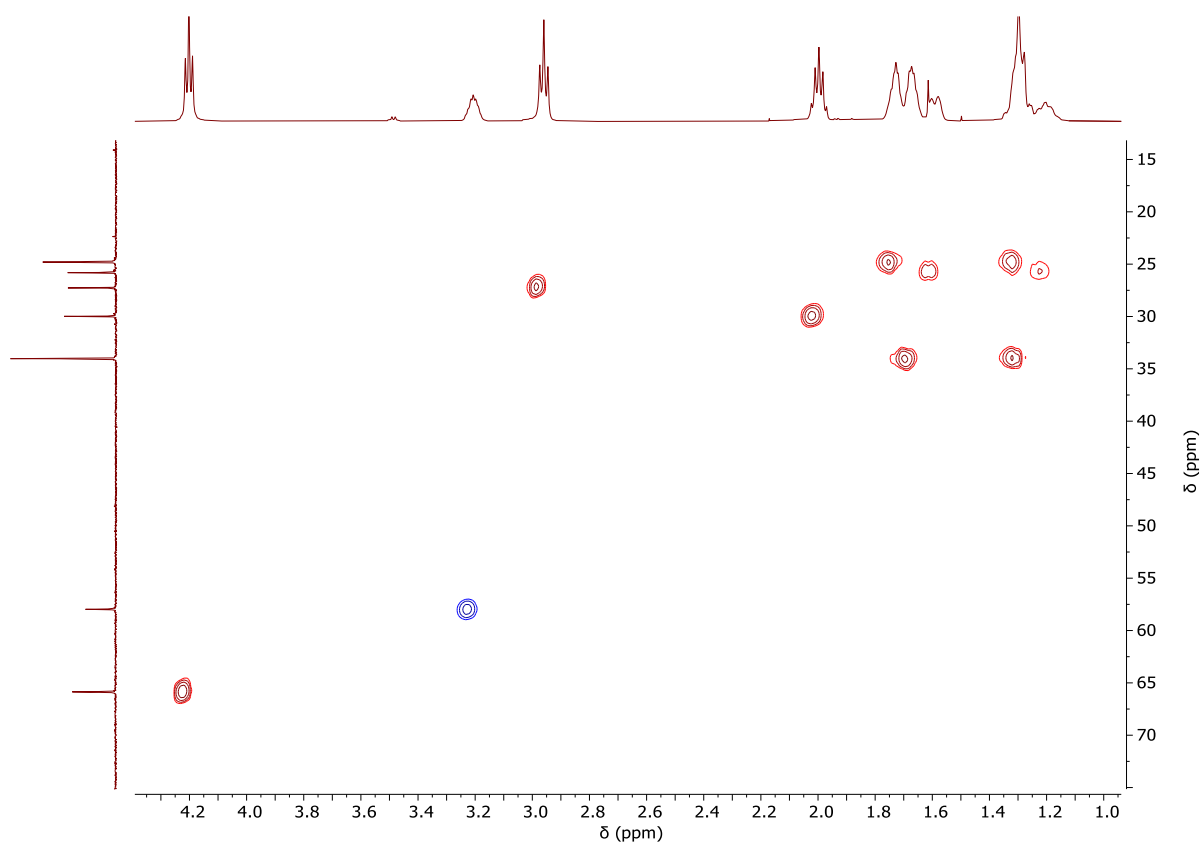


**Figure S 54:**  $^1\text{H}$  -  $^{13}\text{C}$  HSQC NMR spectrum (500MHz,  $\text{CDCl}_3$ ) of isolated CyNCS/OX copolymer (table 2, run 9).

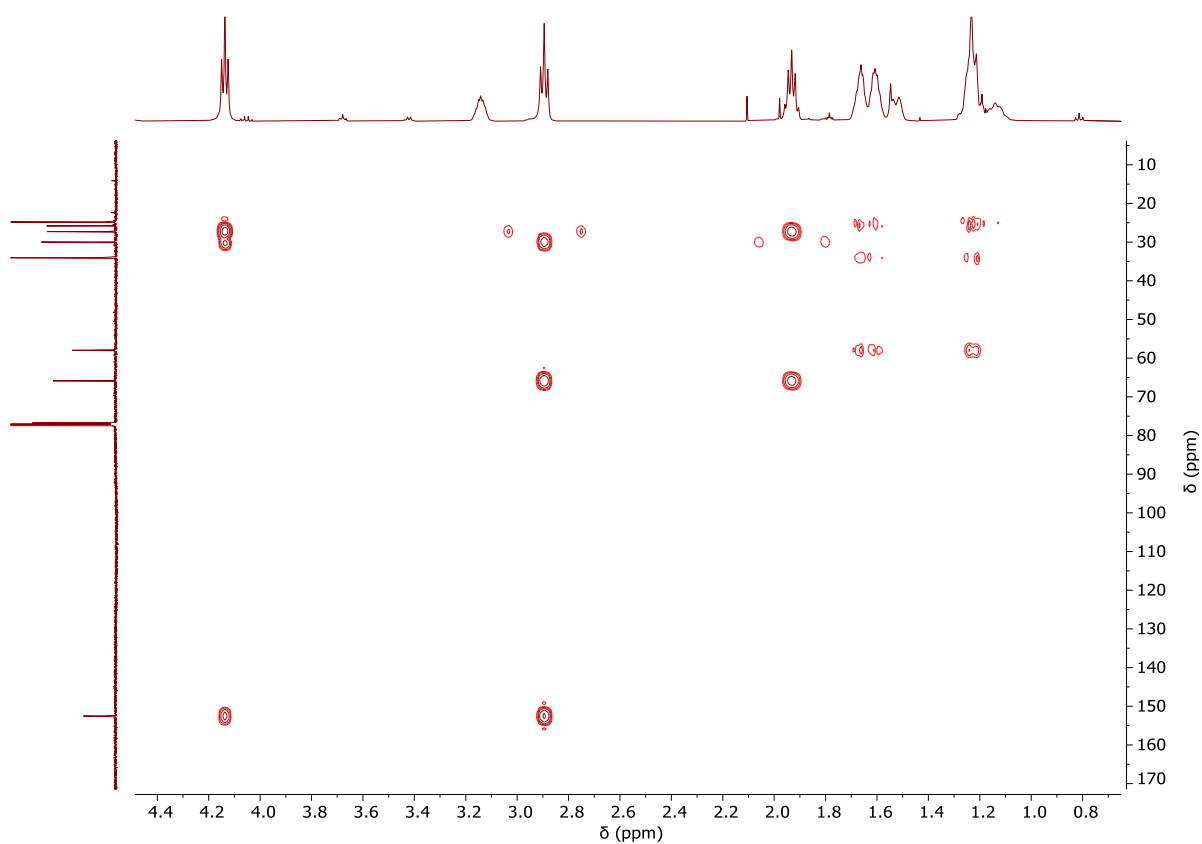


**Figure S 55:**  $^1\text{H}$  -  $^{13}\text{C}$  HMBC NMR spectrum (500MHz,  $\text{CDCl}_3$ ) of isolated CyNCS/OX copolymer (table 2, run 9).

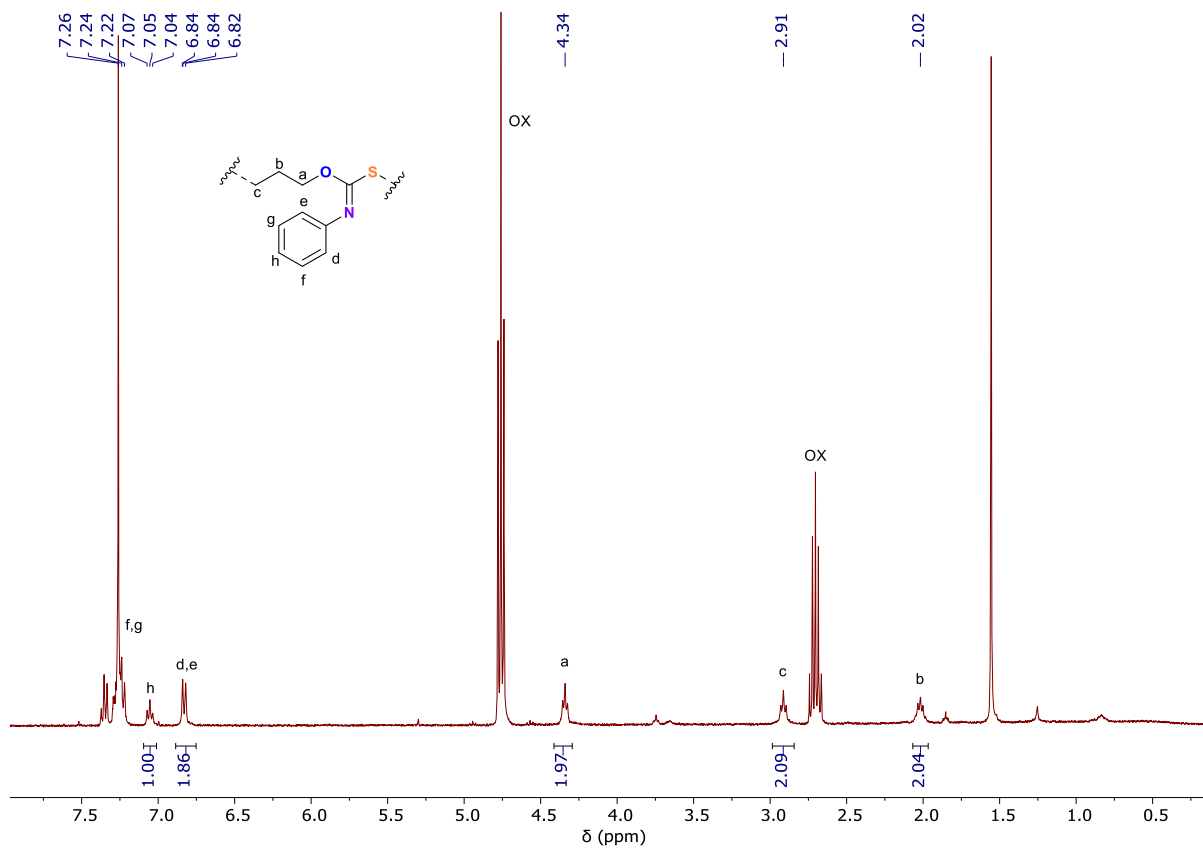


**Figure S 56:** <sup>1</sup>H NMR spectrum (400MHz, CDCl<sub>3</sub>) the final aliquot from PhNCS/OX ROCOP (table 2, run 8).

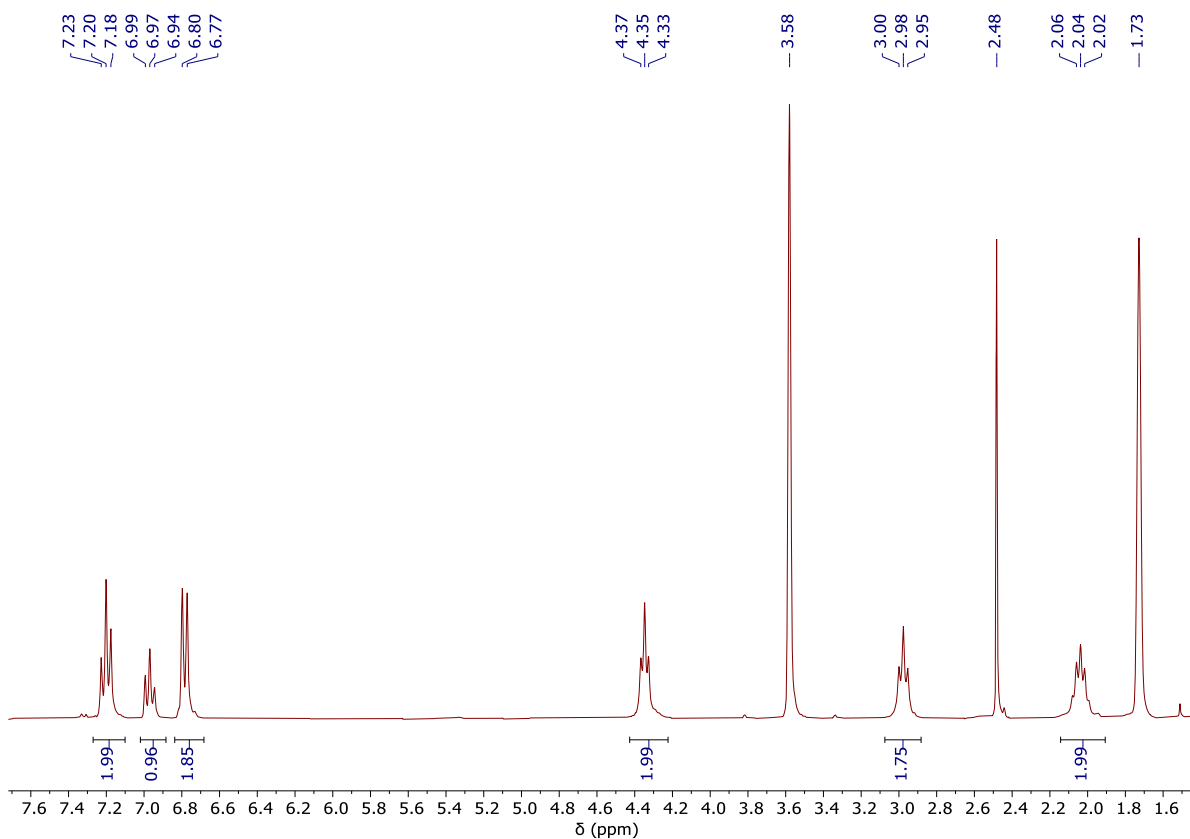


**Figure S 57:** <sup>1</sup>H NMR spectrum (300MHz, C<sub>4</sub>D<sub>8</sub>O) of isolated PhNCS/OX copolymer (table 2, run 8). Peak assignments as per Fig. S 56. <sup>13</sup>C and 2D NMR spectra unavailable due to insolubility.

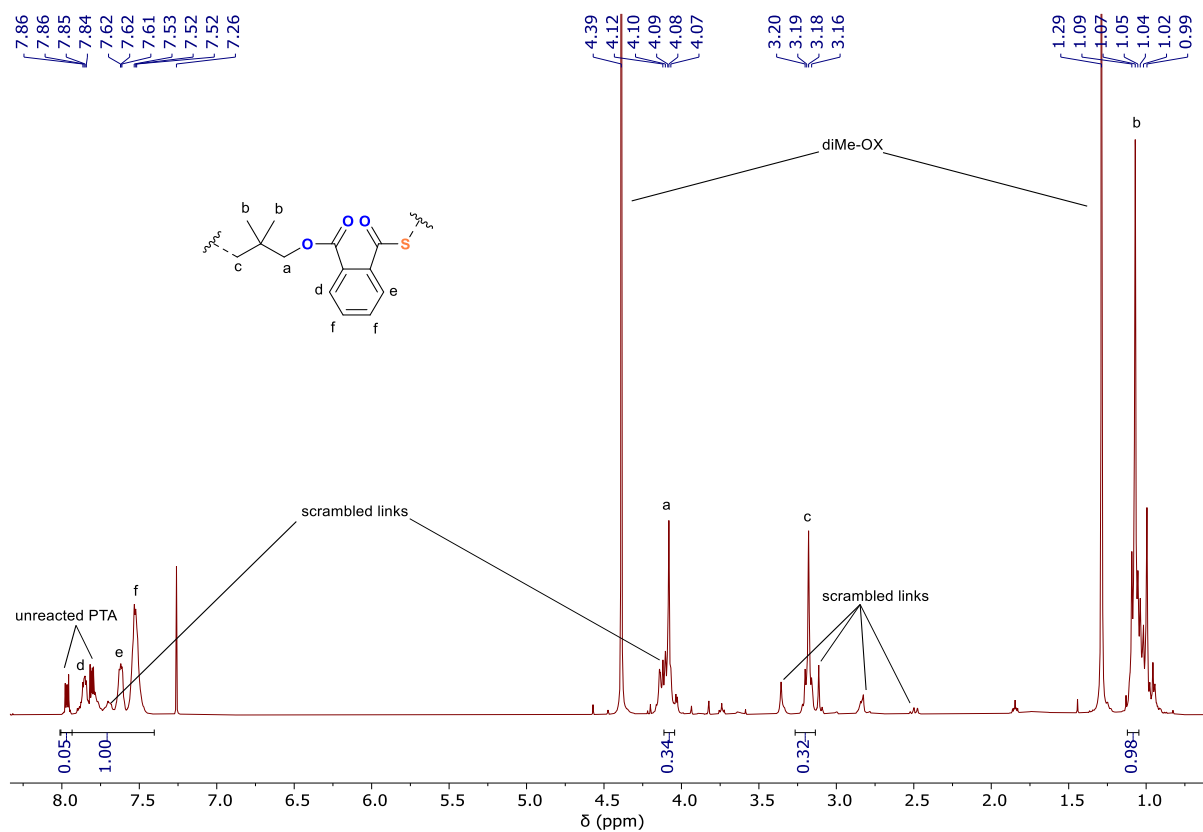


**Figure S 58:**  $^1\text{H}$  NMR spectrum (400MHz,  $\text{CDCl}_3$ ) of the final aliquot from PTA/ OX- $\text{Me}_2$  ROCOP (table 2, run 3).

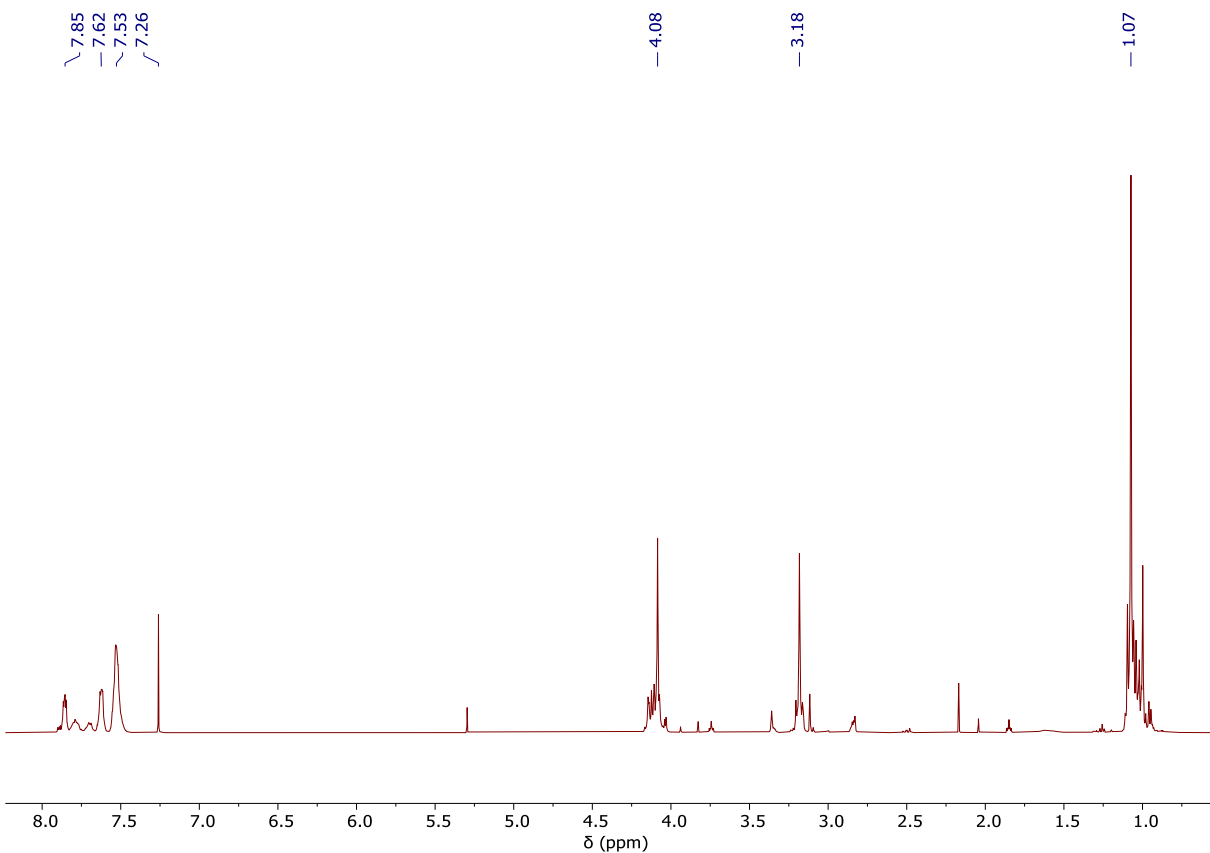


**Figure S 59:**  $^1\text{H}$  NMR spectrum (500MHz,  $\text{CDCl}_3$ ) of isolated PTA/ OX- $\text{Me}_2$  copolymer (table 2, run 3). Peak assignments as per Fig. S 58.

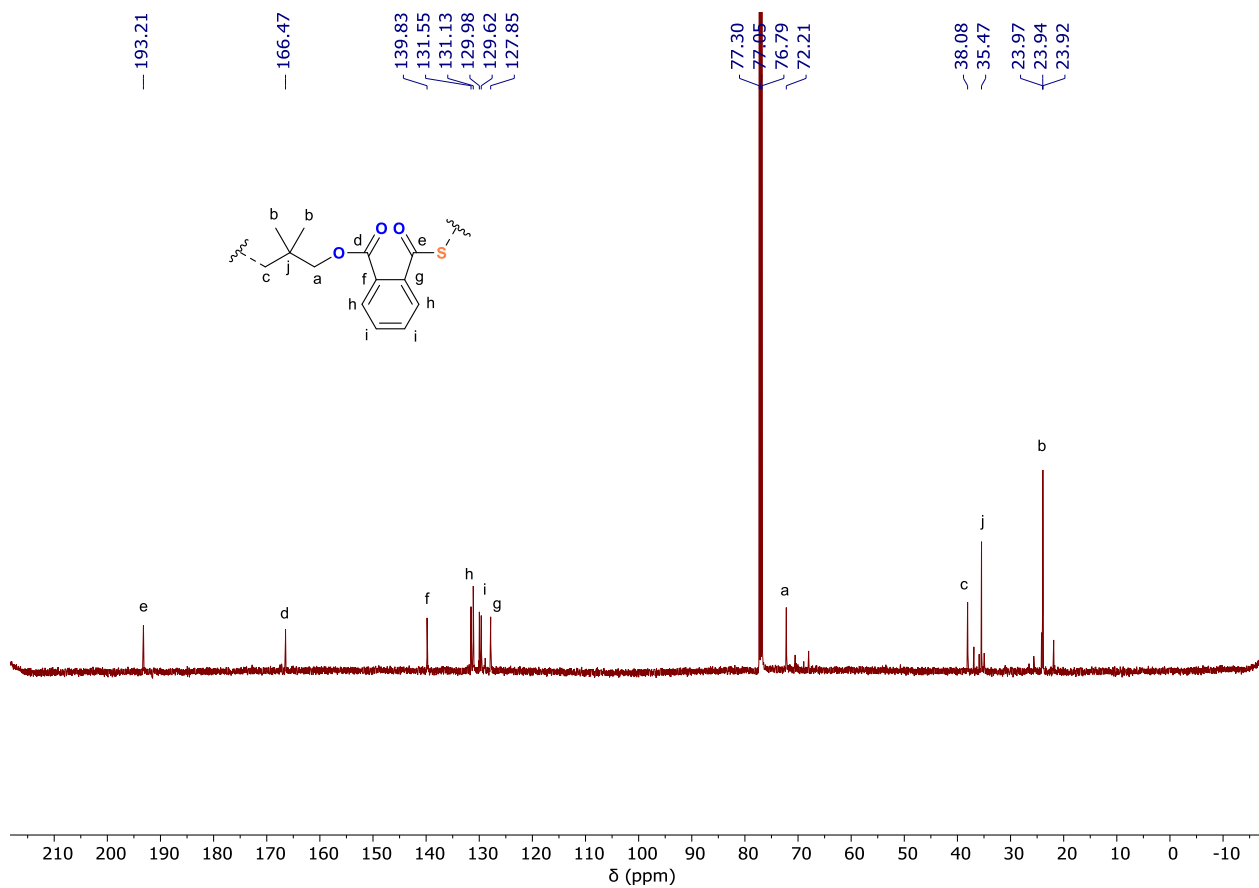


Figure S 60:  $^{13}\text{C}$  NMR spectrum (500MHz,  $\text{CDCl}_3$ ) of isolated PTA/ OX- $\text{Me}_2$  copolymer (table 2, run 3).

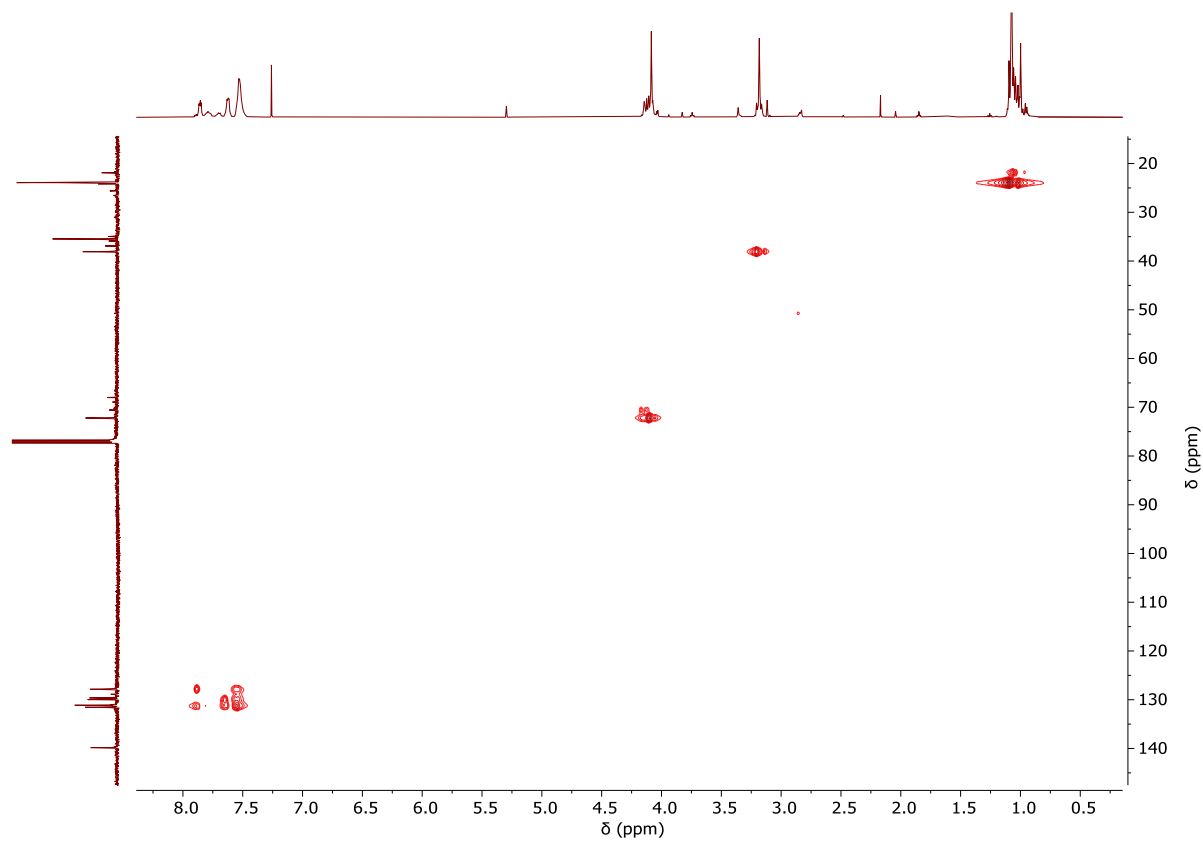
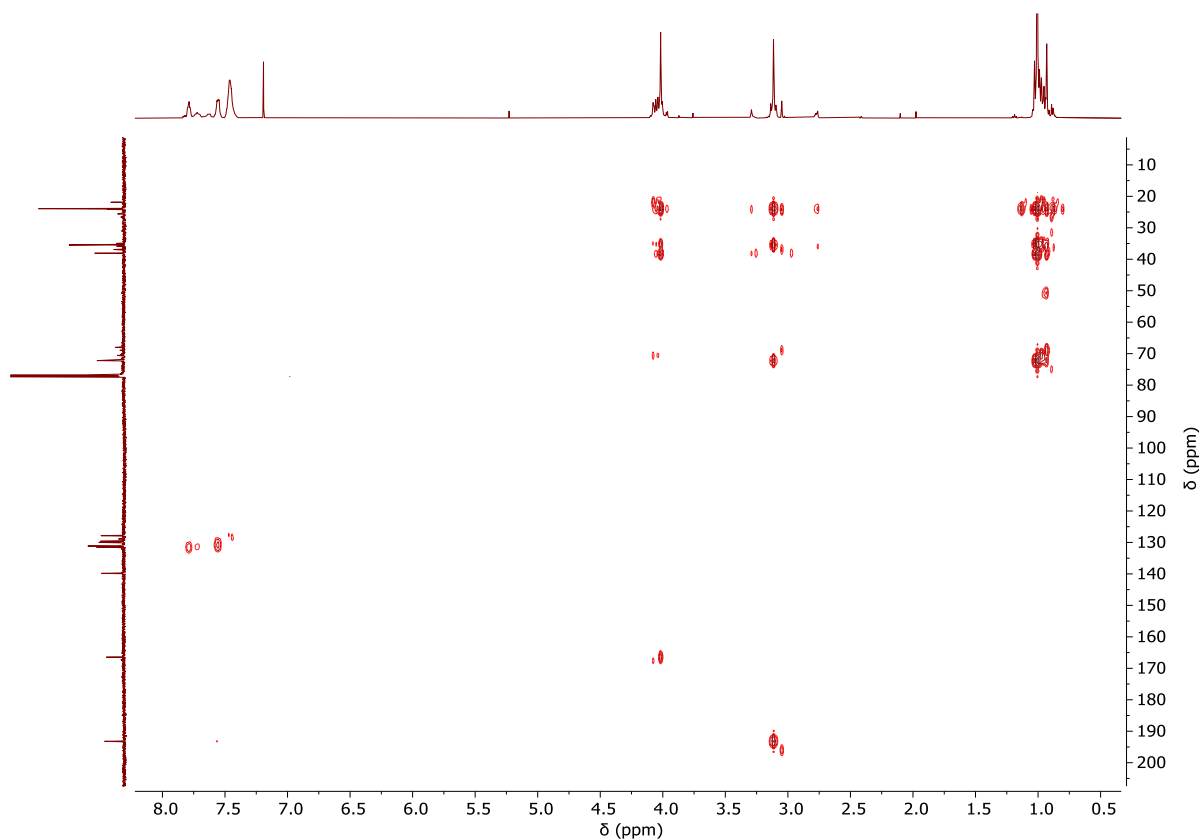


Figure S 61:  $^1\text{H}$  -  $^{13}\text{C}$  HSQC NMR spectrum (500MHz,  $\text{CDCl}_3$ ) of isolated PTA/ OX- $\text{Me}_2$  copolymer (table 2, run 3).



**Figure S 62:**  $^1\text{H}$  -  $^{13}\text{C}$  HMBC NMR spectrum (500MHz,  $\text{CDCl}_3$ ) of isolated PTA/ OX- $\text{Me}_2$  copolymer (table 2, run 3).

$\swarrow$  7.86  
 $\swarrow$  7.86  
 $\swarrow$  7.60  
 $\swarrow$  7.53  
 $\swarrow$  7.26
 
 $\swarrow$  4.24  
 $\swarrow$  4.23
 

 $\swarrow$  3.44  
 $\swarrow$  3.42  
 $\swarrow$  3.32  
 $\swarrow$  3.28
 

 $\swarrow$  1.13  
 $\swarrow$  1.07

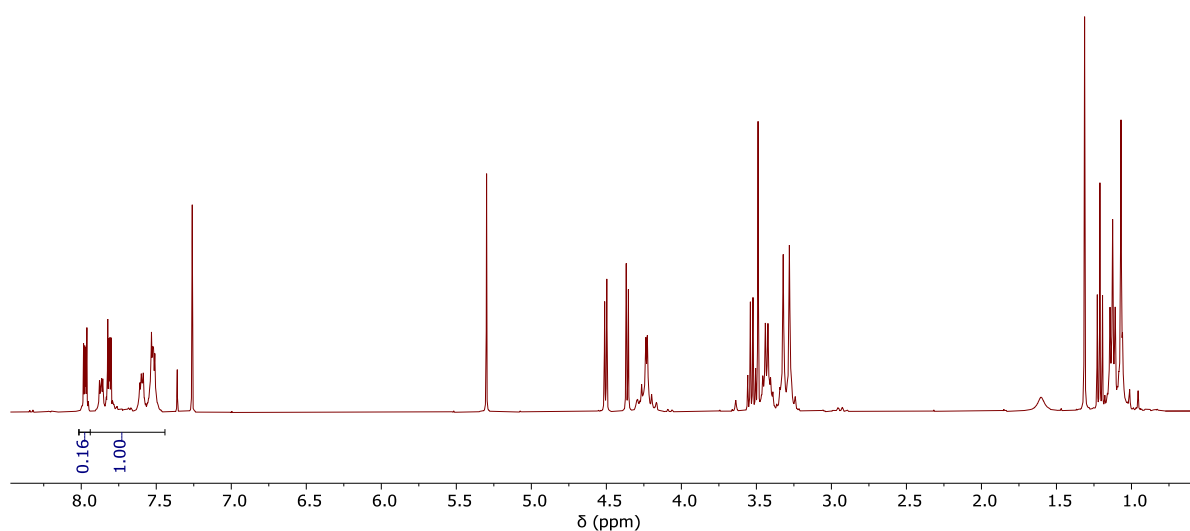


**Figure S 63:**  $^1\text{H}$  NMR spectrum (400MHz,  $\text{CDCl}_3$ ) of the final aliquot from PTA/OX-OEt ROCOP (table 2, run 4). Peak assignments as per Fig. S 64.

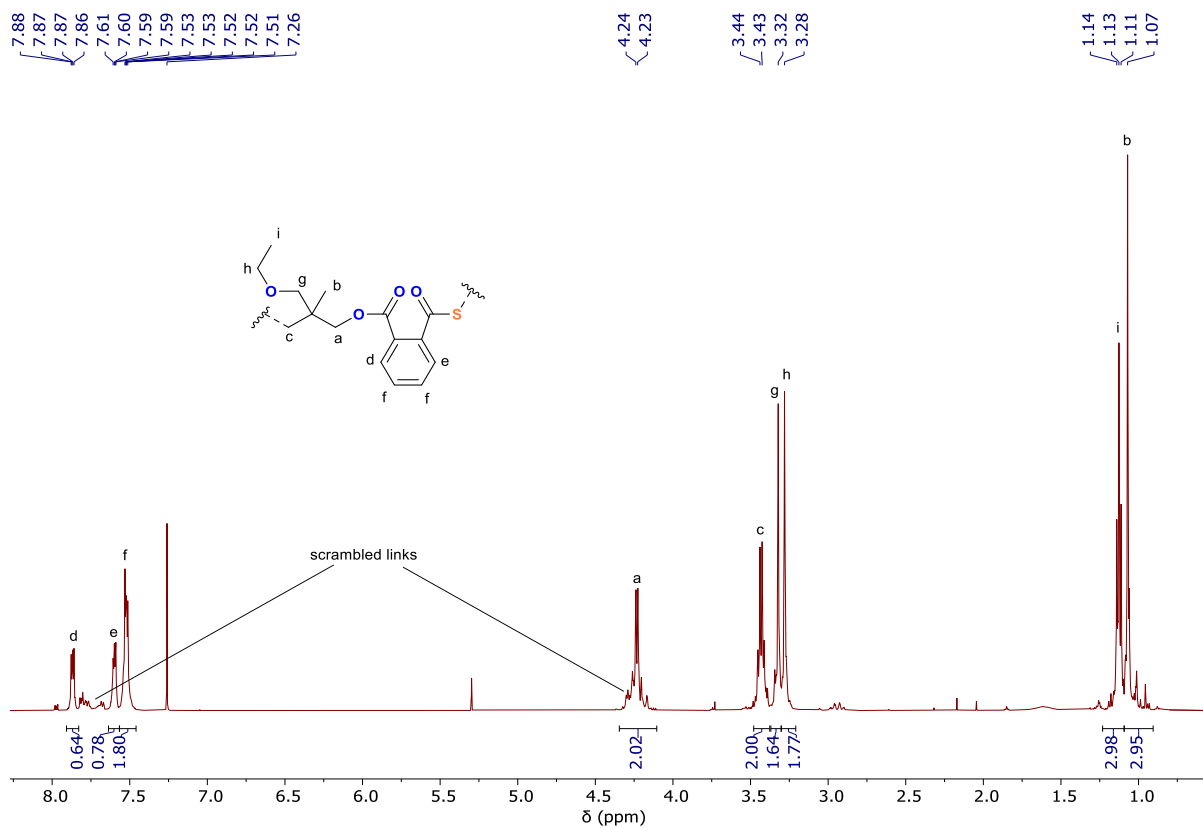


Figure S 64:  $^1\text{H}$  NMR spectrum (500MHz,  $\text{CDCl}_3$ ) of isolated PTA/OX-OEt copolymer (table 2, run 4).

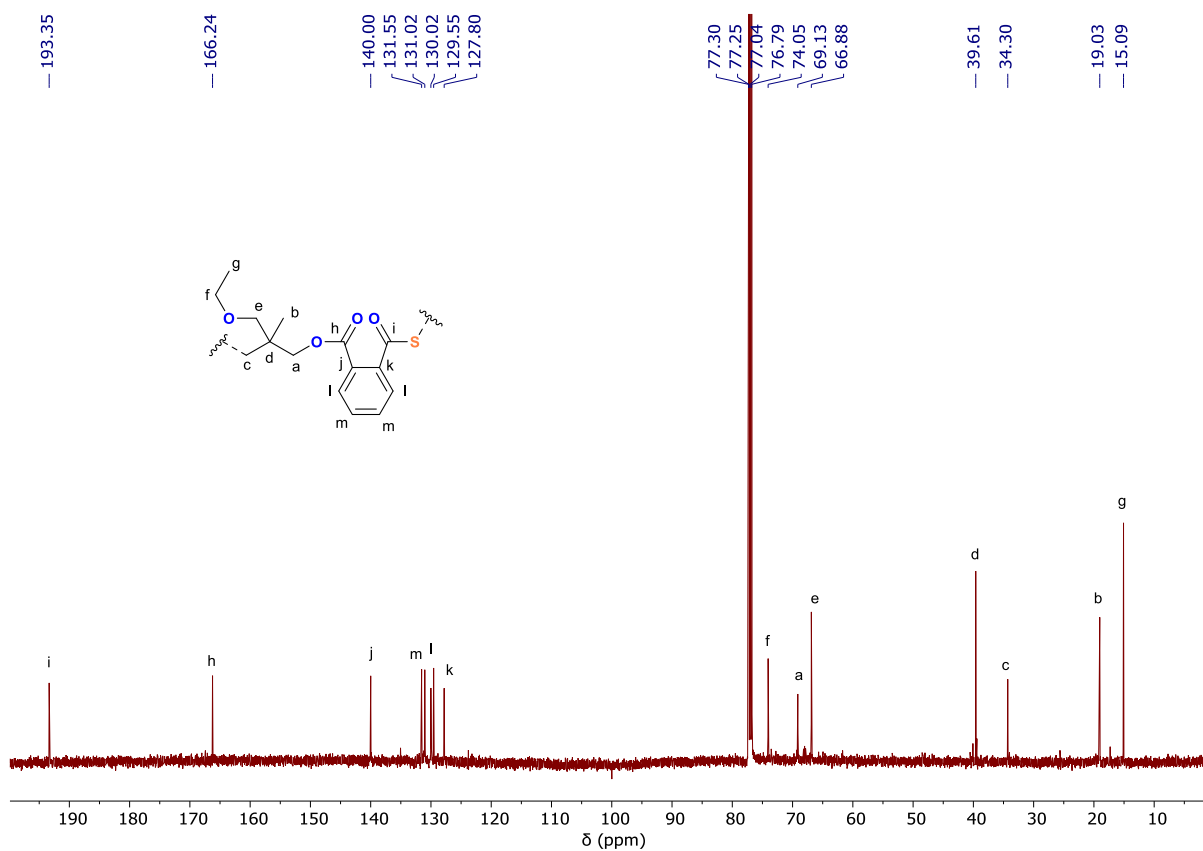
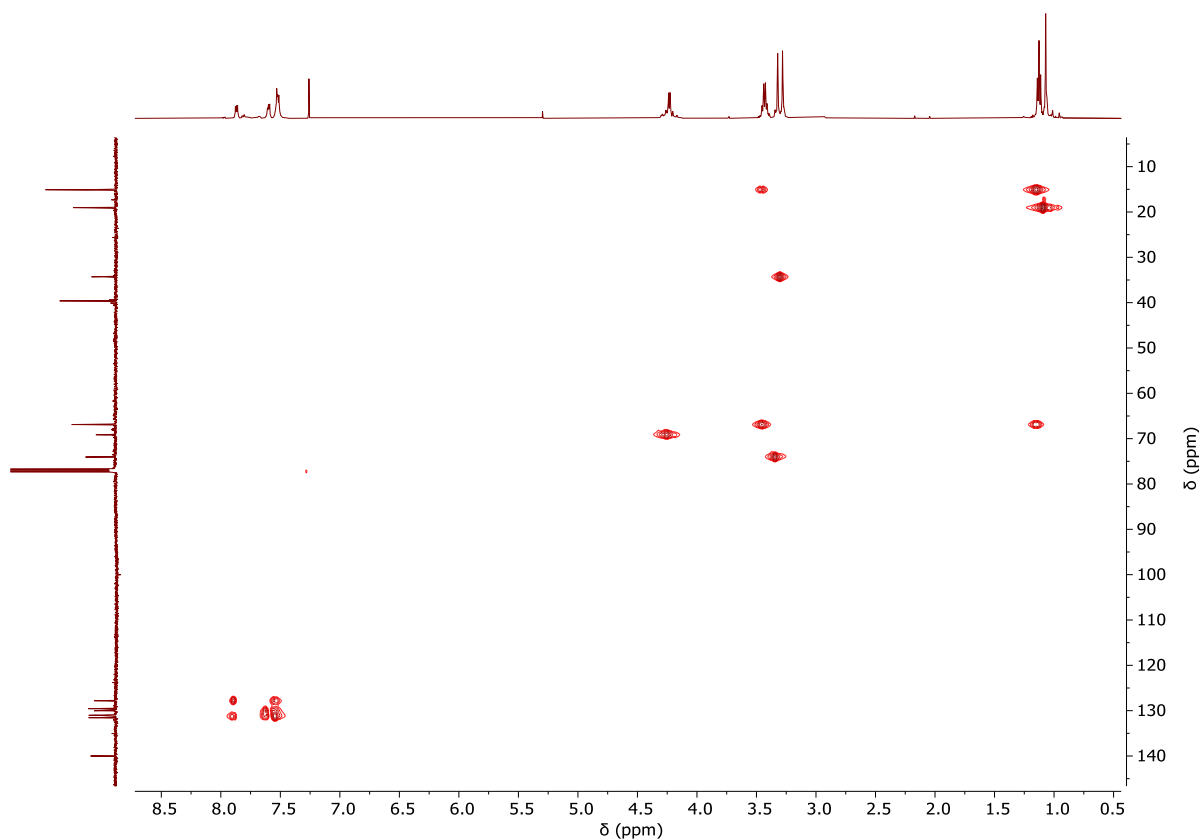
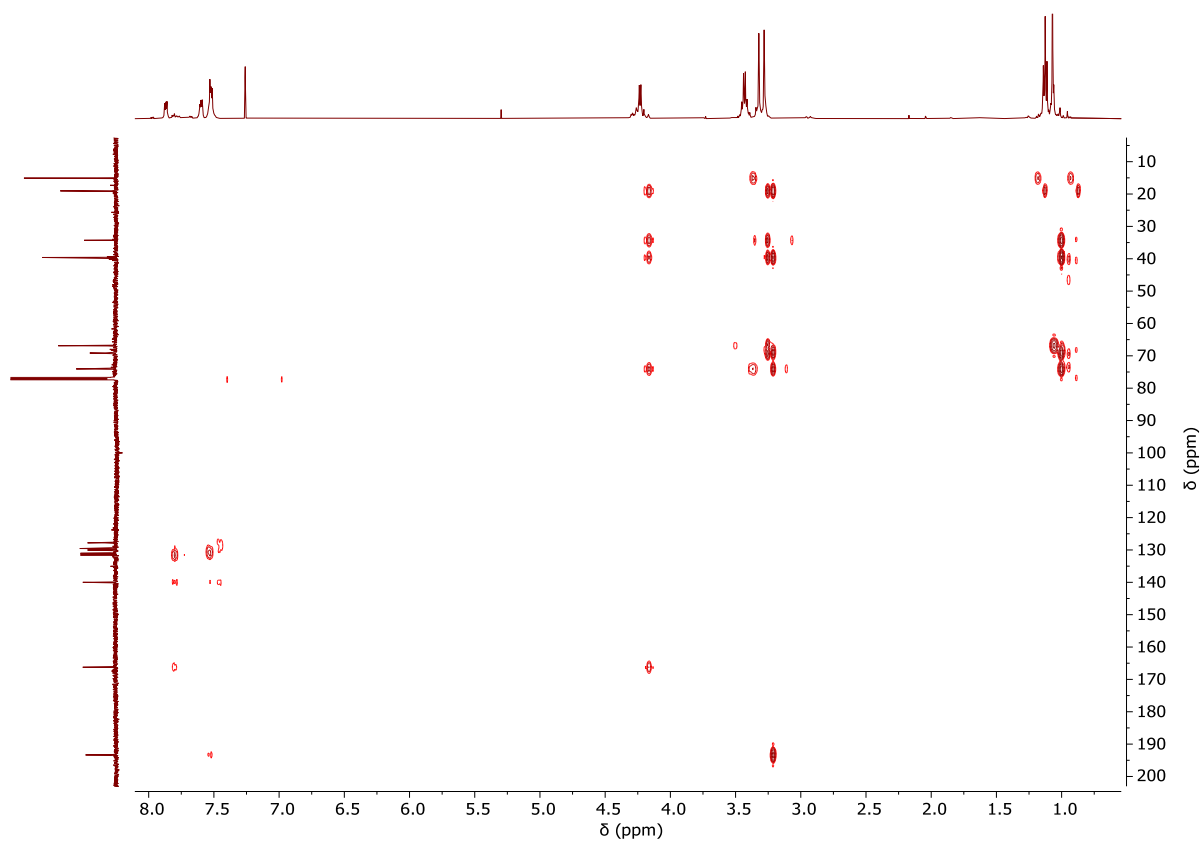


Figure S 65:  $^{13}\text{C}$  NMR spectrum (500MHz,  $\text{CDCl}_3$ ) of isolated PTA/OX-OEt copolymer (table 2, run 4).



**Figure S 66:**  $^1\text{H} - ^{13}\text{C}$  HSQC NMR spectrum (500MHz,  $\text{CDCl}_3$ ) of isolated PTA/OX-OEt copolymer (table 2, run 4).



**Figure S 67:**  $^1\text{H} - ^{13}\text{C}$  HMBC NMR spectrum (500MHz,  $\text{CDCl}_3$ ) of isolated PTA/OX-OEt copolymer (table 2, run 4).

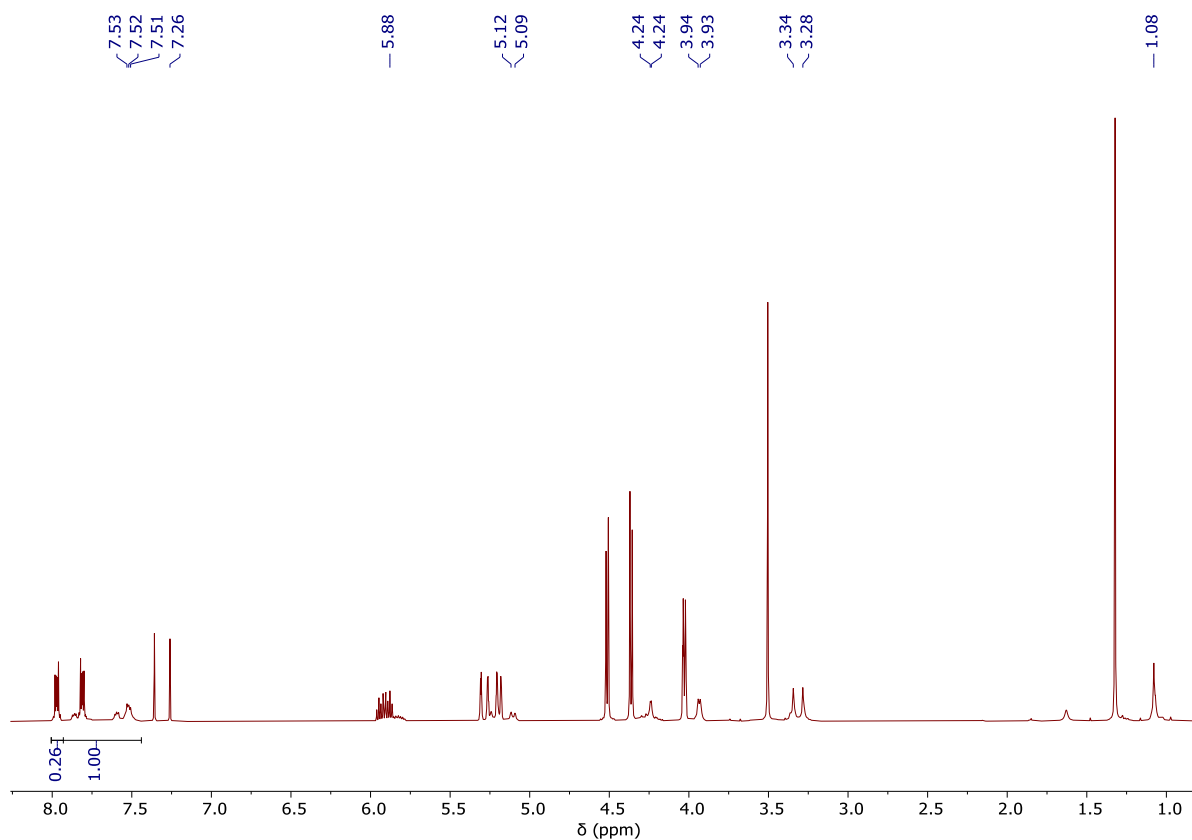


**Figure S 68:**  $^1\text{H}$  NMR spectrum (400MHz,  $\text{CDCl}_3$ ) of the final aliquot from PTA/OX-OAll ROCOP (table 2, run 6). Peak assignments as per Fig. S 69.

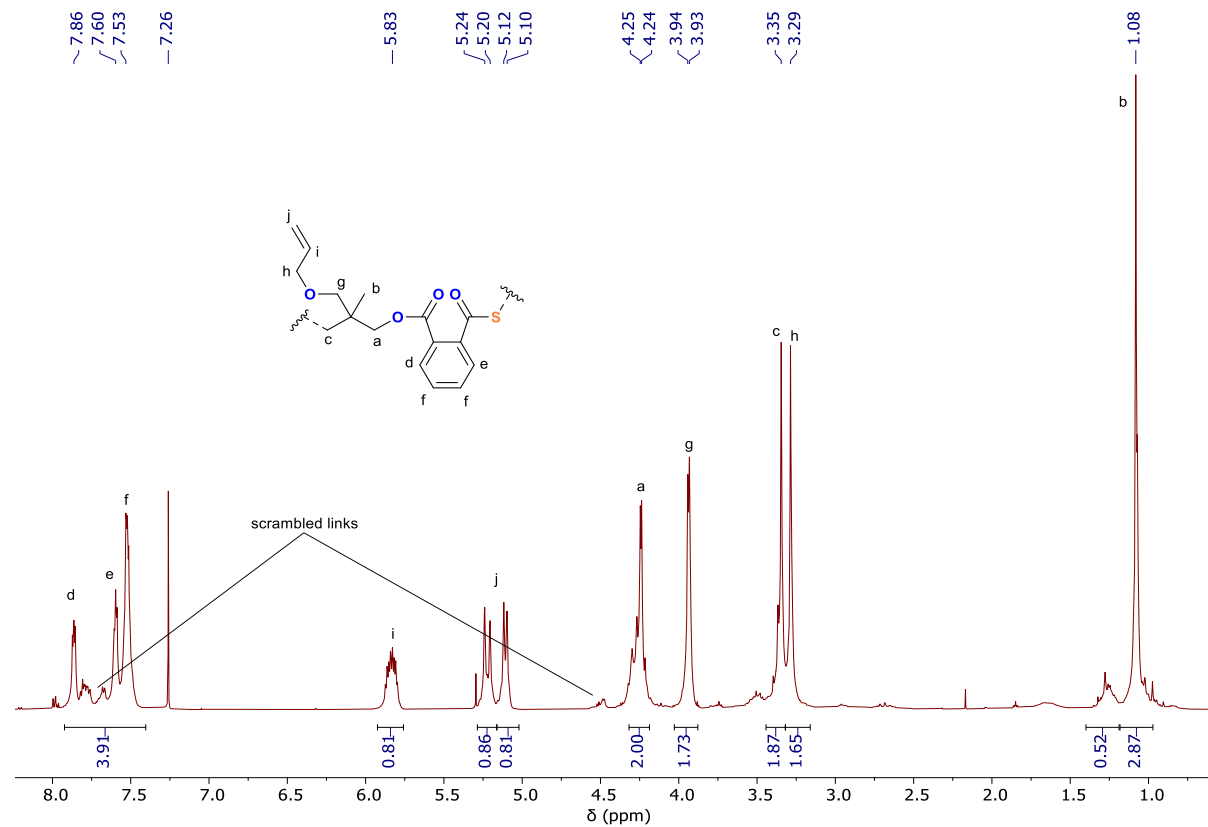


**Figure S 69:**  $^1\text{H}$  NMR spectrum (500MHz,  $\text{CDCl}_3$ ) of isolated PTA/OX-OAll copolymer. (table 2, run 6).



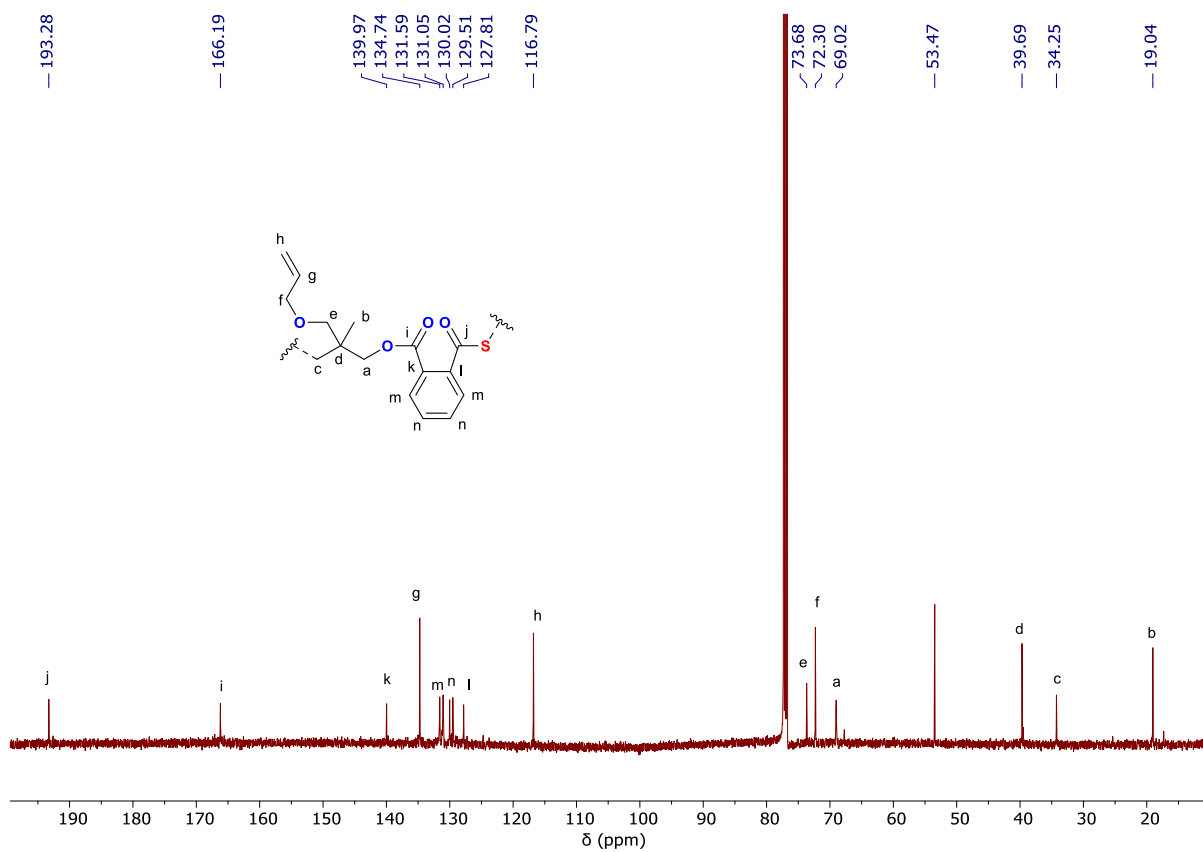


Figure S 70:  $^{13}\text{C}$  NMR spectrum (500MHz,  $\text{CDCl}_3$ ) of isolated PTA/OX-OAll copolymer. (table 2, run 6).

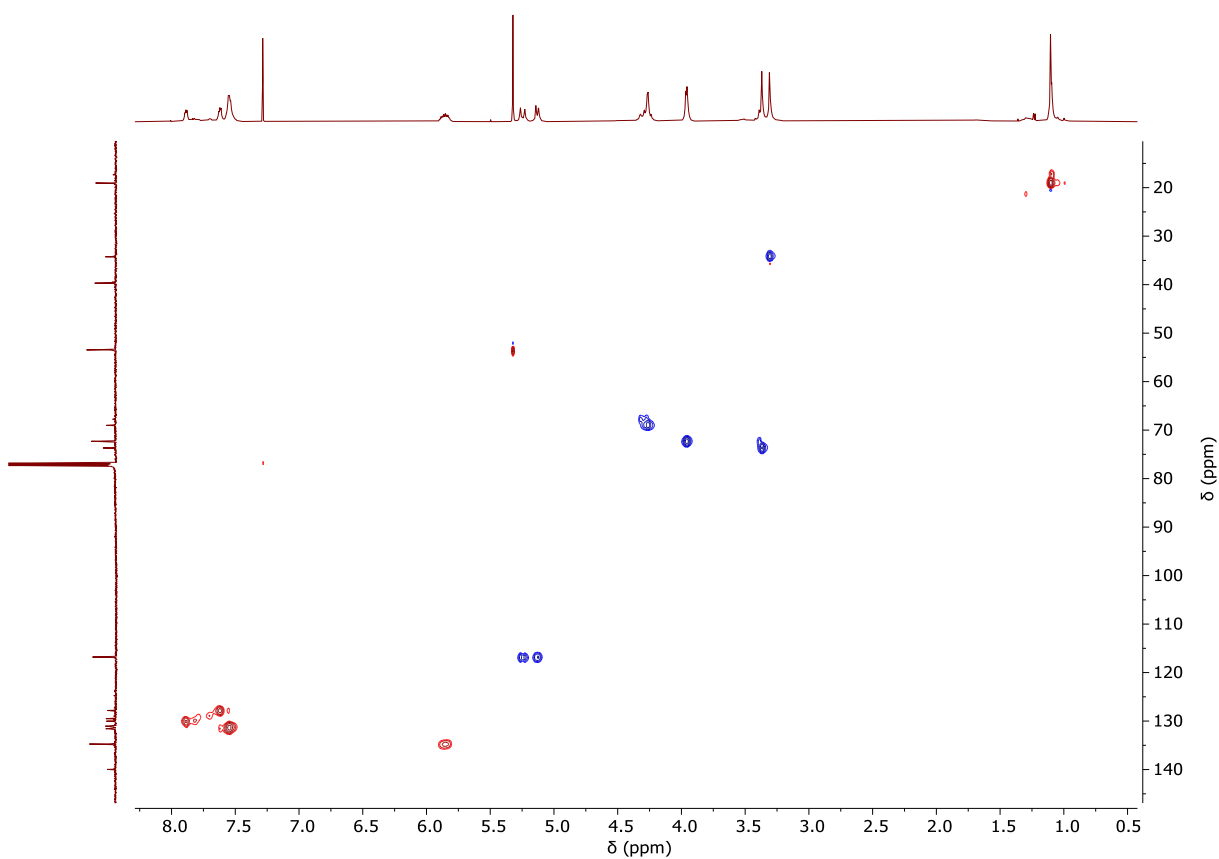


Figure S 71:  $^1\text{H} - ^{13}\text{C}$  HSQC NMR spectrum (500MHz,  $\text{CDCl}_3$ ) of isolated PTA/OX-OAll copolymer (table 2, run 6).

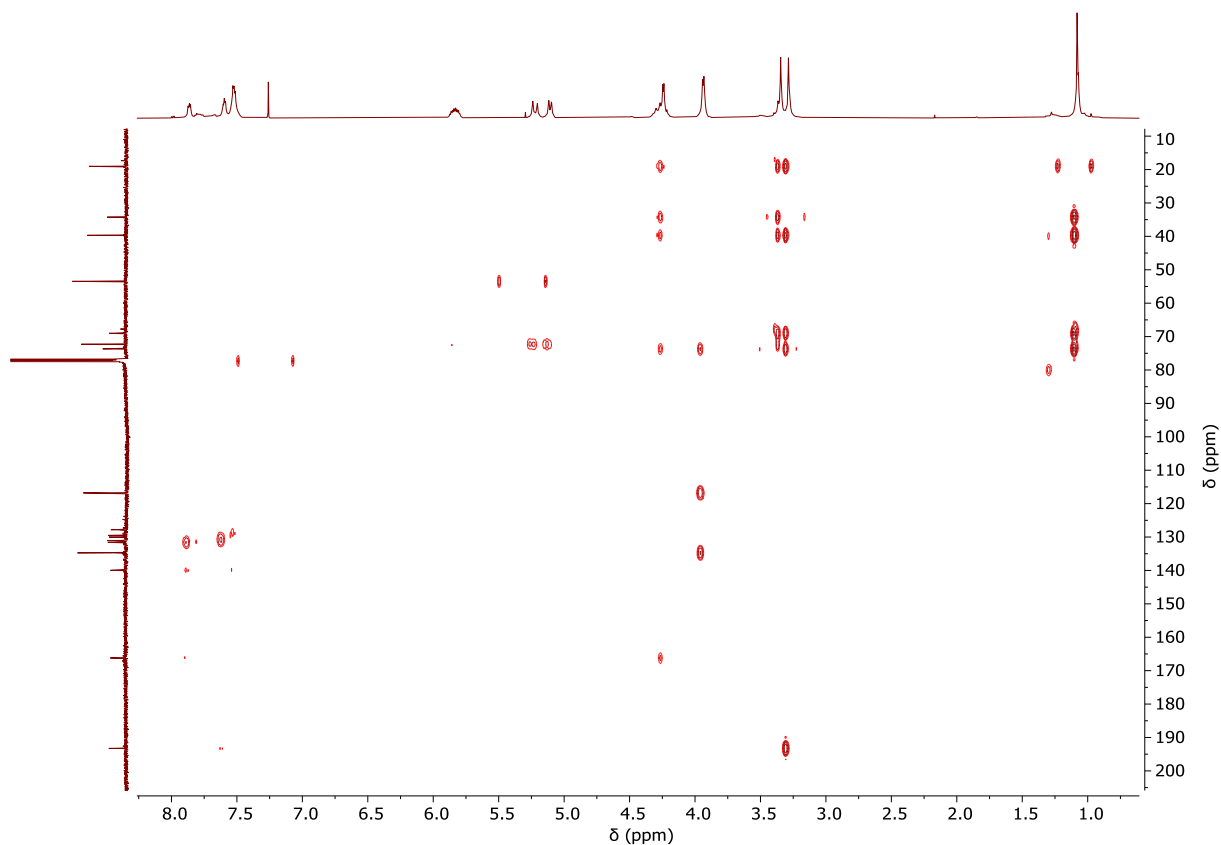


Figure S 72:  $^1\text{H} - ^{13}\text{C}$  HMBC NMR spectrum (500MHz,  $\text{CDCl}_3$ ) of isolated PTA/OX-OAll copolymer (table 2, run 6).

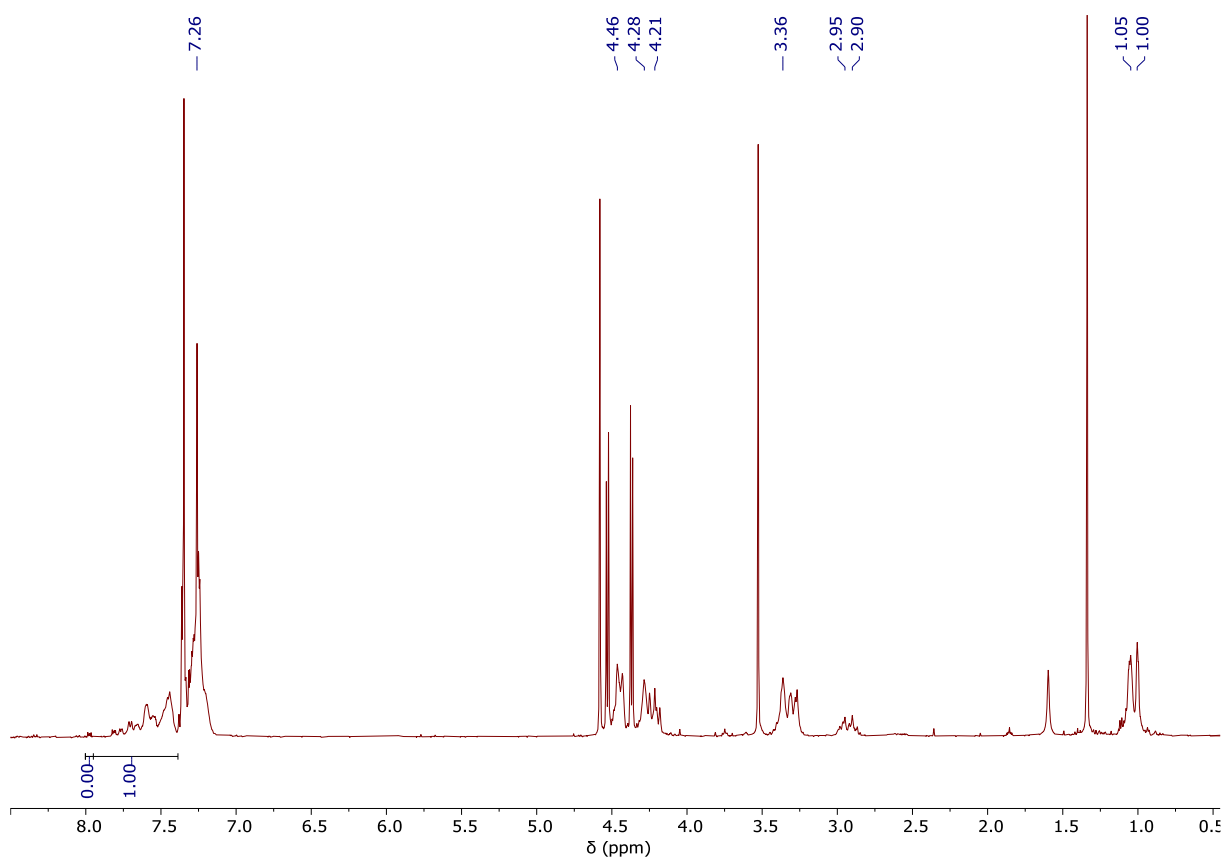


Figure S 73:  $^1\text{H}$  NMR spectrum (400MHz,  $\text{CDCl}_3$ ) of the final aliquot from PTA/OX-OBn ROCOP (table 2, run 5). Peak assignments as per Fig. S 74.

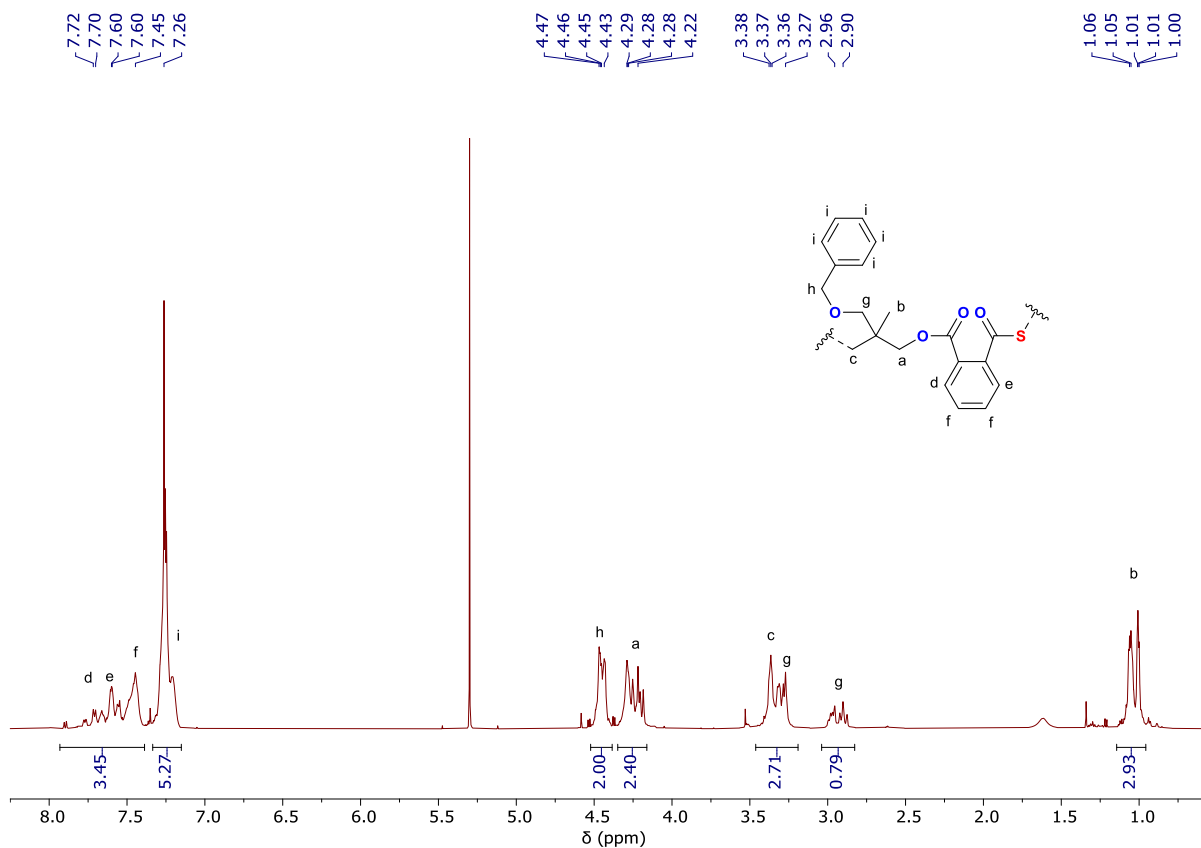


Figure S 74:  $^1\text{H}$  NMR spectrum (500MHz,  $\text{CDCl}_3$ ) of isolated PTA/OX-OBn copolymer. (table 2, run 5).

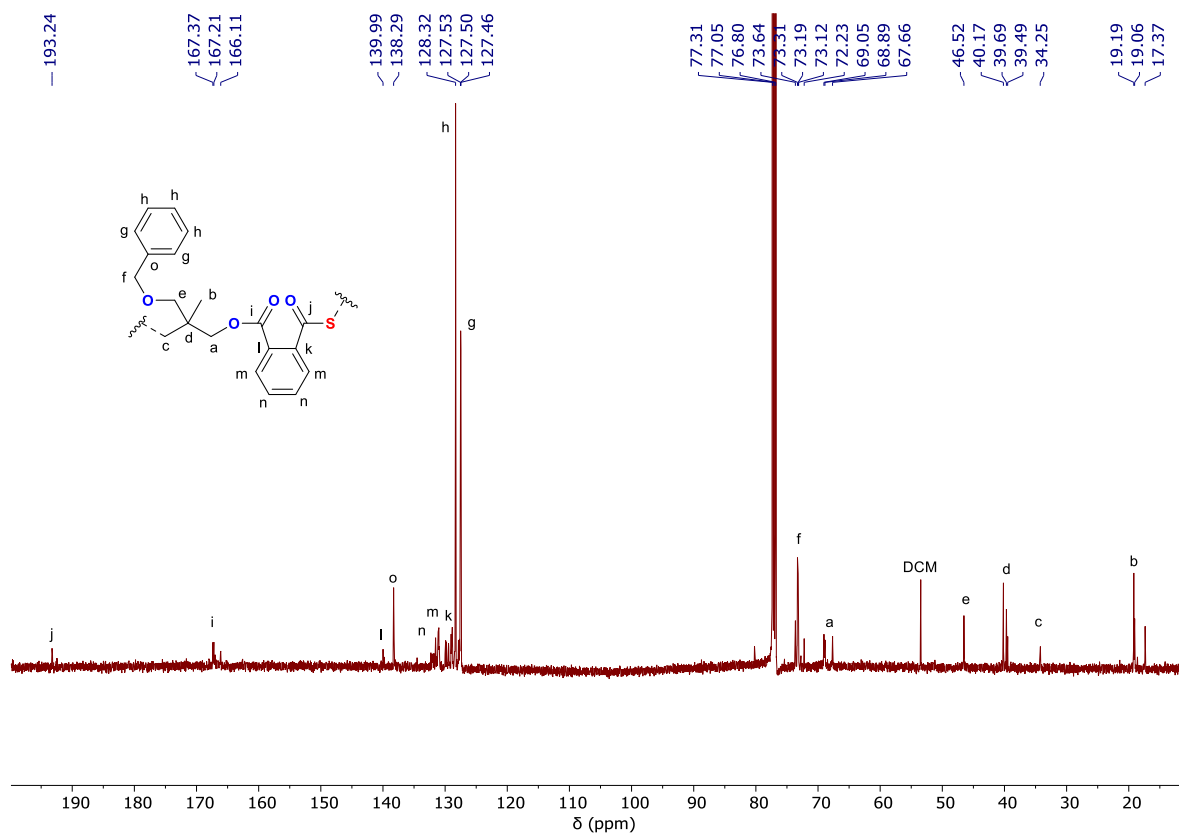


Figure S 75:  $^{13}\text{C}$  NMR spectrum (500MHz,  $\text{CDCl}_3$ ) of isolated PTA/OX-OBn copolymer. (table 2, run 5).

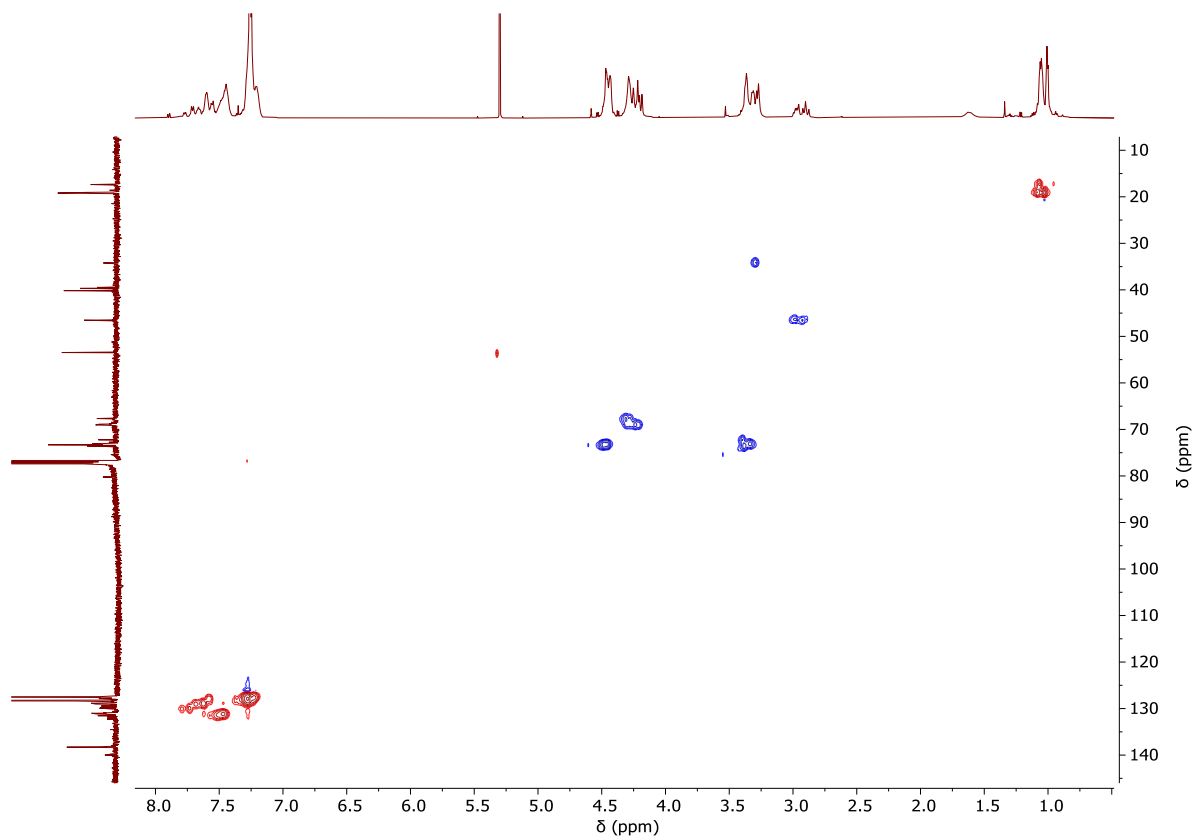


Figure S 76:  $^1\text{H} - ^{13}\text{C}$  HSQC NMR spectrum (500MHz,  $\text{CDCl}_3$ ) of isolated PTA/OX-OBn copolymer (table 2, run 5).

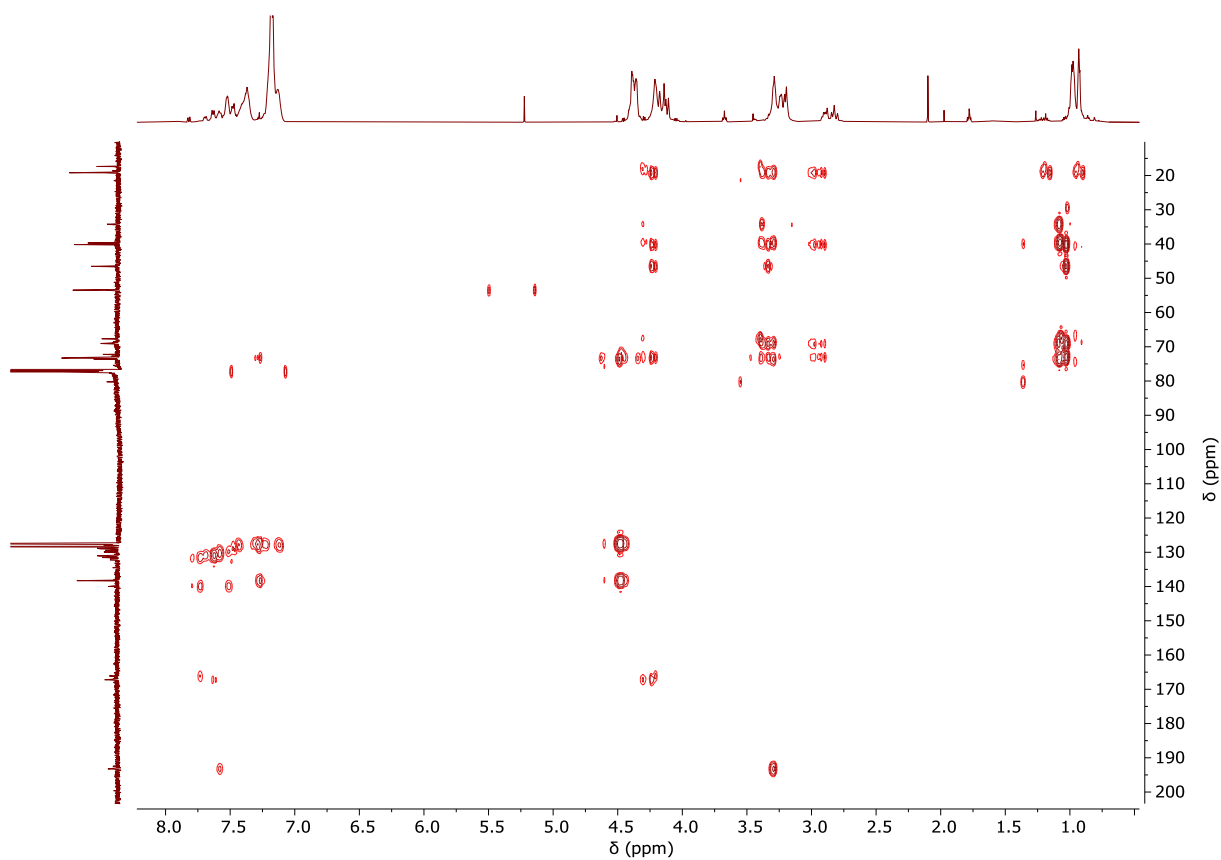


Figure S 77:  $^1\text{H} - ^{13}\text{C}$  HMBC NMR spectrum (500MHz,  $\text{CDCl}_3$ ) of isolated PTA/OX-OBn copolymer (table 2, run 5).

## Gel Permeation Chromatography (GPC):

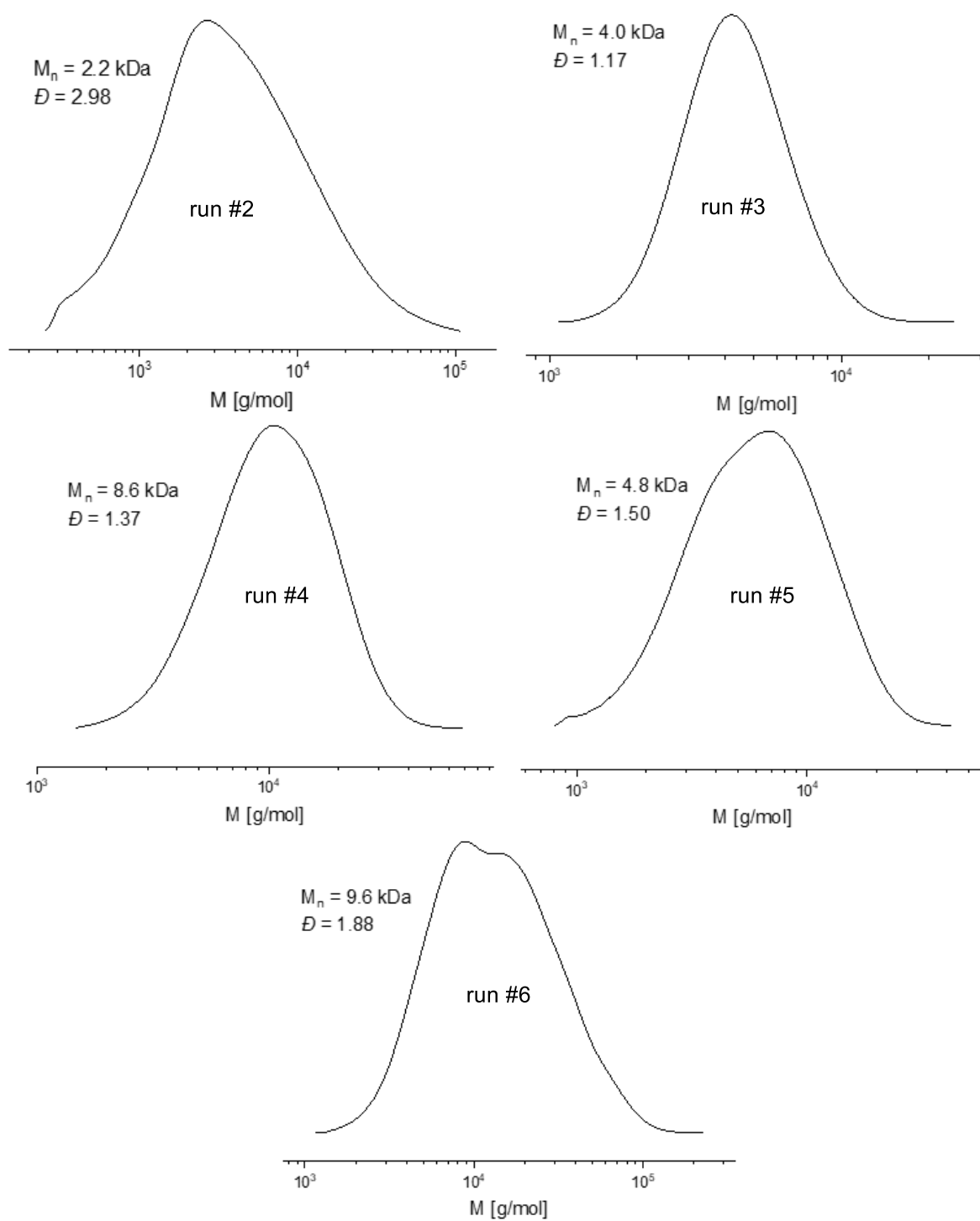
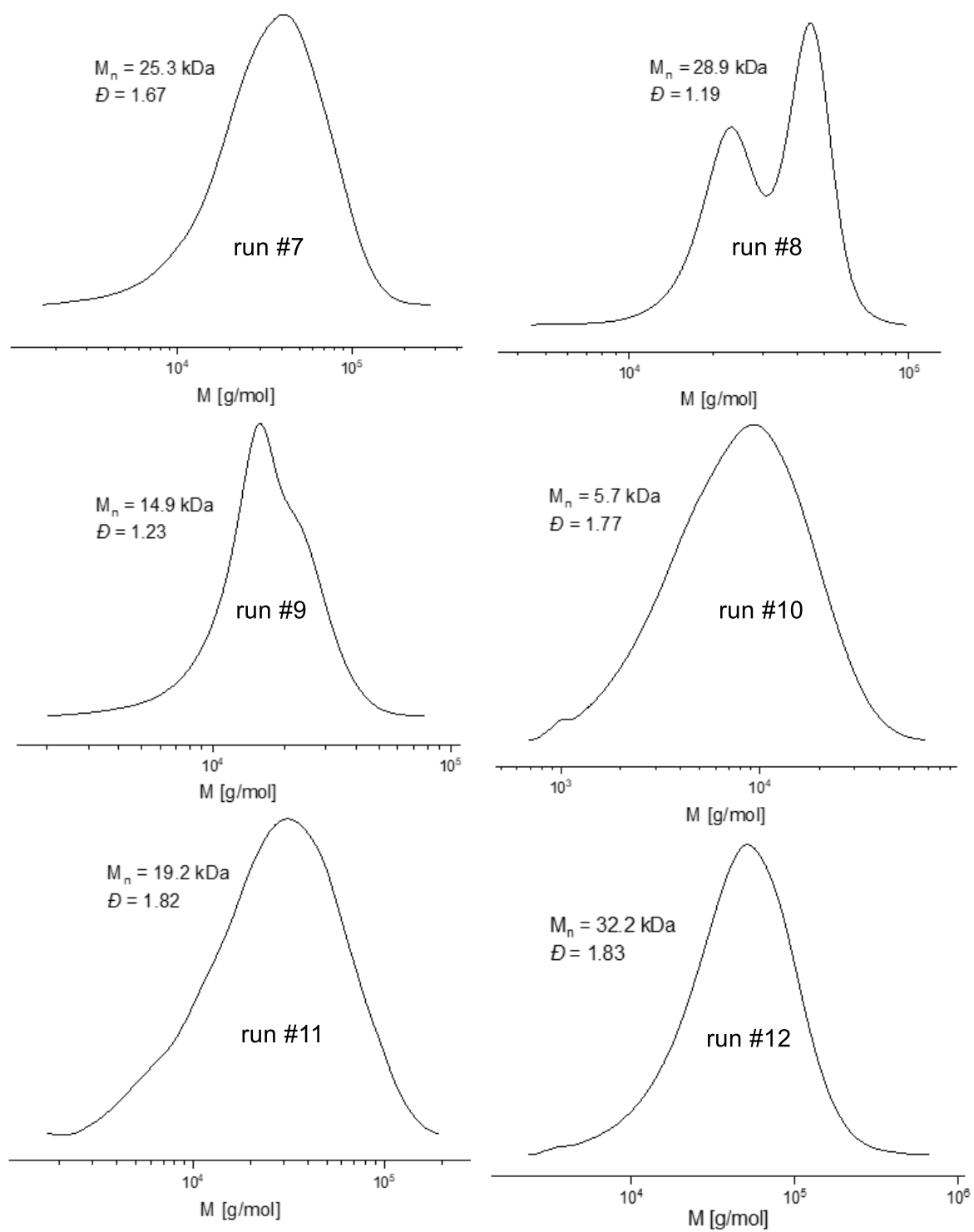


Figure S 78: GPC traces corresponding to table 2, run #2 - #6.



**Figure S 79:** GPC traces corresponding to table 2, run #7 - #12.

Section S4: Thermal Analysis – TGA, DSC

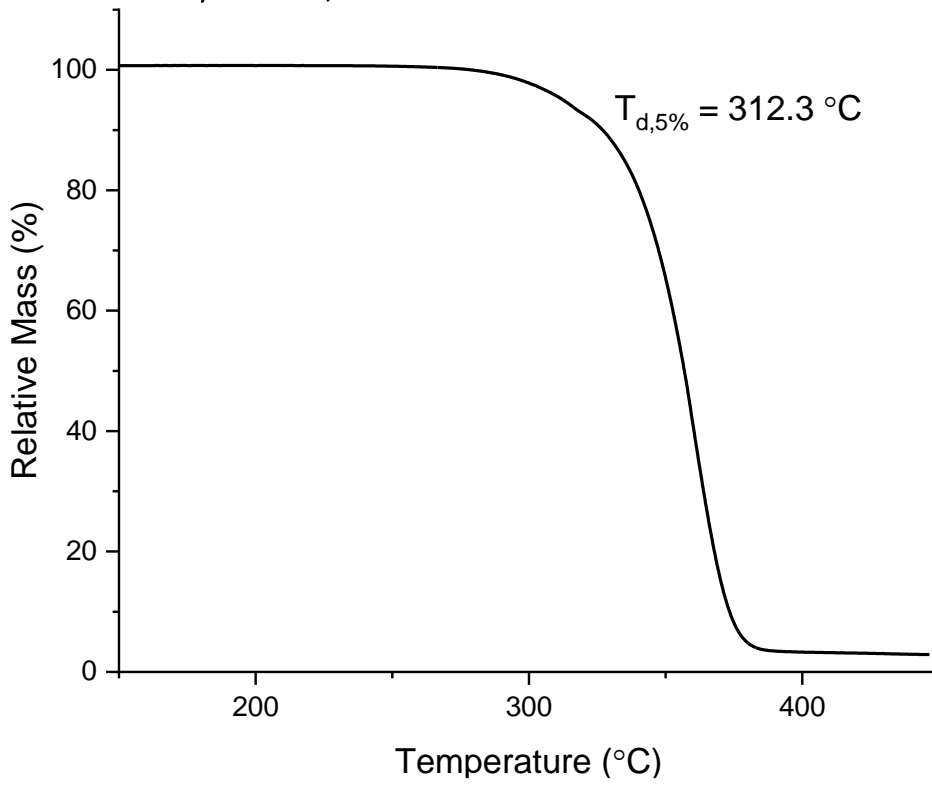


Figure S 80: TGA data of PTA/OX copolymer corresponding to table 2, run 1.

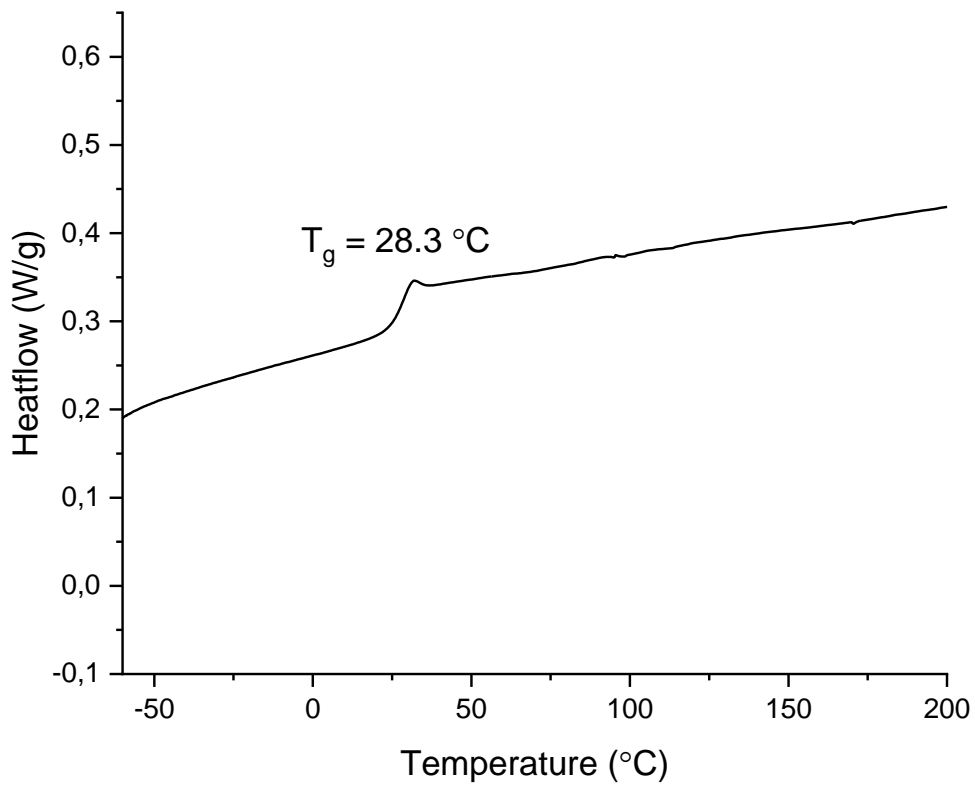


Figure S 81: DSC data from the 1<sup>st</sup> heating cycle of PTA/OX copolymer corresponding to table 2, run 1.

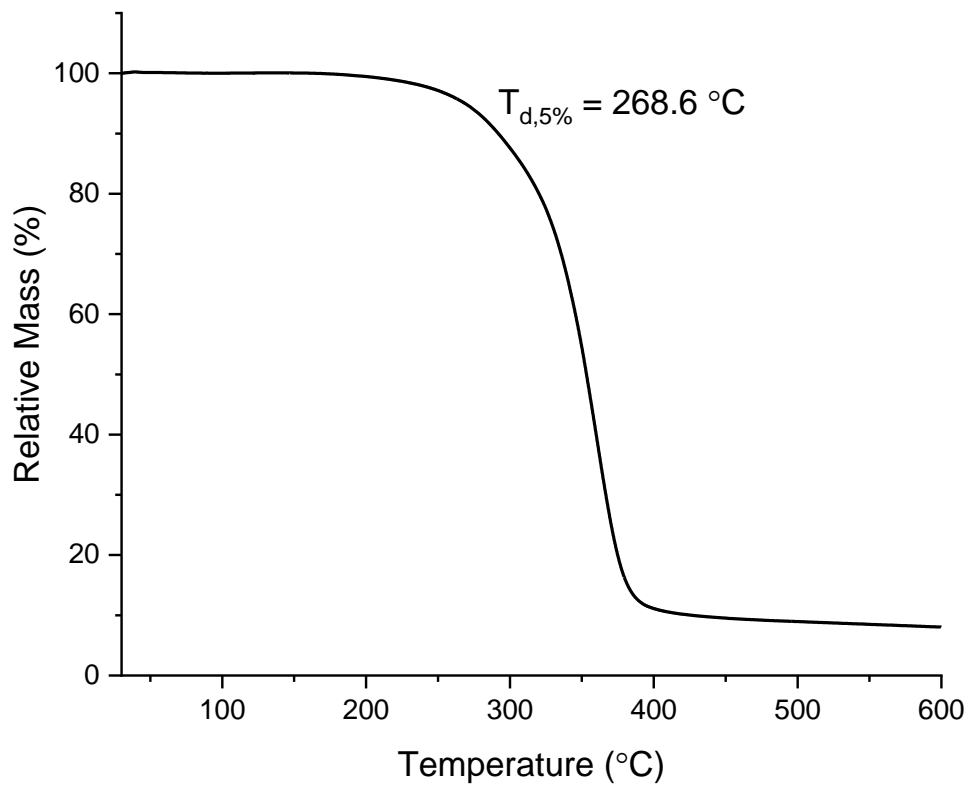


Figure S 82: TGA data of STA/OX copolymer corresponding to table 2, run 2.

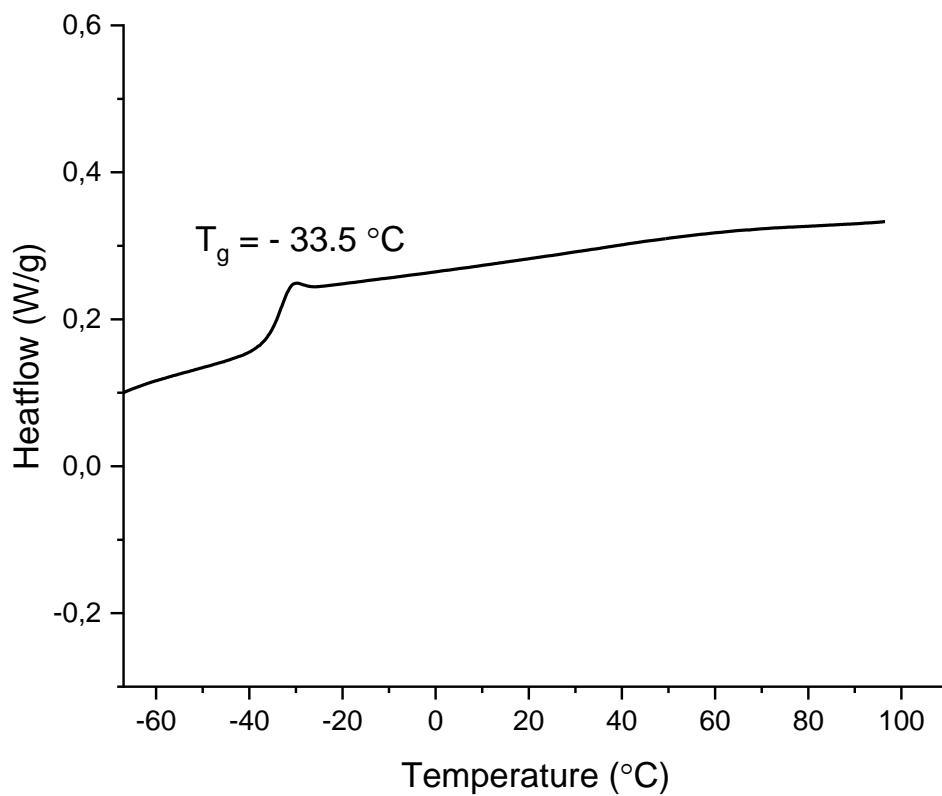


Figure S 83: DSC data from the 1<sup>st</sup> heating cycle of STA/OX copolymer corresponding to table 2, run 2.



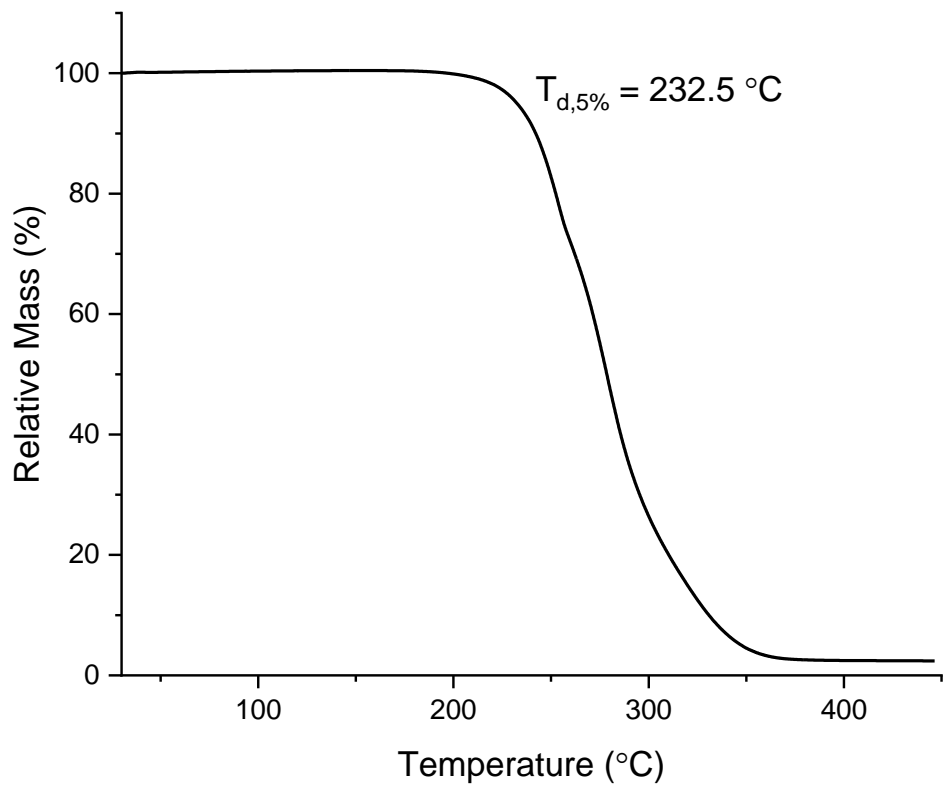


Figure S 84: TGA data of CS<sub>2</sub>/OX copolymer corresponding to table 2, run 3.

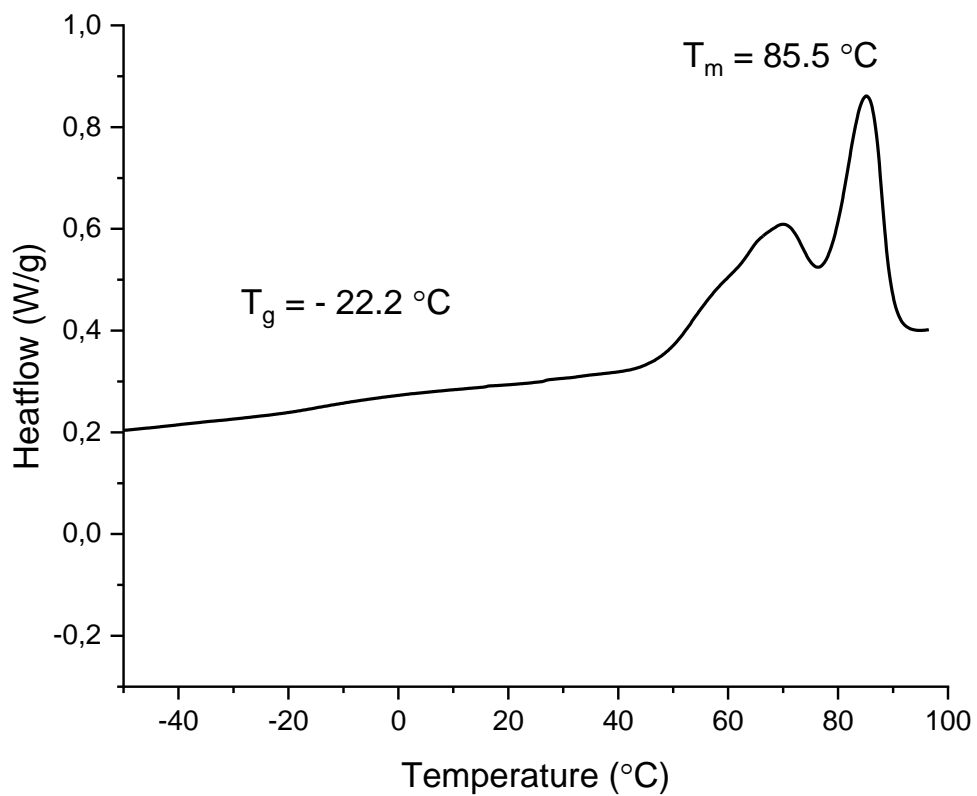


Figure S 85: DSC data from the 1<sup>st</sup> heating cycle of CS<sub>2</sub>/OX copolymer corresponding to table 2, run 3.

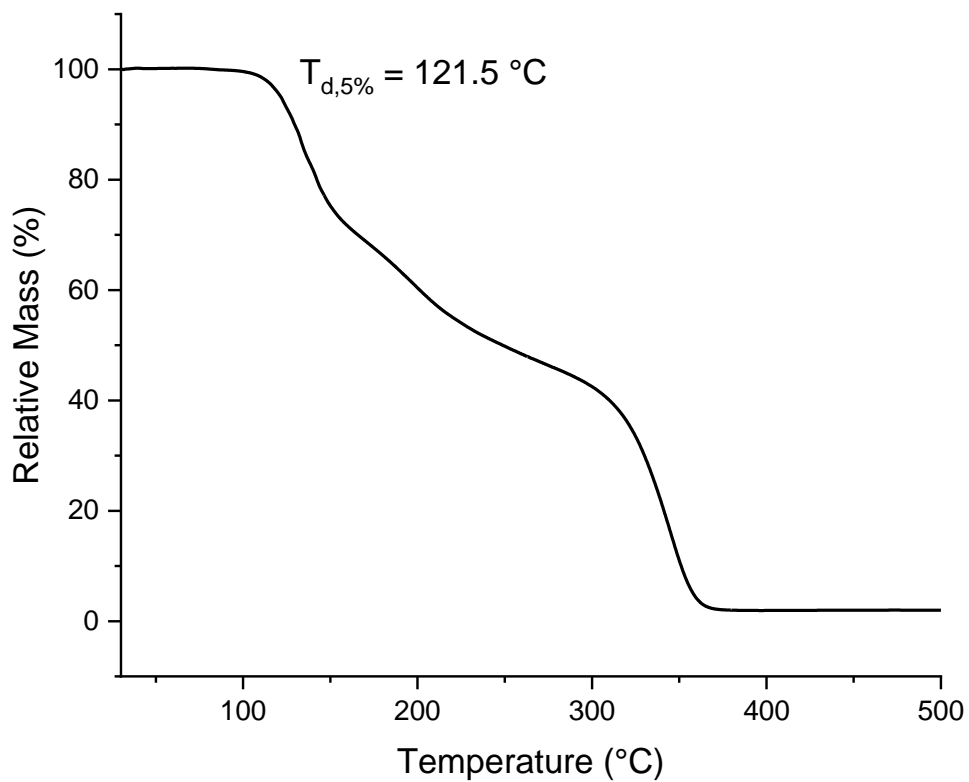


Figure S 86: TGA data of CS<sub>2</sub>/OX copolymer corresponding to table 2, run 4.

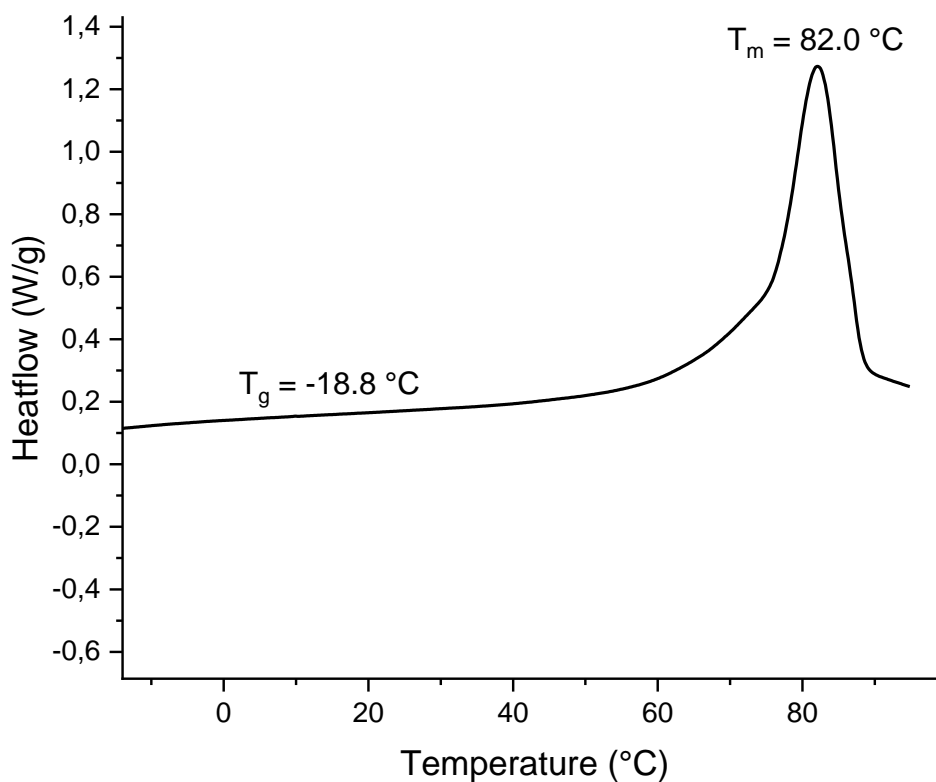


Figure S 87: DSC data from the 1<sup>st</sup> heating cycle of CS<sub>2</sub>/OX copolymer corresponding to table 2, run 4.

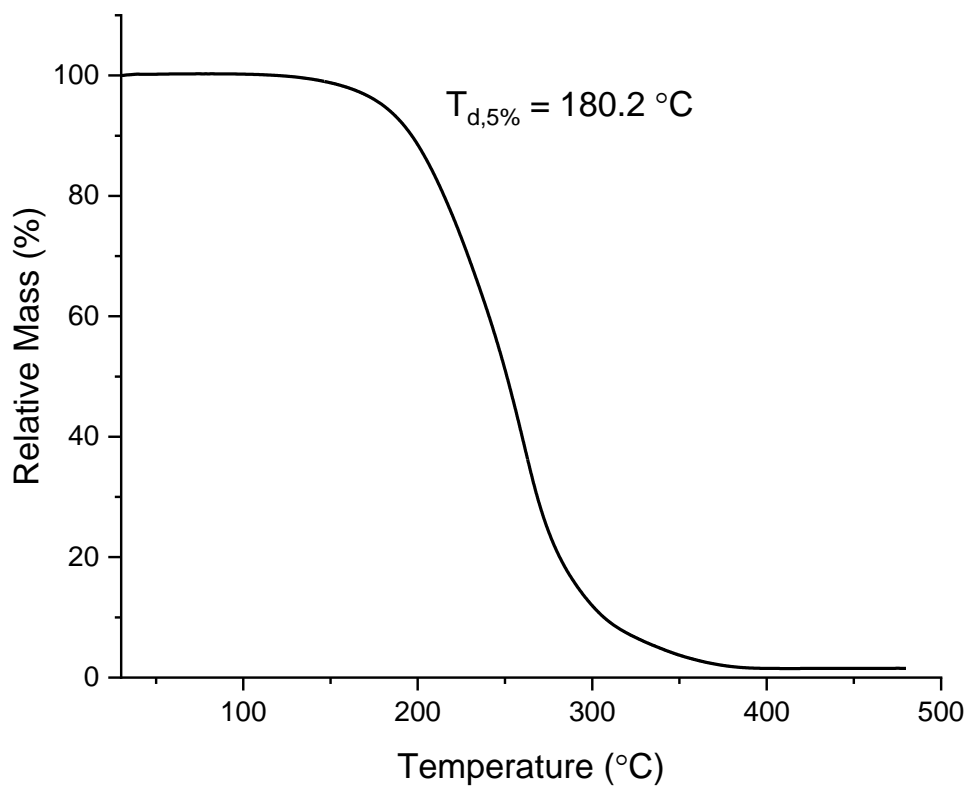


Figure S 88: TGA data of EtNCS/OX copolymer corresponding to table 2, run 5.

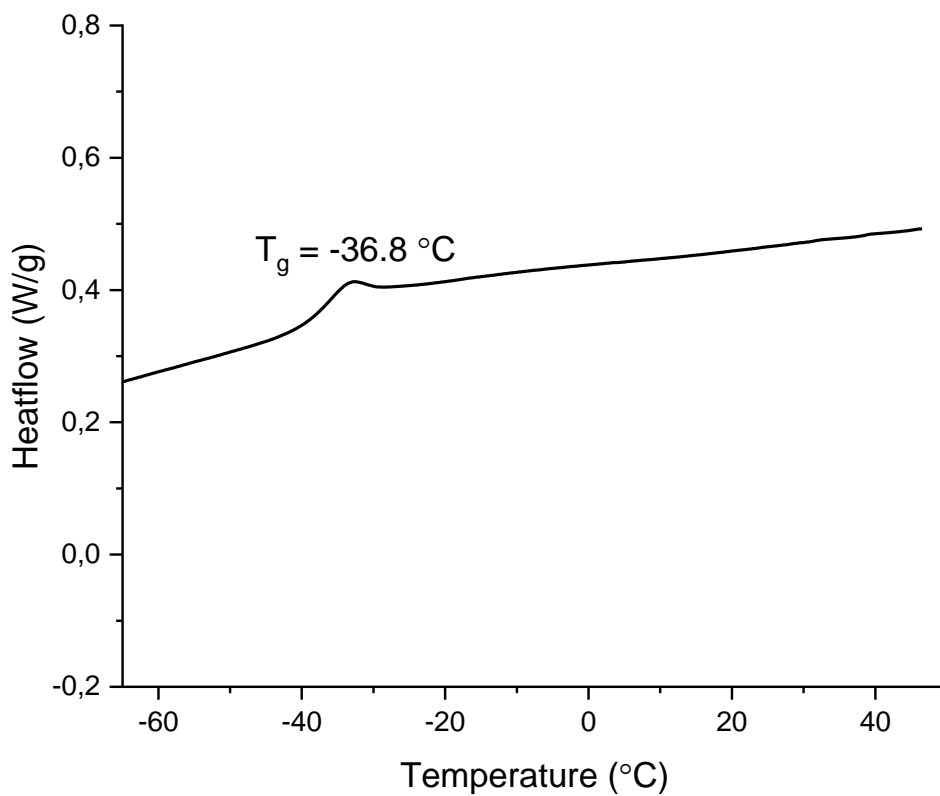


Figure S 89: DSC data from the 1st heating cycle of EtNCS/OX copolymer corresponding to table 2, run 5.

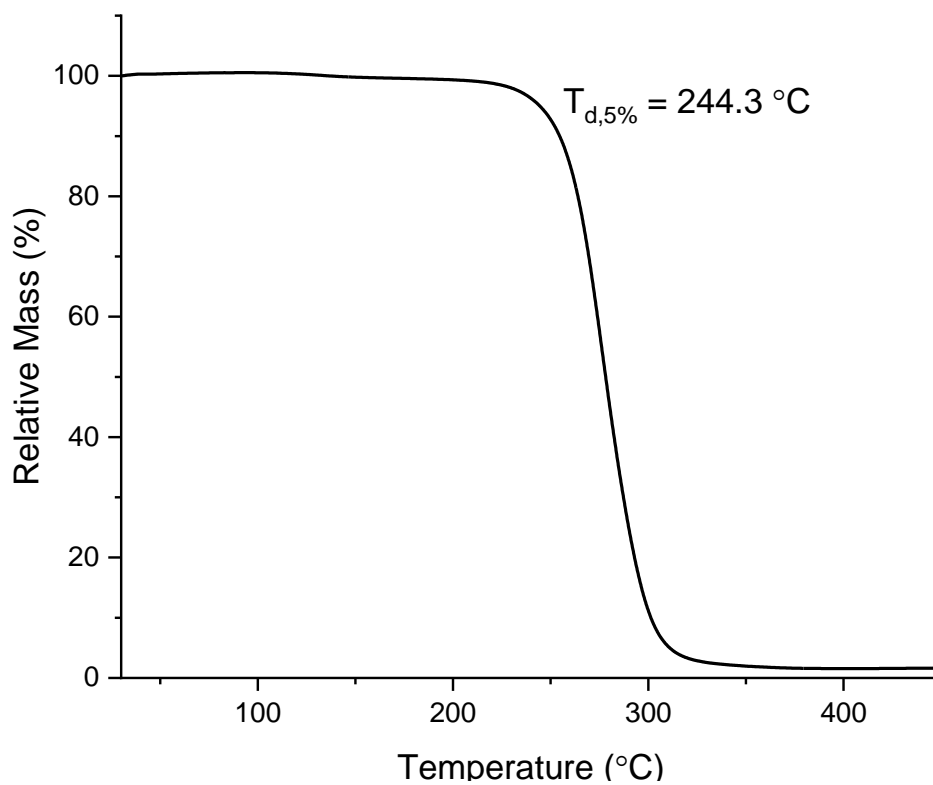


Figure S 90: TGA data of CyNCS/OX copolymer corresponding to table 2, run 6.

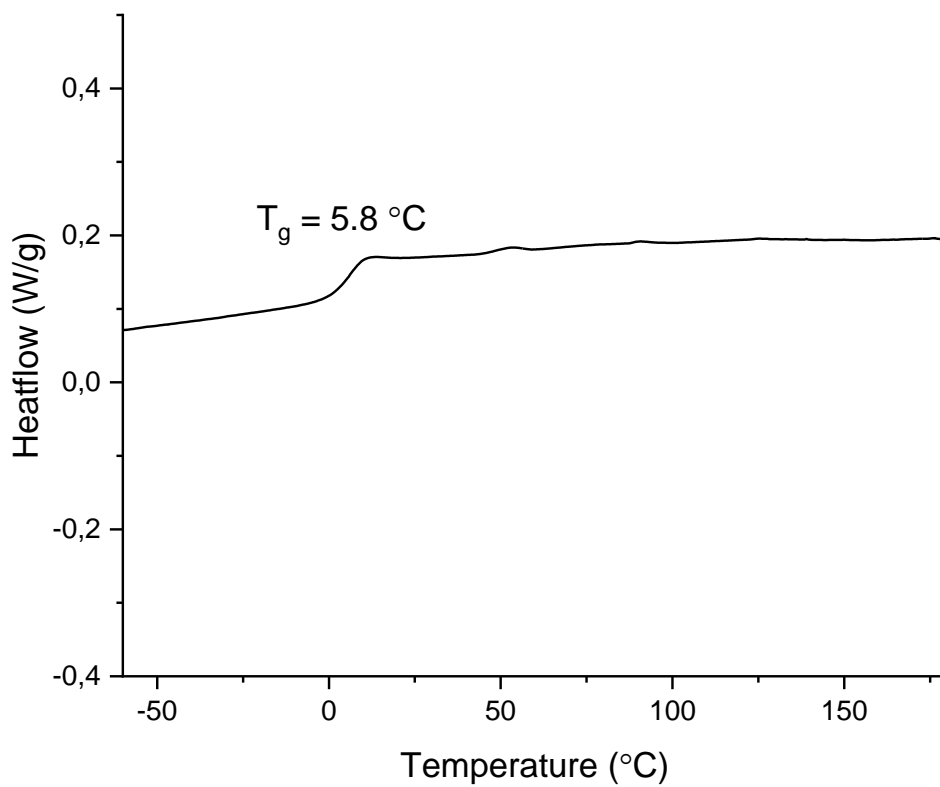


Figure S 91: DSC data from the 1<sup>st</sup> heating cycle of CyNCS/OX copolymer corresponding to table 2, run 6.

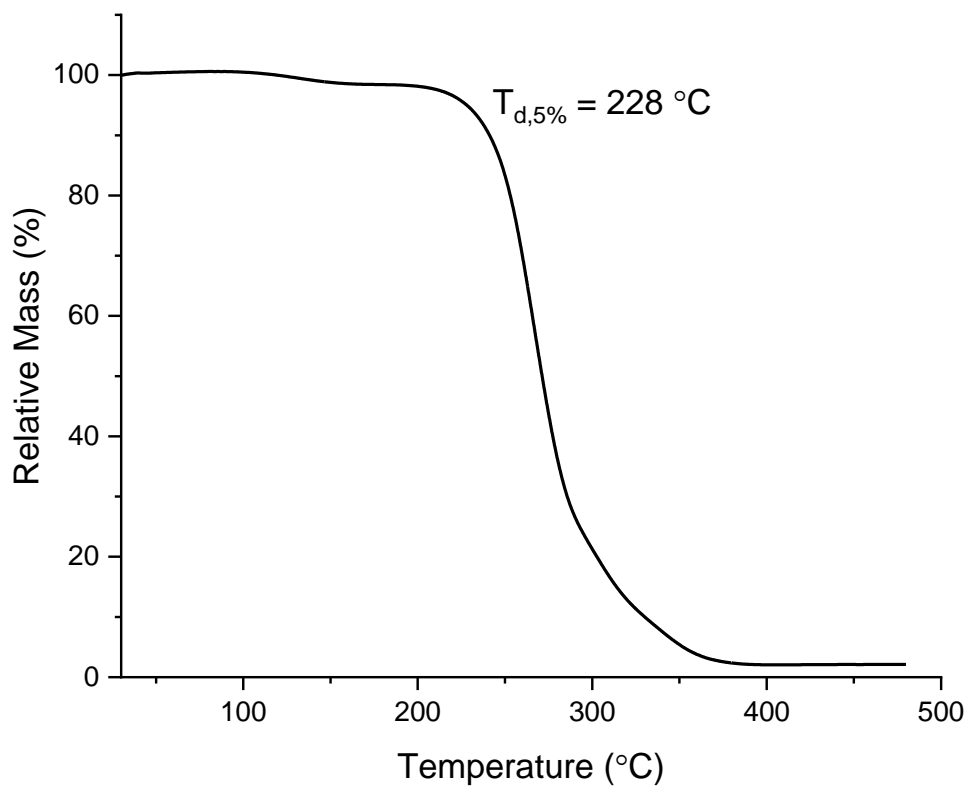


Figure S 92: TGA data of PhNCS/OX copolymer corresponding to table 2, run 7.

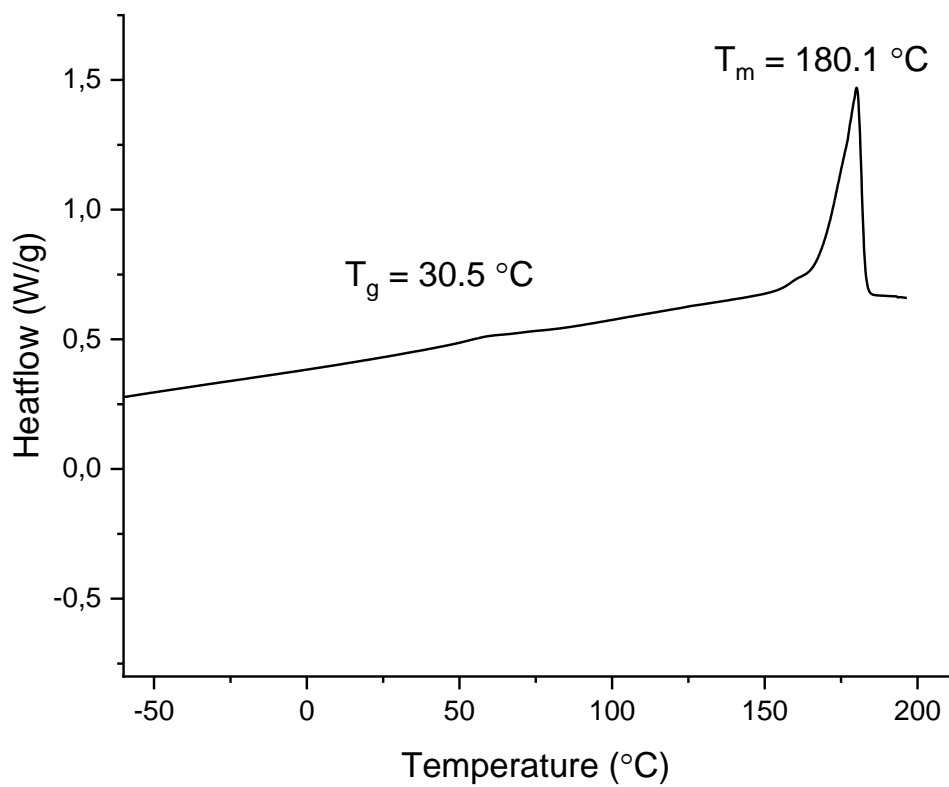


Figure S 93: DSC data from the 1<sup>st</sup> heating cycle of PhNCS/OX copolymer corresponding to table 2, run 7.

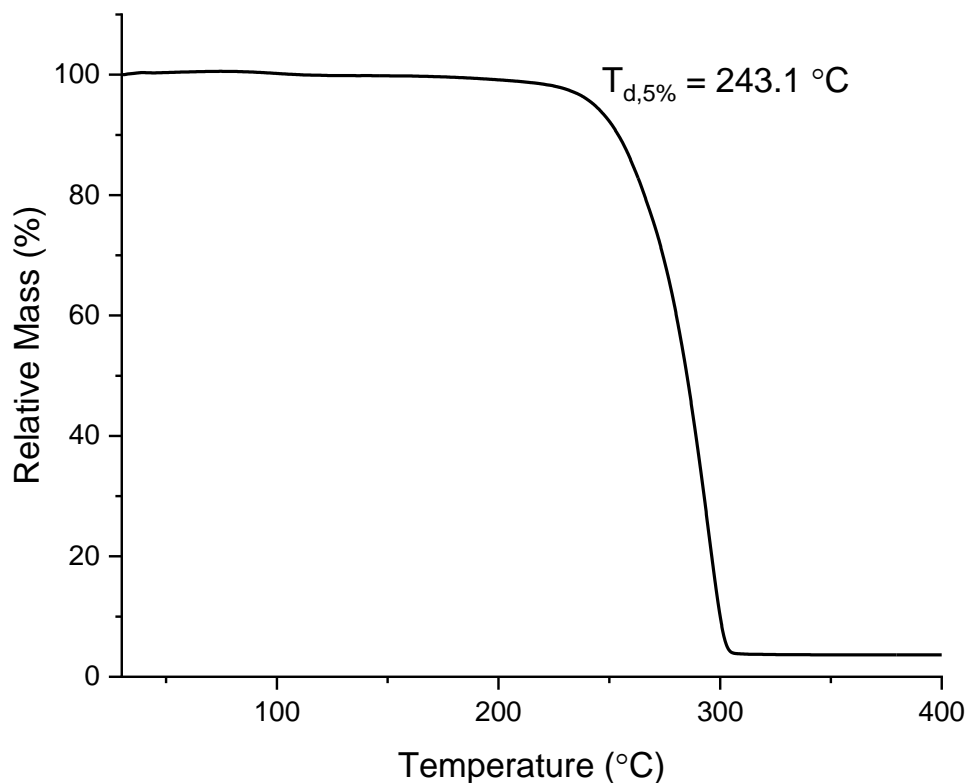


Figure S 94: TGA data of PTA/PO copolymer corresponding to table 2, run 8.

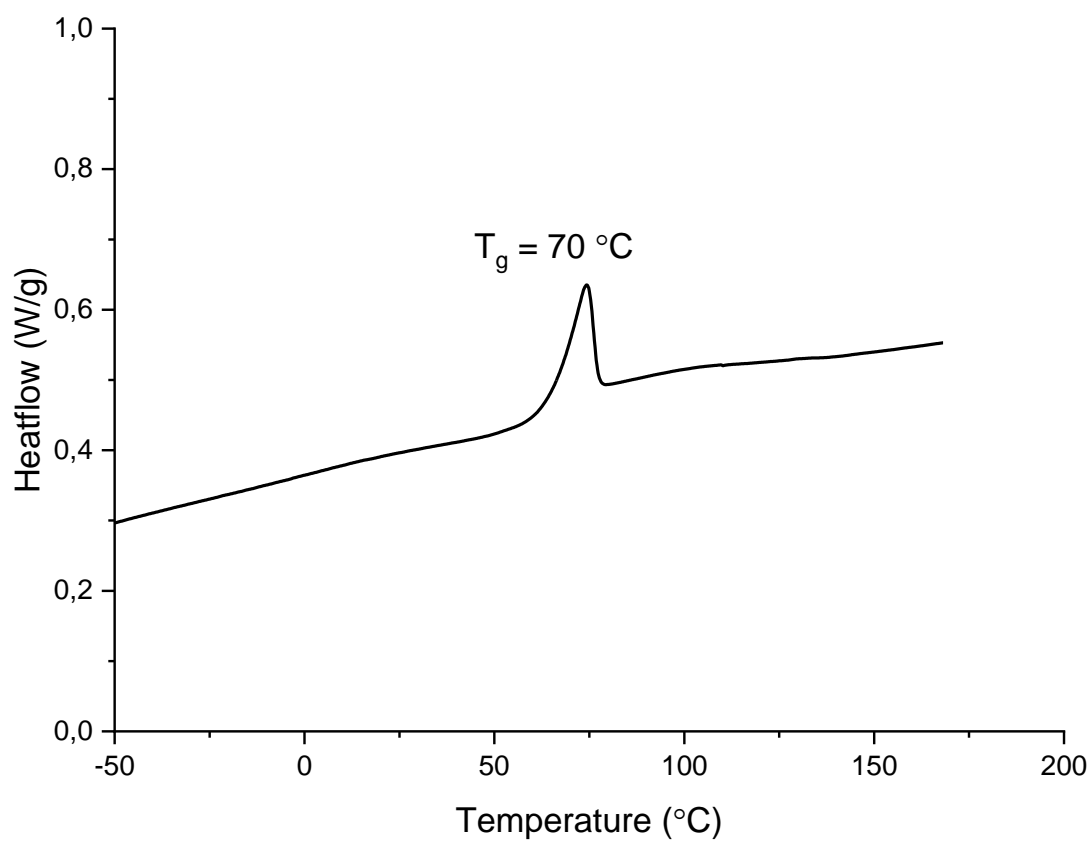


Figure S 95: DSC data from the 1<sup>st</sup> heating cycle of PTA/PO copolymer corresponding to table 2, run 8.

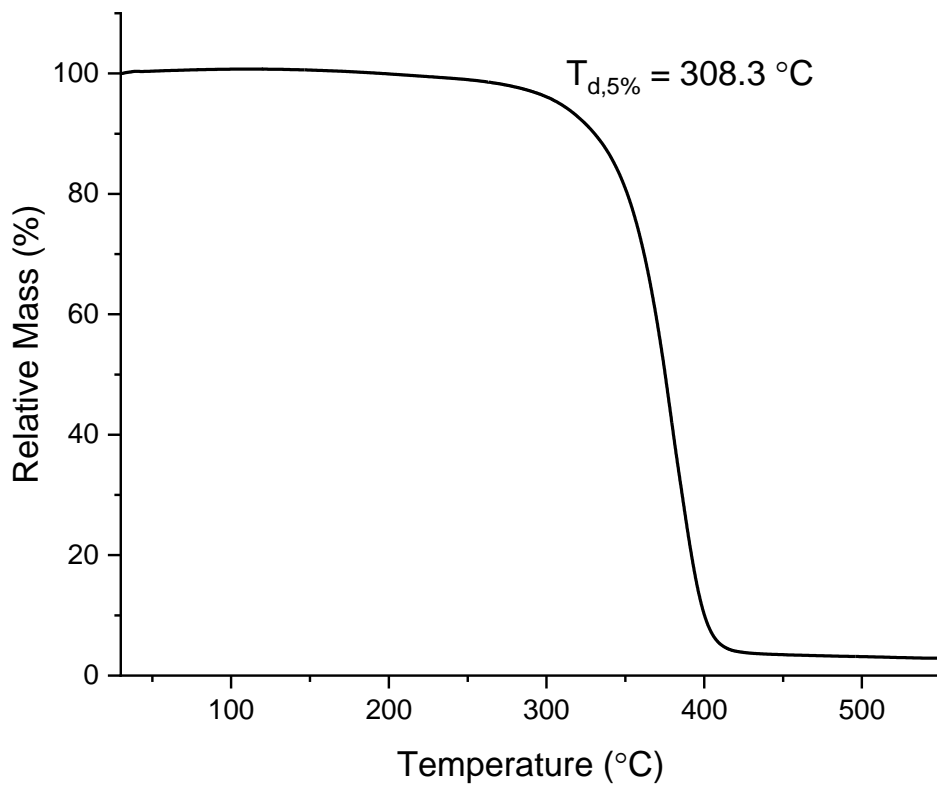


Figure S 96: TGA data of PTA/OX-OAll copolymer corresponding to table 2, run 12.

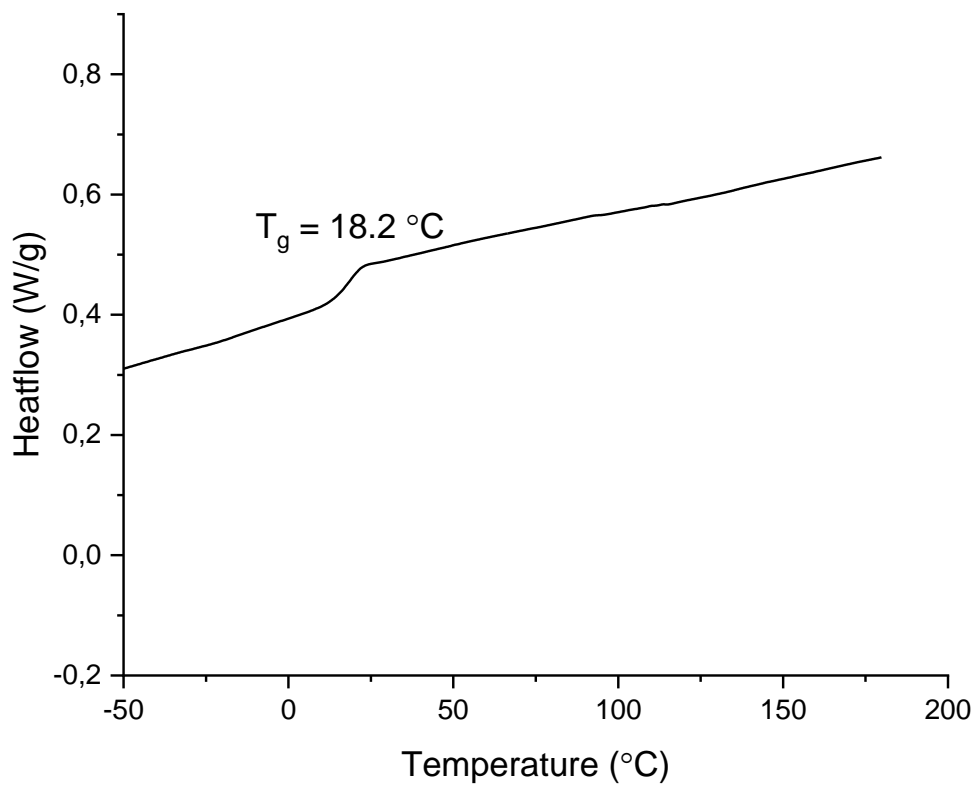


Figure S 97: DSC data from the 1<sup>st</sup> heating cycle of PTA/OX-OAll copolymer corresponding to table 2, run 12.

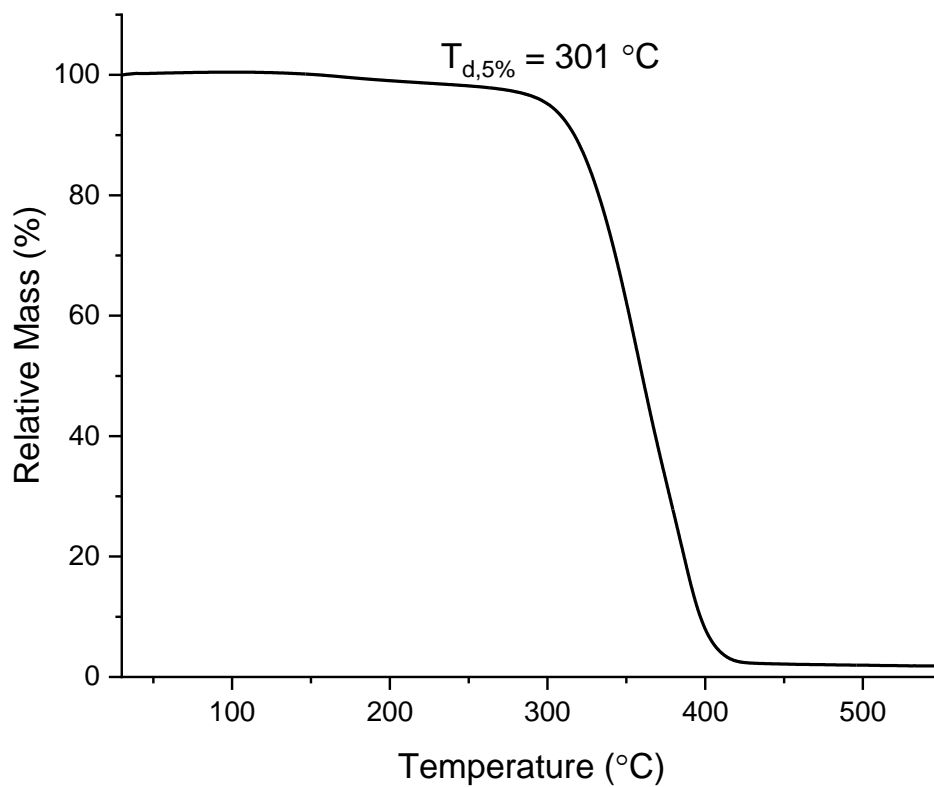


Figure S 98: TGA data of PTA/OX-OBn copolymer corresponding to table 2, run 11.

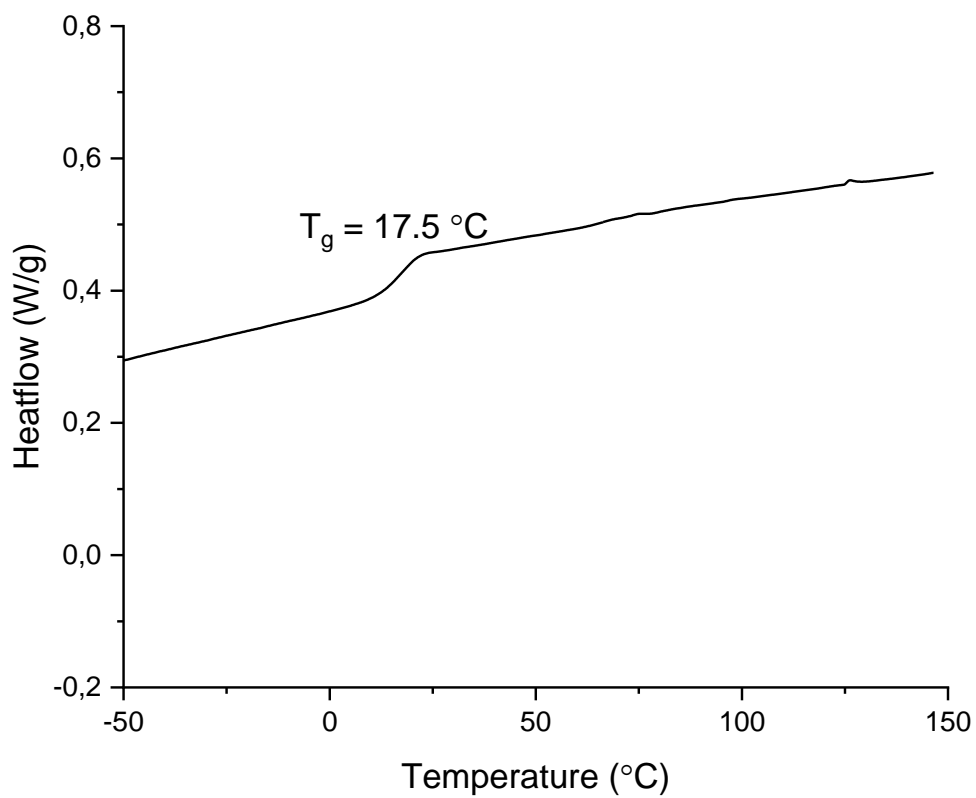


Figure S 99: DSC data from the 1<sup>st</sup> heating cycle of PTA/OX-OBn copolymer corresponding to table 2, run 11.



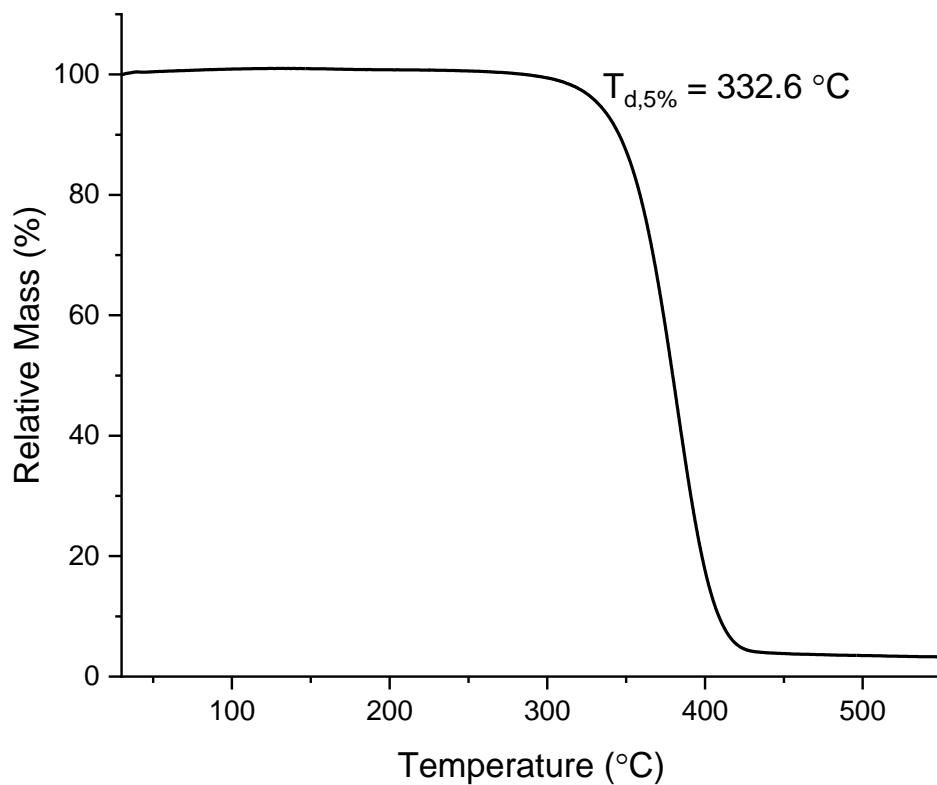


Figure S 100: TGA data of PTA/OX-Me<sub>2</sub> copolymer corresponding to table 2, run 9.

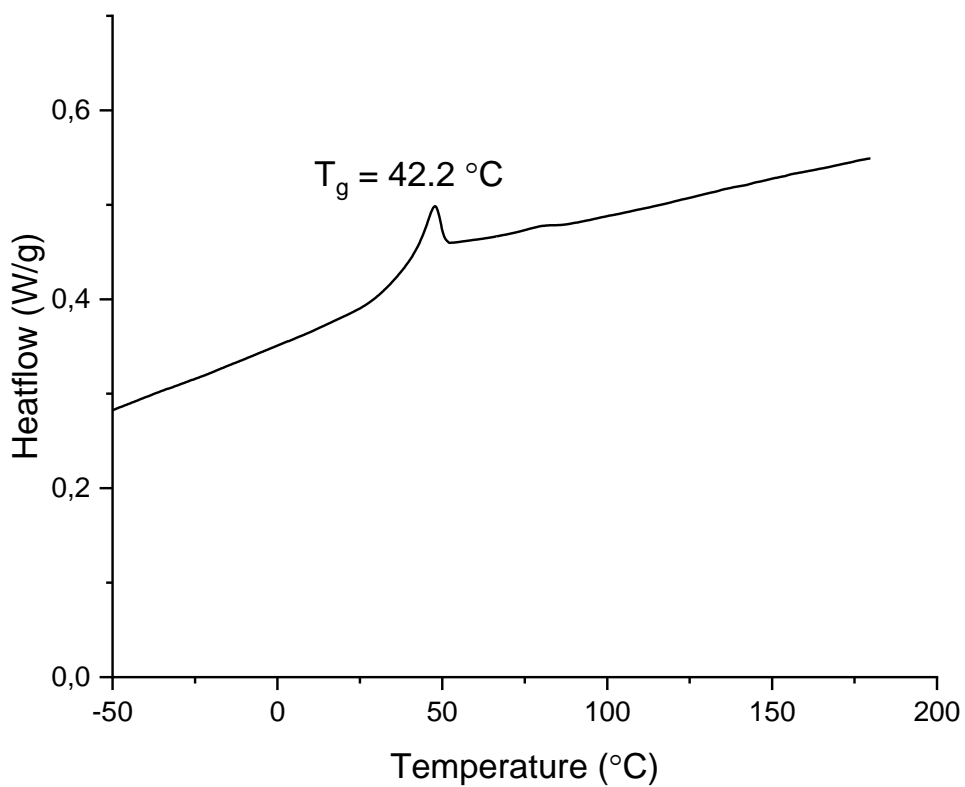


Figure S 101: DSC data from the 1<sup>st</sup> heating cycle of PTA/OX-Me<sub>2</sub> copolymer corresponding to table 2, run 9.

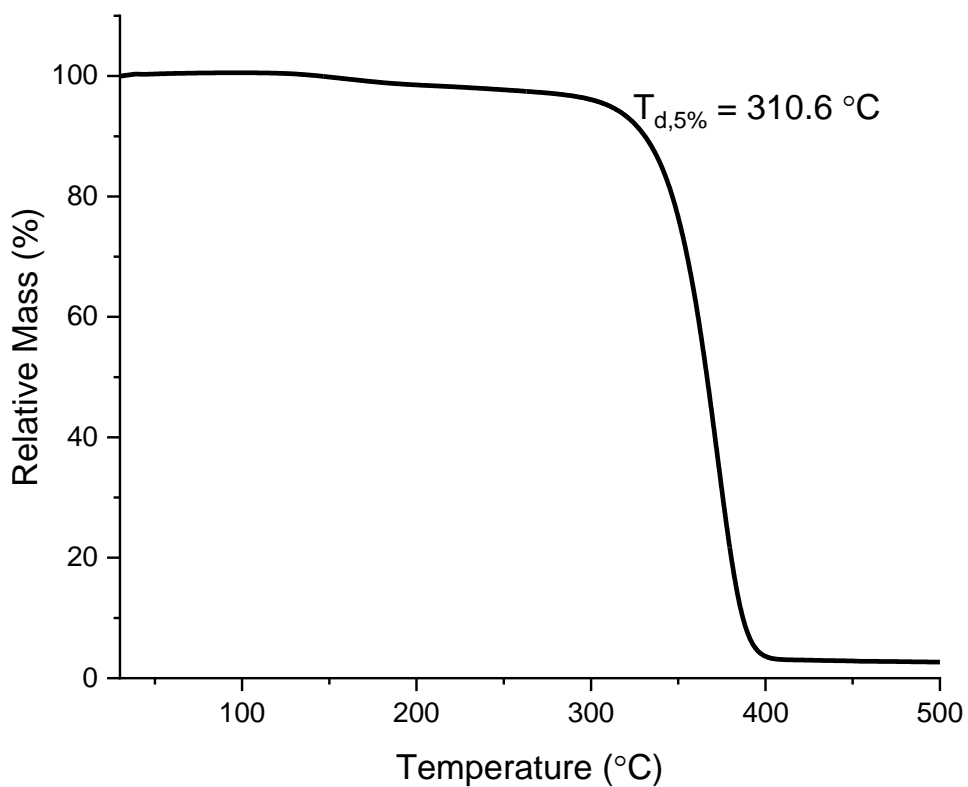


Figure S 102: TGA data of PTA/OX-OEt copolymer corresponding to table 2, run 10.

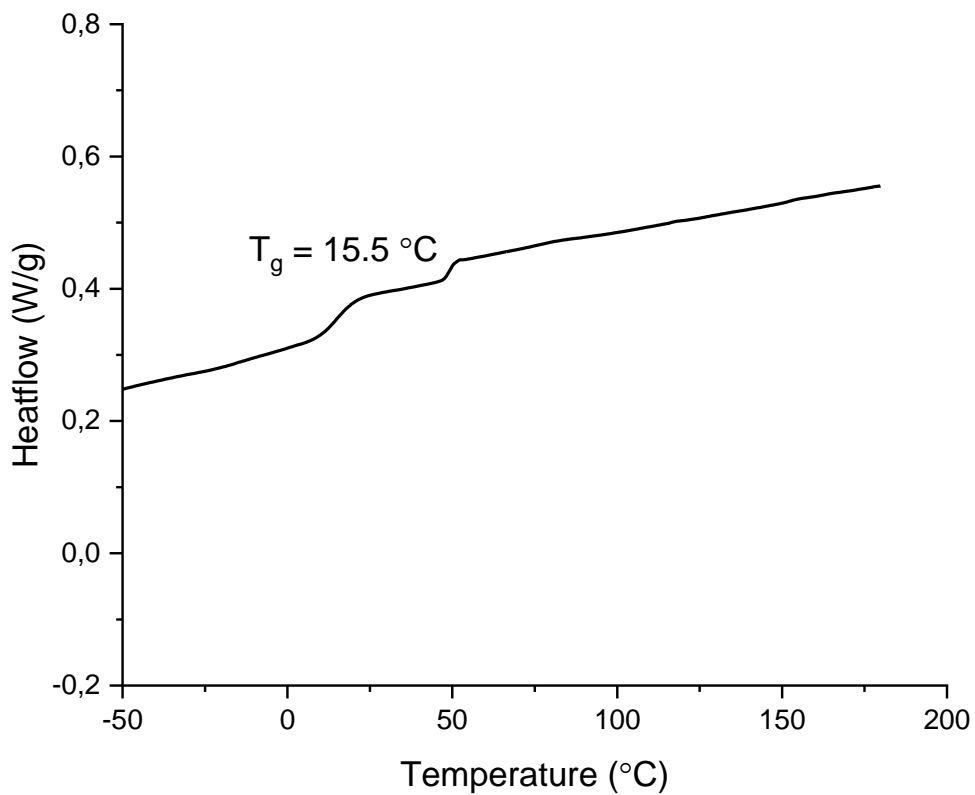
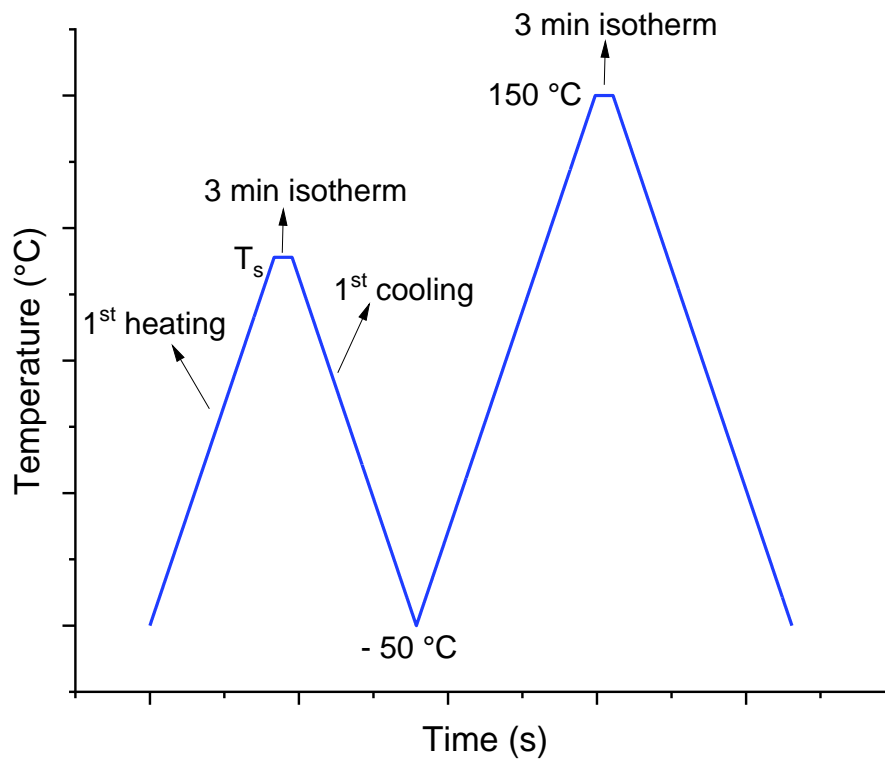


Figure S 103: DSC data from the 1<sup>st</sup> heating cycle of PTA/OX-OEt copolymer corresponding to table 2, run 10.

## Section S5: Self nucleation experiments



**Figure S 104:** DSC procedure for the experiment.

Since the semi-crystalline polymers do not crystallize from a fully molten state, a self-nucleation (SN) technique was used since it allows us to study the crystallization in polymers.<sup>[7]</sup> Figure S 95 shows the procedure used for the SN. Three different  $T_s$  were selected, the  $T_s$  exactly at the peak of the melting temperature, the highest  $T_s$ , exactly where the melting peak ends, and an intermediate  $T_s$  between the two  $T_s$  mentioned. For the study of each  $T_s$  a fresh sample was used.

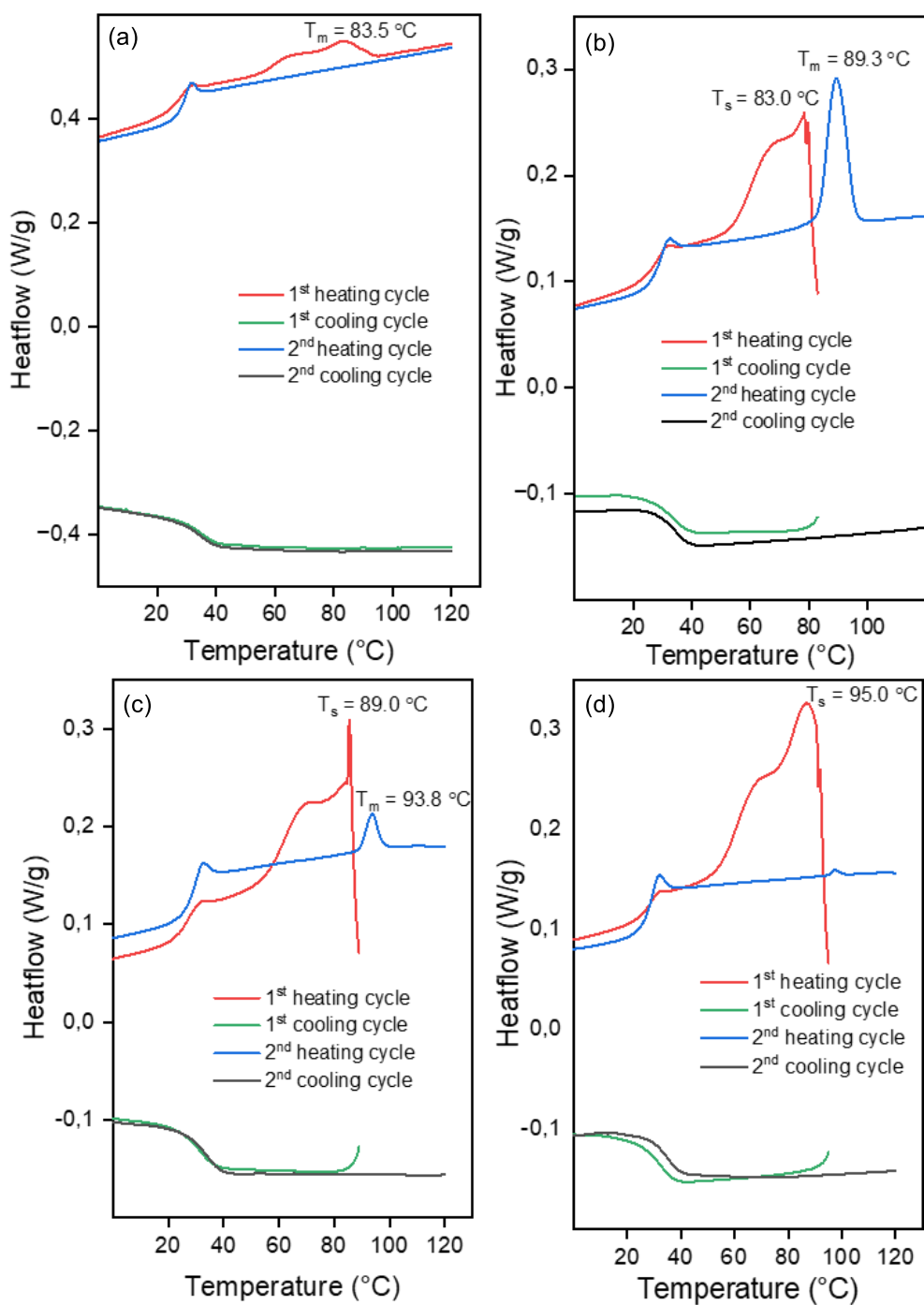


**Figure S 105:** DSC data (clockwise) of PTA/OX copolymer from table 2, run 1. (a) First heating  $> T_m$ , (b) First heating to  $T_s = 83\text{ °C}$ , (c) First heating to  $T_s = 89\text{ °C}$ , (d) First heating to  $T_s = 95\text{ °C}$ .

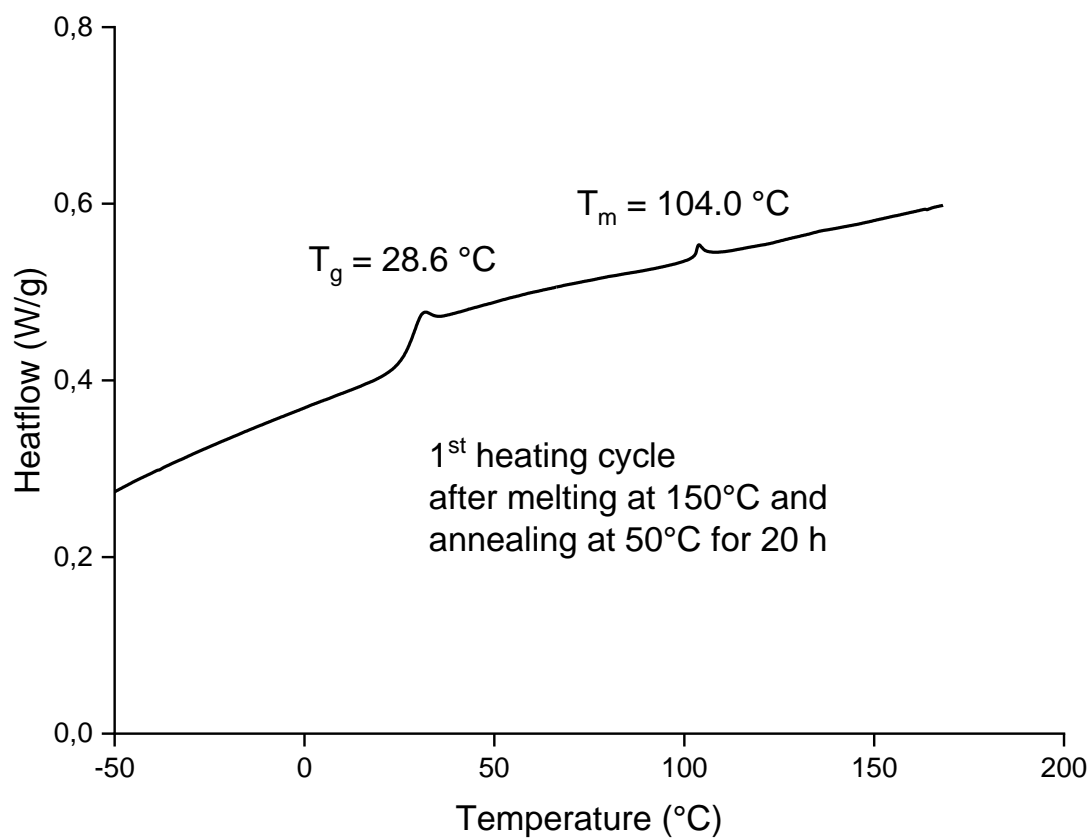


**Figure S 106:** DSC data from 1<sup>st</sup> heating cycle of PTA-OX copolymer after melting at 150°C and annealing at 50°C for 20 h.

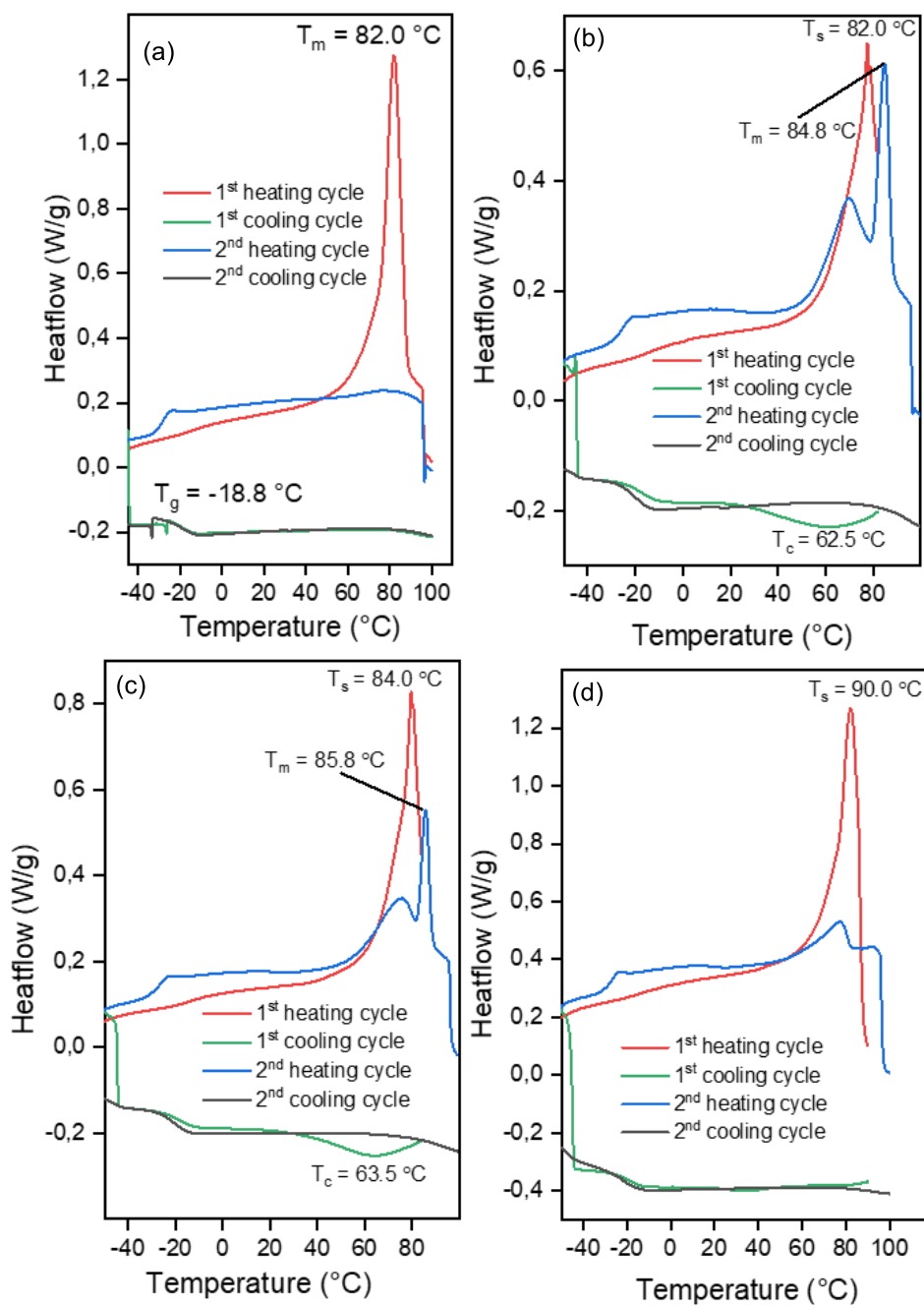


**Figure S 107:** DSC data (clockwise) of CS<sub>2</sub>/OX copolymer from table 2, run 4. (a) First heating > T<sub>m</sub>, (b) First heating to T<sub>s</sub> = 82 °C, (c) First heating to T<sub>s</sub> = 84 °C, (d) First heating to T<sub>s</sub> = 90 °C

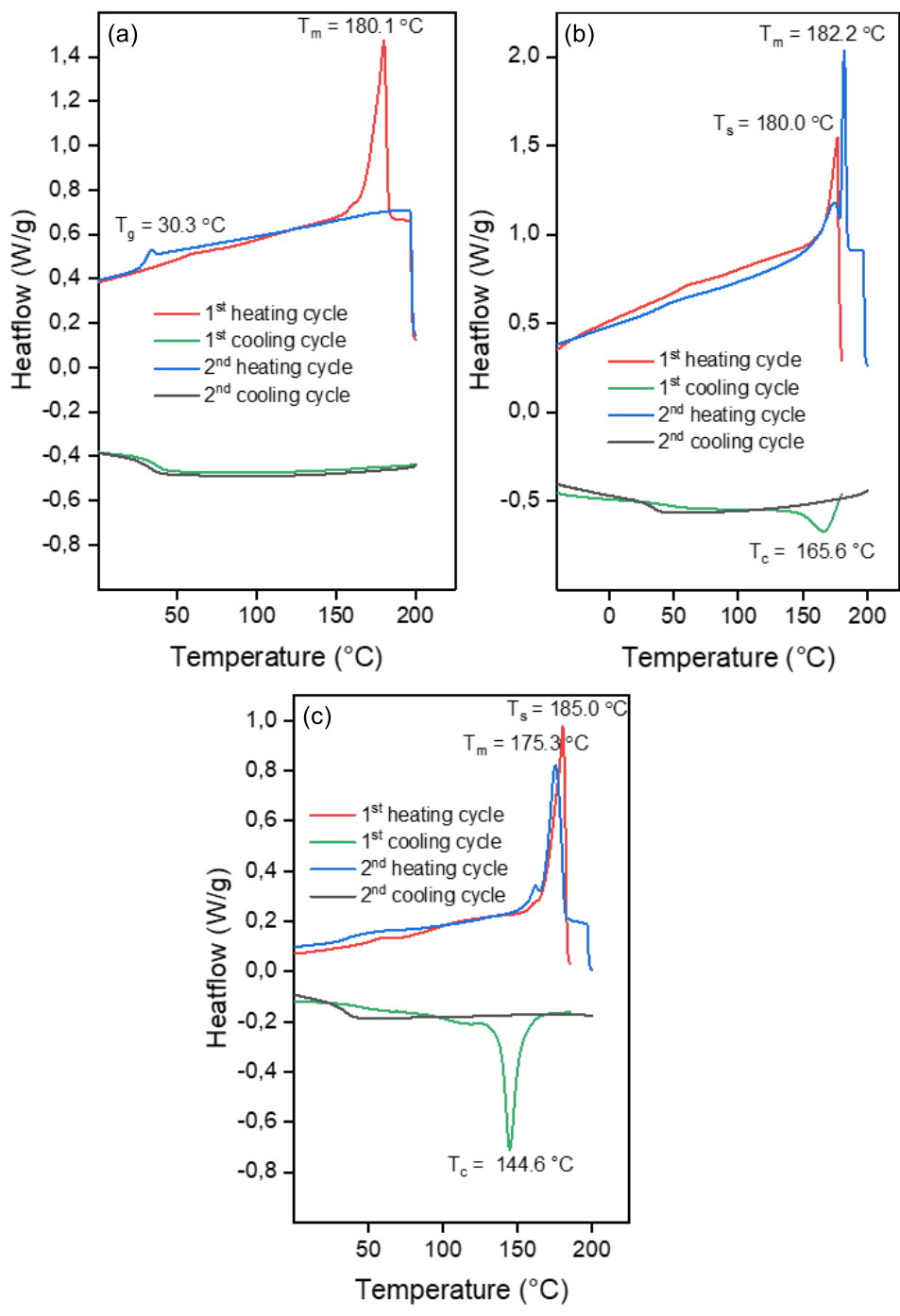


**Figure S 108:** DSC data (clockwise) of PhNCS/OX copolymer from table 2, run 7. (a) First heating  $> T_m$ , (b) First heating to  $T_s = 180^\circ\text{C}$ , (c) First heating to  $T_s = 185^\circ\text{C}$ .

## Section S6: Insitu IR experiments

### Procedure:

The appropriate amount of catalyst, cocatalyst and the monomers were added to an oven dried schlenk tube equipped with a magnetic stirrer inside an argon filled glovebox. It was then brought outside the glovebox and the IR probe was fixed under Ar flow. It was then placed in a pre-heated oil bath at the 80 °C for the specified time. The insitu IR measurement was started once the temperature stabilized and an IR spectrum was recorded every 15 seconds.

1: To determine the dependence of reaction rate on phthalic thioanhydride (PTA).

1eq. KOAc@18C6: 1eq. BEt<sub>3</sub>: 300eq. PTA: 2000 eq. OX was added to a schlenk tube and fitted with the IR probe under a flow of Ar. The measurement was stopped when PTA consumption was complete. The IR peaks corresponding to unreacted PTA at 834, 947 and 1219 cm<sup>-1</sup> and the PTA-OX copolymer at 915, 1089, 1129, 1253 and 1575 cm<sup>-1</sup> were assigned using isolated IR spectrum and then analysed further.

2: To determine the dependence of reaction rate on oxetane.

1eq. KOAc@18C6: 1eq. BEt<sub>3</sub>: 1000eq. PTA: 300 eq. OX was added to a schlenk tube along with 1 mL tetrahydrofuran (THF). The IR probe was fixed under a flow of Ar. The measurement was stopped after 12 h. The IR data of THF was subtracted from the data. The peak corresponding to unreacted OX at 977 cm<sup>-1</sup> was selected for further analysis.

**Analysis:** The change in area under the curve for the selected peaks, to a two-point baseline was computed. The raw data was normalised and plotted as a function of conc. (%) vs time.

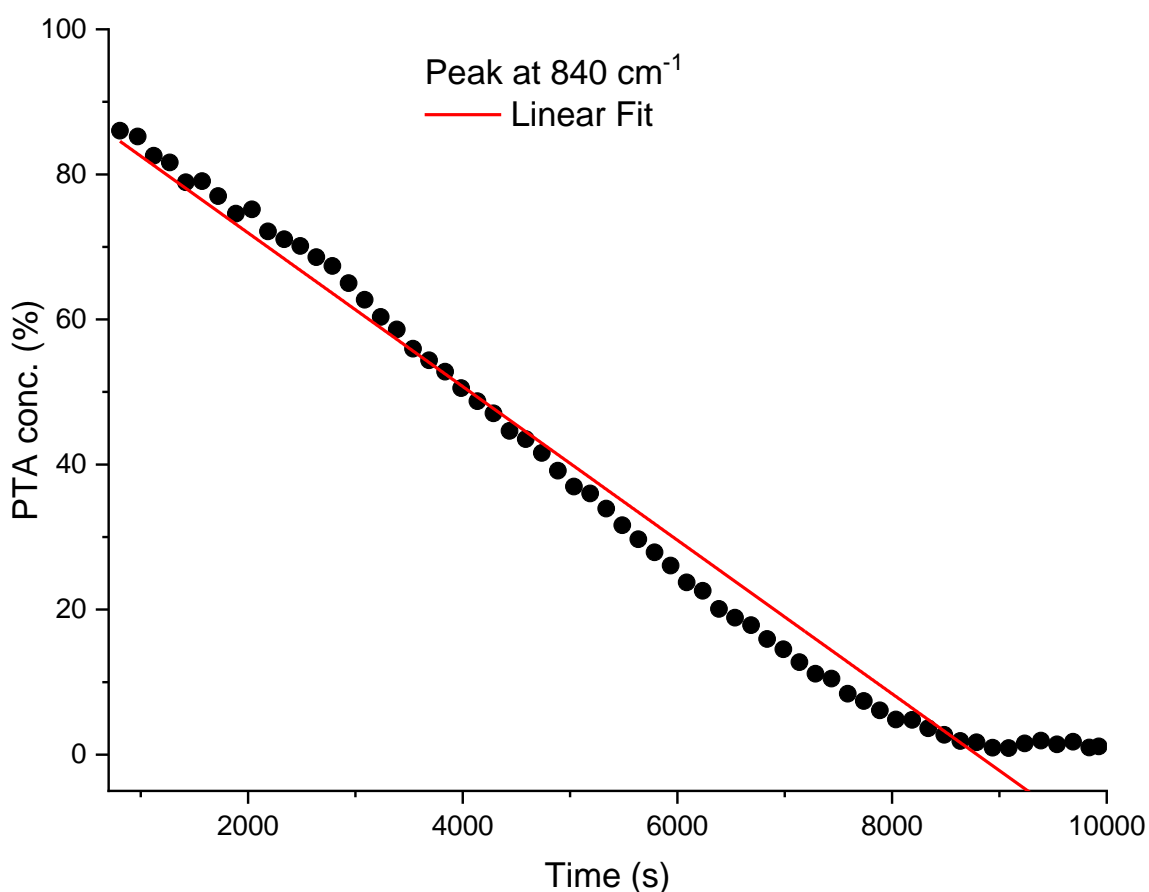


Figure S 109: Graph of PTA conc. (%) vs. time



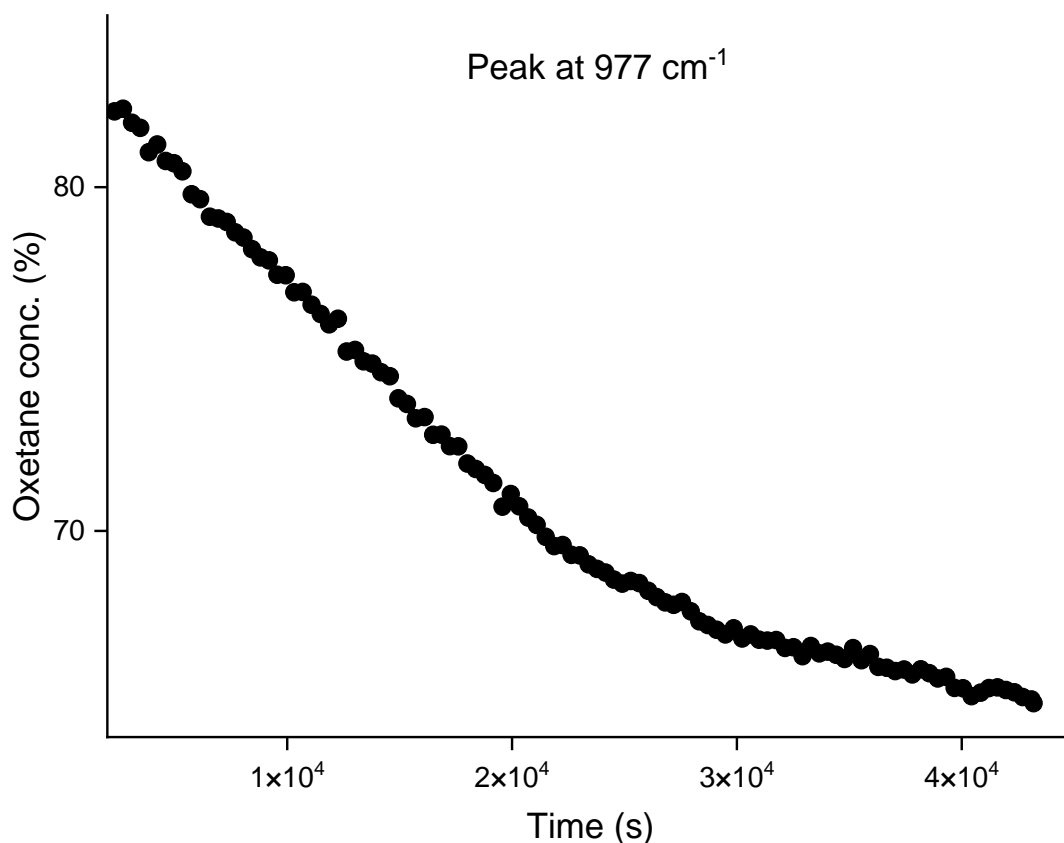


Figure S 110: Graph of oxetane conc. (%) vs. time.

#### Section S7: References

1. M.R. Stühler, C. Gallizioli, S.M. Rupf and A.J. Plajer, *Polym. Chem.*, **2023**, 14, 4848-4855
2. D. C. Wilson, S. Liu, X. Chen, E. A. Meyers, X. Bao, A. V. Prosvirin, K. R. Dunbar, C. M. Hadad and S. G. Shore, *Inorg. Chem.*, **2009**, 48, 13, 5725–5735
3. R. Ahlrichs, M. Bär, M. Hacer, H. Horn and C. Kömel, *Chem. Phys. Lett.*, **1989**, 162, 165–169.
4. (a) J.P. Perdew, *Phys. Rev. B*, **1986**, 33, 8822-24. (b) A.D. Becke, *J. Chem. Phys.*, **1996**, 104, 1040-1046.
5. S. Grimme, J. Antony, S. Ehrlich and H. Krieg, *J. Chem. Phys.*, **2010**, 132, 154104-154119.
6. A. Klampt, *WIREs Comput. Mol. Sci.*, **2011**, 1, 699-709.
7. J. Stephan, J. L. Olmedo-Martínez, C. Fornacon-Wood, M. Stühler, M. Dimde, D. Braatz, R. Langer, A. J. Müller, H. Schmalz and A. J. Plajer, *Angew. Chem. Int. Ed.*, **2024**, 63, e202405047